

**DEVELOPMENT OF MULTIFUNCTIONAL SIRNA DELIVERY SYSTEMS
AND THEIR APPLICATIONS IN MODULATING GENE EXPRESSION IN A
CARDIAC ISCHEMIA-REPERFUSION MODEL**

A Dissertation
Presented to
The Academic Faculty

by

Jie Liu

In Partial Fulfillment
of the Requirements for the Degree
Doctor of Philosophy in Biomedical Engineering

Georgia Institute of Technology
December 2013

Copyright © Jie Liu 2013

**DEVELOPMENT OF MULTIFUNCTIONAL SIRNA DELIVERY SYSTEMS
AND THEIR APPLICATIONS IN MODULATING GENE EXPRESSION IN A
CARDIAC ISCHEMIA-REPERFUSION MODEL**

Approved by:

Dr. Ying Luo, Advisor
Department of Biomedical Engineering
Peking University

Dr. Michael E. Davis, Advisor
Department of Biomedical Engineering
*Georgia Institute of Technology &
Emory University*

Dr. Haifeng Chen
Department of Biomedical Engineering
Peking University

Dr. Zhifei Dai
Department of Biomedical Engineering
Peking University

Dr. Khalid Salaita
Department of Chemistry
Emory University

Date Approved: Nov 15, 2013

To my parents,
Min Zhang and Mianhu Liu

ACKNOWLEDGEMENTS

I would like to acknowledge everyone that helped me during my journey of pursuing the PhD degree. Thank you to everyone that gave me help, support, and guidance along the way. Without your kindness, I could hardly finish all the work in this dissertation.

I would like to thank my advisor Dr. Ying Luo, who widened my horizon for science and gave me the opportunity to exploit the exciting area of gene delivery. I still remembered our starting time when there were only 3 students, and she showed me how to build up a mature lab competent for both chemical and biological research from two empty rooms in a short time. She is a role model for me that let me know how a good scientist thinks and performs. Except the guidance for my research, she is also very generous to provide me opportunities to figure out my strengths and career direction, like the chances for international conferences, the Joint PhD Program with Georgia Tech/Emory, and the industry internship. Thank you for being so supportive during these years.

Many thanks to my co-advisor Dr. Michael Davis. Thank you for taking me as an exchange student in your lab and helping me in so many different ways. I was not familiar with animal studies or cardiovascular diseases before, and to be honest, in the first few weeks I was pressured facing many new words and new techniques. Your patience and optimistic attitude eased my tension. And I also learned how to be efficient at work and meanwhile enjoy the time after work, reaching a good balance between work and life, inspired by you. The whole experience at Emory campus was incredible.

My committee members –Dr. Haifeng Chen, Dr. Zhifei Dai, and Dr. Khalid Salaita – have been giving me great advices for my research work, the presentation, the dissertation, and future career. The points they mentioned during our discussion made me have deeper understanding and further considerations of my research and experimental details. Time difference is always a big problem when it comes to the time for pre-defense and defense. I'm grateful for your patience during the process of time coordination. Thanks a lot for all the contributions made.

I want to give credits for my labmates, past and present. As in a relatively new lab, we are the founders for different research areas in our lab, establishing the new systems and experiment protocols from almost nothing. We spent days and nights together, and we shared the joys when things work well and the frustrations if the results turned out to be opposite against expectation. No matter what, we always support each other. I'm so glad to have you guys during the five years. Thank you, Xiaopeng Liu, Tao Shi, Bing Lv, Liyang Jiang, Kai Wang, Wei Zhang, Jinyang Wang, Ni Su, Fang Wang, Jiong Chen, Suwei Zhu, Hao Cai, Xiang Yin, Jiaying Liu, and Xi Gu.

I also would like to thank all the labmates in Davis Lab. Going to a foreign country where people speak different languages would be a big challenge, but all of you made it much easier for me to fit in the new environment. I still remembered the time when I got some PFA powder flown into my eyes accidently and ended up into the emergency room. Almost everyone went to the emergency room with me and kept me accompanied, and even Mike dropped by from home. That's the warmest and most touching moment I ever

had. Although only stayed for one year, I already feel strongly connected with this big family. Thank you so much, Archana Boopathy, Srishti Bhutani, Milton Brown, Bernadette Cabigas, Pauline Che, Kristin French, Warren Gray, Raffay Khan, Mario Martinez, Karl Pendergrass, Inthu Somasuntharam, Catherine, Dave, Marcos and Sheridan.

My parents have been my biggest support along the way. Though they didn't prefer Biomedical Engineering to be my major at the beginning, they got my back for every major decision I made. Whenever I felt frustrated and depressed, they encouraged me to pick it up again and never give up the dream that I truly want. Whenever I need help, they would try every effort to make things easier. I couldn't be luckier to have them as my parents. Now it's time for me to take care of them and be their biggest support in the future.

Last but not least, to my boyfriend Chen Wang. He's the one that almost went through all the experience with me during these five years. I know I could be emotional and sometimes unreasonable when I got upset after defeated by the troubles at experiments, but he never gave up on me. He cheered me up when I was depressed, talked me through the troubles when I became calm, and reminded me to move forward instead of being satisfied with current situation after I made some progress. His tolerance and protection guarded me through this long journey. People say when you find the right person, you'll know it, because everything just feels natural, no need for worries and suspicions. I think I've already found the one.

TABLE OF CONTENTS

	Page
ACKNOWLEDGEMENTS	iv
LIST OF TABLES	ix
LIST OF FIGURES	x
LIST OF ABBREVIATIONS	xiii
SUMMARY	xvi
CHAPTER	
1 INTRODUCTION	1
1.1 Motivation	1
1.2 Research Objectives	2
1.3 Specific Aims	4
1.4 Background	6
2 DEVELOPMENT OF A DEGRADABLE CATIONIC POLYMER TO SILENCE GENE EXPRESSION IN VITRO	22
2.1 Introduction	22
2.2 Results	24
2.3 Discussion	33
3 DEVELOPMENT OF A NEUTRAL CROSSLINKED DENDRIMERIC SYSTEM TO SILENCE GENE EXPRESSION IN VITRO	37
3.1 Introduction	37
3.2 Results	39

3.3 Discussion	55
4 DOWN-REGULATION OF AT1R IN CARDIAC TISSUE BY DELIVERING SPECIFIC SIRNA TO PRESERVE CARDIAC FUNCTION POST-MI	59
4.1 Introduction	59
4.2 Results	61
4.3 Discussion	73
5 SUMMARY AND FUTURE DIRECTIONS	78
5.1 Peptide polymers in siRNA delivery	78
5.2 Neutral crosslinked dendrimeric systems	80
5.3 Dendrimeric delivery systems in cardiac tissue	83
5.4 Concluding remark	85
APPENDIX A: MATERIALS AND METHODS	87
REFERENCES	97
VITA	115

LIST OF TABLES

	Page
Table 4.1: Size and zeta-potential of siRNA-loaded particles	64
Table A.1: Primer sequences used in qPCR	95

LIST OF FIGURES

	Page
Figure 1.1: Scheme of a typical dendrimer	11
Figure 2.1: Scheme of the synthesis of dPOA	25
Figure 2.2: siRNA loading capacity of arginine peptides assessed by fluorescent dye exclusive assay	26
Figure 2.3: Zeta-potentials of R9/siRNA and dPOA/siRNA complexes at N/P=3 and N/P=5	27
Figure 2.4: Nuclease resistance of siRNA-loaded arginine peptide particles	28
Figure 2.5: GSH treatment for dPOA/siRNA and PLR/siRNA complexes	29
Figure 2.6: Cytotoxicity of arginine peptides	30
Figure 2.7: Fluorescence microscopy observation and flow cytometry analysis of cy3-siRNA loaded particles	31
Figure 2.8: Cell viability upon the treatment of dPOA and RGD-g-dPOA	32
Figure 2.9: Gene silencing efficiency of siRNA-loaded dPOA particles and siRNA-loaded RGD-d-dPOA particles in A549-luci and HepG2 cells	33
Figure 3.1: Flow cytometry analysis of binding and internalization efficiency of different saccharide-modified PAMAM-HYDs with HepG2 cells	41
Figure 3.2: The structure of the neutral dendrimer of GalNAc-PAMAM-HYD and the H^1 -NMR spectrum of GPHs with varied GalNAc modifications	42
Figure 3.3: Schematic process of preparing siRNA-loaded crosslinked particles for siRNA delivery	43
Figure 3.4: Complexation of siRNA with PAMAM-HYD and GPH dendrimers at pH 5.0 and pH 7.4	44
Figure 3.5: Zeta-potentials of dendrimer-siRNA mixtures	45

Figure 3.6: siRNA encapsulation efficiency in the crosslinked systems	46
Figure 3.7: siRNA encapsulation efficiency in crosslinked particles made from GPHs with varied GalNAc modification levels	47
Figure 3.8: Sizes of the siRNA-loaded crosslinked particles at varied glutaraldehyde concentrations and GalNAc modification levels	48
Figure 3.9: Zeta-potentials of siRNA-loaded crosslinked particles	49
Figure 3.10: Size distribution of siRNA-loaded crosslinked particles and polyelectrolyte particles	50
Figure 3.11: siRNA release from the crosslinked particles at the acidic condition	51
Figure 3.12: Cytotoxicity of neutral dendrimer PAMAM-HYD and cationic dendrimer G5.0 PAMAM on HepG2 cells and HUVECs after 24 h incubation	52
Figure 3.13: Cytotoxicity of siRNA-loaded crosslinked particles in HepG2 cells	52
Figure 3.14: Gene silencing effect of the siRNA-loaded crosslinked particles	53
Figure 3.15: Cellular internalization of neutral dendrimers and siRNA-loaded crosslinked particles	54
Figure 4.1: Scheme of tadpole dendrimers and H^1 -NMR analysis	62
Figure 4.2: Gel retardation assay of G4.0 PAMAM and tadpole dendrimers	63
Figure 4.3: Size distribution of siRNA-loaded tadpole dendrimer particles	64
Figure 4.4: Cytotoxicity of siRNA-loaded tadpole dendrimer particles in primary neonatal CMs	65
Figure 4.5: Cellular internalization of FITC-siRNA loaded tadpole dendrimer particles in cardiomyoblast H9C2 cells	66
Figure 4.6: siRNA encapsulation efficiency in crosslinked particles made from GPHs with varied GalNAc modification	67
Figure 4.7: Expression of AT1R, AT2R, and Col-1 in the left ventricle tissue upon the delivery of siRNA-loaded tadpole dendrimer particles	69
Figure 4.8: Ejection fraction of different treatment groups at the 3 day after injection	70

Figure 4.9: End-systolic volume and end-diastolic volume of different treatment groups	71
Figure 4.10: Infarct size of different treatment groups	72
Figure 4.11: Characteristics of the optimized tadpole dendrimers	73

LIST OF ABBREVIATIONS

ADH	Adipic acid dihydrazide
AMD	Age-related macular edema
Ang II	Angiotensin II
ANOVA	Analysis of variation
ARB	Angiotensin receptor blocker
AT1R	Angiotensin II type 1 receptor
AT2R	Angiotensin II type 2 receptor
BCA	Bicinchoninic acid
CPP	Cell penetrating peptide
CM	cardiomyocytes
CVD	Cardiovascular disease
DAPI	4',6-diamidino-2-phenylindole
DME	Diabetic macular edema
DMEM	Dulbecco's Modified Eagle Medium
DNA	Deoxyribonucleic acid
dPOA	Degradable poly(oligo-arginine)
dsRNA	Double-stranded RNA
ECM	Extracellular matrix
EF	Ejection fraction
EDV	End diastolic volume
ESV	End systolic volume

FBS	Fetal bovine serum
FITC	Fluorescein isothiocyanate
GPC	Gel permeation chromatography
GPH	GalNAc-PAMAM-Hydrazide
GSH	Glutathione
IMTP	Ischemic myocardium-targeted peptide
IR	Ischemia-reperfusion
MI	Myocardial infarction
mRNA	Messenger ribonucleic acid
MTT	3- (4,5-Dimethylthiazol-2-yl)-2,5-diphenyltetrazolium bromide
MTS	[3-(4,5-dimethylthiazol-2-yl)-5-(3-carboxymethoxyphenyl)-2-(4-sul fophenyl)-2H-tetrazolium
NAION	Non-arteritic ischemic optic neuropathy
NHS	N-hydroxysuccinimide
ODN	Oligodeoxynucleotide
PAA	Polyacrylic acid
PAMAM	Polyamido amine
PAMAM-HYD	PAMAM-hydrazide
PBS	Phosphate buffered saline
PEG	Poly(ethylene glycol)
PEI	Polyethyleneimine
PGAA	Poly(glycoamidoamines)
PIGF	Placental growth factor

PLGA	Poly(lactic-co-glycolic acid)
PLL	Poly L-lysine
PLR	Poly-L-arginine
PPI	Polypropyleneimine
PV	Pressure-volume
RAAS	Renin-Angiotensin-Aldosterone System
RdRP	RNA dependent RNA Polymerase
RISC	RNA Induced Silencing Complex
RNA	Ribonucleic acid
RNAi	RNA interference
ROS	Reactive oxygen system
SEM	Standard error of measurements
siRNA	Small interfering ribonucleic acid
SOD	Superoxide dismutase
SPDP	N-succinimidyl-3-(2-pyridyldithiol)propionate
TAT	Trans-Activator of Transcription
TBE	Tris/Borate/EDTA
TTC	2,3,5-triphenyltetrazolium chloride
UTMD	Ultrasound-targeted microbubble destruction
VEGF	Vascular endothelial growth factor
WHO	World Health Organization

SUMMARY

RNA interference (RNAi) is a conservative post-transcriptional gene silencing mechanism that can be mediated by small interfering RNAs (siRNAs). Given the effectiveness and specificity of RNAi, the administration of siRNA molecules is a promising approach to cure diseases caused by abnormal gene expression. However, as siRNA is susceptible to degradation by nucleases and it can hardly penetrate cell membranes due to its polyanionic nature, a successful translation of the RNAi mechanism for therapeutic purposes is contingent on the development of safe and efficient delivery systems. This dissertation described the development of novel siRNA delivery systems on the basis of polymeric and dendrimeric materials and also demonstrated the application of one optimized delivery system to deliver therapeutic siRNAs in a cardiovascular disease model *in vivo*. We studied a linear peptide polymer made from cell penetrating peptide monomers and investigated the contribution of the polymeric structure, degradability, and ligand conjugation to the siRNA loading capacity, biocompatibility, and transfection efficiency of polymeric materials. With the obtained knowledge and experience, we invented a neutral crosslinked delivery system aiming to solve the inherent drawbacks of traditional cationic delivery systems that are based on electrostatic interactions. The new concept utilized buffering amines to temporarily bind siRNA and a crosslinking reaction to immobilize the formed particles, and targeting ligands modified on the neutral dendrimer surface further enhanced the interactions between the delivery vehicles and target cells.

The obtained delivery system allowed stability, safety, controllability, and targeting ability for siRNA delivery, and the method developed here could be transformed to other polymeric or dendrimeric cationic materials to make them safer and more efficient. To exploit the therapeutic potential of siRNA delivery, we developed a tadpole-shaped dendrimeric material to deliver siRNA against an Angiotensin II receptor in a rat ischemia-reperfusion model. Our results showed that the nonaarginine-conjugated tadpole dendrimer was capable of delivering siRNA effectively to cardiac cells both *in vitro* and *in vivo*, and the successful down-regulation of the Angiotensin II receptor preserved the cardiac functions and reduced the infarct size post-myocardial infarction. This dissertation paves a way for transforming multifunctional non-viral siRNA delivery systems into potent therapeutic strategies for the management of cardiovascular diseases.

CHAPTER 1

INTRODUCTION

Gene therapy is becoming increasingly attracting to improve human health. The discoveries revealed by the human genome project demonstrated the underlying genetic causes for inherited diseases [1], and it is estimated that more than 10,000 human diseases relate with genetic abnormalities. With the rapid development of academic researches and modern techniques, numerous gene targets that are deregulated or dysfunctional under particular circumstances have been identified for critical diseases. Therefore, increasing the expression of protective genes or decreasing the expression of pathogenic genes or harmful genes could be a potent strategy for disease management.

1.1 Motivation

The discovery of RNA interference (RNAi) mechanism widens the door for gene therapy [2-6]. The high specificity and high efficiency of RNAi make the fine regulation of a target gene become possible. To utilize the endogenous post-transcriptional gene silencing mechanism, appropriate trigger molecules need to be introduced into target cells to initiate the RNAi process, and the most efficient triggers are small interfering RNA (siRNA) and microRNA. Compared to microRNAs and other types of molecules that are capable of suppressing RNA translations, such as ribozymes, DNAzymes, antisense oligonucleotides (ASO), and decoys, siRNA molecules own unique strengths [7]. They have completely matched double-stranded structures, which makes them relatively stable compared to single-stranded RNAs. It is easy to design and synthesize the siRNA sequence against a particular gene simply based on the base-pairing principle, without concerning

the design of complicated structures as seen in ribozymes and DNAzymes. The development of siRNA therapeutics is paving a way for realizing the personalized therapy and meeting the unmet clinical needs [8].

However, the knowledge of gene abnormalities upon illnesses is far behind from being fully translated for therapeutic purposes due to the lack of safe and efficient delivery systems. Currently, clinical trials of gene therapy are dominated by viral vectors, unfortunately with the risks of mutagenesis, immunogenicity, and virus leakage [9], while chemically synthesized carriers are more controllable but less efficient. Most clinical trials using siRNA molecules as the drug molecules aim for local treatments, such as the ocular system, which is relatively less challenging; however, problems with the systemic delivery and the delivery to other organs that are deep in the human body still remain unsolved. Such situation greatly restricts the application of RNAi therapeutics. This dissertation focuses on the development of novel delivery systems based on polymers and dendrimers first *in vitro* and then translating such delivery systems in a cardiovascular disease model *in vivo*.

1.2 Research Objectives

A competent siRNA delivery system should be able to overcome at least 2 biological barriers, the negatively charged cell membrane and the intracellular endosomal membrane. As to the systemic delivery systems, penetrating the endothelial layer is another hurdle to conquer. Except these basic requirements, the siRNA loading efficiency, vehicle stability, toxicity, and degradability are also worth considering. To produce a qualified delivery system, the key factors that finally affect the delivery efficiency need to be figured out, and such knowledge would provide hints and directions for a novel and

applicable design. With this purpose, polymers and dendrimers were studied in this dissertation.

Polymeric materials are highly diverse regarding the structures, sizes, and functions, allowing a great space for the design toward a particular aim. At present, polymers have been widely used as delivery vehicles [10, 11]. Some are composed of unified monomers, while some are hybrids of various components that can realize different actions. The properties and performance of a polymeric material associate with many factors, and sometimes even a slight variation may lead to a significant distinction. To understand the underlying mechanism, in the first part of the dissertation a synthesized linear polymer composed of oligo-peptide monomers was studied to understand how the size and the degradability affect the characteristics of the polymer as well as the final transfection efficiency *in vitro*, and whether the introduction of an integrin-binding ligand could improve the efficacy was also studied.

Dendrimers are popular and promising in constructing drug delivery systems [12, 13]. They have defined chemical structures with tunable numbers of branches, peripherals, and generations, so they can be designed to deliver a certain category of cargoes with controllable loading efficiency and affinity. As to siRNA delivery, dendrimers hold an additional advantage of the endosomal escape ability to release siRNA into cytoplasm where the RNAi takes place. The nature of dendrimers is suitable for siRNA delivery; however, their toxicities bring safety concerns when it comes to the translation for therapeutic purposes. In the second part of the dissertation, the surface characteristic of the original cationic dendrimer was redesigned, and a crosslinking strategy was invented for constructing neutral siRNA delivery vehicles with the reformed dendrimeric materials.

Myocardial infarction (MI) is a life-threatening cardiovascular disease that was usually caused by the occlusion of coronary arteries due to floating atherosclerotic plaques. Even if patients can survive from the initial attack, the following loss of heart muscle contractility and progressive ventricle dysfunction can hardly be prevented. Currently, the only definite cure is the heart transplantation, but the availability of heart donors and the risk of consistent activations of the immune system may present as potential issues, thus the treatment of cardiovascular diseases demands a significant breakthrough. Till now gene therapy rarely expands to cardiac tissue because of the lack of suitable delivery vehicles. In the third part of the dissertation, with the knowledge and experience obtained in the first two parts, a hybrid material of dendrimers and polymers was developed into a siRNA delivery system and was exploited in a cardiovascular disease model.

1.3 Specific Aims

The central hypothesis of this dissertation is that the design of multifunctional polymeric materials will lead to a safe and efficient siRNA delivery system with potential cardiovascular applications. The central hypothesis was studied following three specific aims.

Specific Aim 1: Investigate the key factors of polymeric materials based on degradable cationic polymers

We hypothesized that a degradable backbone could alleviate the toxicity from high-density charges and meanwhile preserve the strengths of the polymeric structure. We used an oxidative condensation method to synthesize polymeric oligo-arginine peptides linked with reducible disulfide bonds, and the performances of the obtained materials were evaluated for physiochemical properties and transfection efficiency in cancer cell lines,

using the short oligo-arginine and a non-reducible arginine polymer in comparison. To investigate the contribution of functional ligands, a RGD peptide was further modified on the reducible arginine polymer, and the transfection efficiency of the un-modified and modified materials were compared.

Specific Aim 2: Develop a neutral crosslinked dendrimeric system to overcome the drawbacks of traditional cationic systems

We hypothesized that the neutral peripherals of a dendrimer is the key to reduce toxicity, and its buffering amines at the joint points could be utilized to carry siRNA at low pH. We developed a novel category of neutral dendrimers by replacing their surface cationic groups with physiologically non-charged hydrazides and targeting saccharide molecules, and we established a method to construct the neutral crosslinked delivery vehicles based on a crosslinking reaction. The siRNA loading efficiency, particle size, stability, controlled release of siRNA, and targeting capability were studied with varied crosslinker concentrations and saccharide densities on the dendrimer surface.

Specific Aim 3: Exploit the therapeutic potential of an optimized siRNA delivery system in a cardiac ischemia-reperfusion model

We hypothesized that the suppression of AT1R by RNAi would prevent Ang II activation and preserve cardiac functions after MI injury. We developed several tadpole-shaped dendrimeric materials for siRNA delivery with different CPP modifications and screened out a potent material that showed the strongest performance *in vitro*. The selected tadpole dendrimer was used to delivery siRNA against AT1R intramyocardially in a rat ischemia-reperfusion model. Gene expression levels of AT1R and relative genes in cardiac tissue as well as cardiac functions, with or without siRNA delivery, were examined

and compared after the treatment.

Successful completion of the dissertation would lead to novel non-viral siRNA delivery systems for gene therapy, such as for cardiovascular diseases.

1.4 Background

1.4.1 RNAi mechanism and RNAi therapeutics

RNAi mechanism

Since Andrew Fire and Craig Mello revealed the mechanism of RNAi, it has been extensively employed in basic investigations of gene functions and regulations of gene expression levels with engineering or therapeutic purposes. Two main pathways have been identified in the RNAi mechanism, the siRNA pathway and microRNA pathway.

siRNA molecules have completely complementary duplex structures, normally 19-23 nt in the length with 2 nt overhangs at 3' terminals. siRNA can be produced from long double-stranded RNAs (dsRNAs) by a endoribonuclease Dicer or be introduced exogenously into cytoplasm, and then a protein complex named as RNA Induced Silencing Complex (RISC) incorporates siRNA and activates it by discarding its sense strand. The remaining anti-sense strand guides the RISC to recognize the homologous mRNA, and a local double-stranded structure forms after the base-pairing. An endonuclease in RISC cleaves the double-strand part, leading to the degradation of the specific mRNA. Moreover, the existence of RNA dependent RNA Polymerase (RdRP) further amplifies the amount of small RNA molecules after RNAi initiation. RdRP extends the double-stranded structure of mRNA using the anti-sense strand of siRNA as the primer and the mRNA as the template, and endonucleases cleave the formed double strands into small fragments with similar

structures as siRNAs, which can trigger more RNAi processes. As a result, the RdRP mechanism makes the gene silencing effect even more efficient and sustaining.

The other important pathway is driven by microRNA. microRNA pathway shares the similar mechanism and cellular machineries of siRNA pathway with 3 major differences. First, a mature microRNA is produced from pre-microRNA endogenously via post-transcriptional modifications with P-bodies involved, so the origin of microRNA molecules and initial process of microRNA pathway are different from the siRNA pathway. Second, microRNAs have mismatched parts in their duplexes, presenting like a loop in the center, not completely complementary in the sequences, which leads to the third difference regarding the silencing mechanism. In microRNA pathway, if the leading strand of microRNA is completely complementary to the mRNA, the mRNA will be cleaved and degraded as the siRNA pathway, otherwise the mRNA will be prevented from being translated. In both pathways, the small RNA molecules are the triggers for gene silencing, so the delivery of siRNAs or microRNA mimics to target organs holds promises in treating diseases caused by gene expression disorders.

RNAi therapeutics

Compared to traditional drugs, small RNA molecules, which initiate RNAi in the cytoplasm, have great potentials due to the sequence specificity and ease of design and synthesis. In addition, the RNAi mechanism regulates the targets at the gene expression level instead of simply blocking a receptor or a pathway, which may avoid the risk of causing deficiency or dysfunction in endogenous feedback loops.

Despite all the advantages of RNAi therapeutics, its clinical use has not been fully exploited, because unmodified RNA molecules cannot readily enter cells and are

vulnerable to degradation by RNases. Since Elbashir et al. demonstrated the usage of siRNA duplexes [7], the research focusing on how to deliver siRNA efficiently and controllably has never stopped, but few met the high standard for gene drugs in safety and efficacy. To date, more than 30 clinical trials involving 21 different siRNA or shRNA drugs are in process, targeting 14 diseases, such as HIV/AIDS, cancer/tumor, kidney injury, age-related macular edema (AMD), diabetic macular edema (DME), non-arteritic ischemic optic neuropathy (NAION), familial adenomatous polyposis, etc. Most therapeutic RNA molecules were applied naked or via viral vectors, while 8 trials are using synthetic carriers to deliver RNA molecules via intravenous administrations [14]. Among them six are dependent on liposomes or lipid vehicles [15-17], one is based on cyclodextrin nanoparticles [18], and one employs a degradable polymeric matrix. Though the clinical studies are showing positive results, the development of RNAi therapeutics still stays in an early stage, and the published gene silencing effects, around 20% reduction in gene expression, were not as high as detected *in vitro* [15]. Therefore, new delivery systems for RNAi therapeutics need to be developed to achieve better efficiency and broader applications *in vivo*.

siRNA and microRNA share similar structures as well as similar deficiencies in the delivery process, such as difficulties in overcoming biological barriers and having a short half-life. As the design for siRNA sequence is easy and the target gene is clear and selectable, the development of delivery systems for siRNA set off earlier than that of microRNA. However, with the recent revealing discoveries of functional microRNAs, particularly the ones relating to stem cell differentiation and myocardial regeneration, the microRNA delivery is also gaining increasing attentions [19-21]. Due to their similarities,

it's likely to expand the use of siRNA delivery systems to microRNA, and vice versa.

1.4.2 Synthetic carriers in siRNA delivery

Polymers in siRNA delivery

Polymeric materials, particularly cationic polymers, have been regarded as valuable players in siRNA delivery. Compared to large and flexible DNA plasmids, siRNA molecules are smaller, more rigid, and more sensitive in sequence regarding their affinity to cationic materials [22]. All of these make siRNA harder to be condensed into stable particles and hence require stronger interactions to achieve that goal. Upon such requirements, polymers serve as competent candidates. By changing the structure and the number of repeating units, the molecular weight and characteristics of polymers can be finely adjusted. Large molecule materials are suitable to complex siRNA molecules into nano- or micro-particles through electrostatic interactions and neutralize the anionic charges of the phosphate backbone, enhancing the translocation of siRNA across cell membranes. By forming particles with cationic polymers, siRNA not only becomes more resistant to nuclease digestion but also gains a longer half-life in circulation, especially when some stabilizing polymers are introduced into the vehicles, such as poly(ethylene glycol) (PEG). Meanwhile, polymers also may serve as the scaffold to allow the decoration of other segments with additional functions so as to become “intelligent”, like ligands for endosomal escape, ligands recognizing specific receptors or cells, pH sensitive elements, etc. Therefore, siRNA delivery systems derived from polymers are being exploited by an increasing number of research groups.

Though with great potentials, some basic questions about the acting mechanisms of

polymeric materials have rarely been studied in details. For instance, how the length or size of the polymers affects their performance, how the degradability determines polymers' properties, and how much improvement could be obtained with the modification of functional ligands. Being able to answer these questions will get us further understanding and better perspectives of polymeric delivery systems.

Besides, the toxicity issue of cationic polymers is another big concern. The cations, most likely primary amines, which are the main source of positive charges in polymers, have been found to cause membrane damage, apoptosis pathway activation, and medium depletion [23-26], finally leading to cell death. The toxicity of polymers associates with their molecular weights, as polymers like poly-L-lysine (PLL) [27], poly-L-arginine (PLR) [28], and polyethyleneimine (PEI) [29, 30] induced more severe damages when their molecular weights were high, likely due to the increased number and density of positive charges, whereas decreasing the size of polymers would compromise the efficiency. To find the right balance for cationic polymers between transfection efficiency and safety exhibits as a great challenge even today.

Dendrimers in siRNA delivery

Dendrimers constitute a category of radially-symmetric, highly branched macromolecules, with well-defined and mono-disperse structures. Typical dendrimers are composed of three components: the core, the interior branches, and peripheral groups (Figure 1.1). With a sophisticated design and the control of chemical synthesis, dendrimers of a certain generation can be obtained with a tunable number of peripheral groups. Most dendrimers used in gene delivery prefer primary amines as peripheries, like polyamido amine (PAMAM) and polypropylene imine (PPI), because the high-density positively

charged amines are capable of complexing siRNA directly with strong affinities, leading to the formation of tight polyelectrolyte particles. Also attributed to the chemical activities of amine groups, various functional ligands, including peptides, saccharides, aptamers, and drug molecules, can be selectively modified on the surface of dendrimers with controllable densities and topologies [13, 31-33].

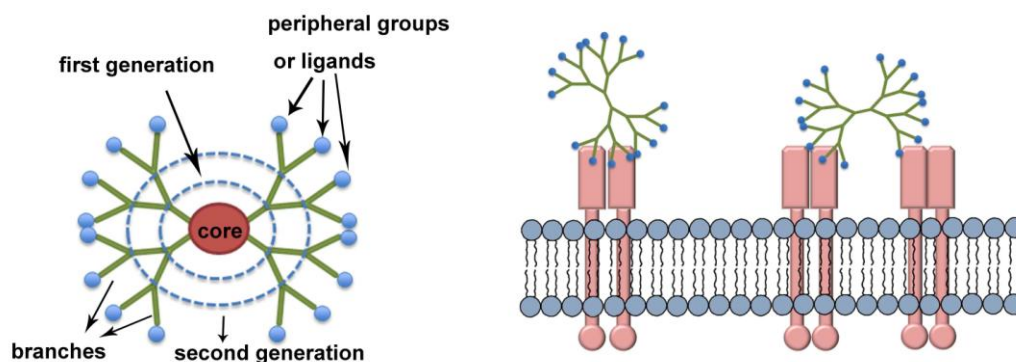


Figure 1.1 Scheme of a typical dendrimer. (a) Component and structure of a dendrimeric material; (b) bioactive dendrimers can interact with specific receptors on cell membranes with potential multivalent effects. Adapted from Liu (2012) [33].

The unique multivalent effect gained from high-density ligands on dendrimers can further amplify the interaction between ligands and their receptors or substrates, and the activities of multivalent ligands exhibit significant enhancements that cannot be gained only by the sum of individual bindings [34, 35]. An increasing number of studies are utilizing the multivalency to achieve enhanced cell binding, highly selective cell recognition, or increased internalization rate of glycodendrimers or peptide dendrimers [36-40].

A charitable nature of amine-derived dendrimers is the buffering capacity attributed to the secondary and tertiary amines inside the structures. These amines tend to capture protons from an acidic environment, so once endocytosized into endosomes — the intracellular acidic “cubicles” with a pH range from 4.5 to 6.5 — the buffering amines become protonated by binding protons inside endosomes. To replenish the losing protons, the symporters on endosome membranes begin to transport protons as well as chloridions into endosomes, and the increased concentration of chloridions triggers the inburst of water in order to balance the osmotic pressure. The series of events finally cause the over-swell of endosomes, and then endosomes break. Such mechanism can accomplish the special task of releasing siRNA cargoes into cytoplasm, as required by siRNA delivery systems.

Undoubtedly, dendrimeric materials are potent candidates for delivering gene cargoes, however, the commonly used cationic dendrimers always associate with toxicity issues, including cytotoxicity, hemolytic/haematological toxicity and *in vivo* toxicity [24, 41-44]. Therefore how to alleviate the toxic issue and whether dendrimeric materials are safe enough for therapeutic applications still remain unsolved.

Cell penetrating peptides in siRNA delivery

Cell penetrating peptides (CPPs) stand for a category of oligo peptides that are rich in basic amino acids, like arginine, lysine, and histidine, which are protonated in a physiological environment. CPPs are able to carry biomacromolecules to across cell membranes. The appearance of the arginine residue in CPPs is more frequent than other amino acids, and it is special because of the guanidine group on its side chain. Except the physiologically cationic characteristic, additionally the guanidine group can interact with the phosphate, sulfate, and carboxylate groups of proteoglycans on cell membranes and

stimulate intracellular signal pathways to change the cytoskeleton structure, resulting in macropinocytosis which internalizes extracellular cargoes into cells [45-47]. Thus, arginine-rich peptides, especially nonaarginine, have been regarded as important components in delivery systems for various types of cargoes. Some research groups used them as direct condensers of gene cargoes [48-53], while some groups modified independent delivery systems with arginine peptides to achieve enhanced internalization [54-59]. The previous results indicate that the smart utilization of CPPs may assist delivery systems to “jump over” some key obstacles in difficult areas, such as primary cells and stem cells.

Nevertheless, according to our previous results and other groups’ studies, nonaarginine alone failed to combine the rod-like siRNA tightly or ensure high gene silencing efficiency constantly [60], probably due to the dissociation of the polyelectrolyte particles during transfection. Similar problems may exist for other types of CPPs. As a result, how to use CPPs wisely and efficiently is an essential question to answer.

1.4.3 Cardiovascular diseases and RAAS

Cardiovascular diseases and Angiotensin II

Cardiovascular disease (CVD) is the leading cause of death over the world. According to the statistics from World Health Organization (WHO), nearly 17.3 million people died from CVDs in 2008, and without interventions the number will increase to 23.3 annually by the year of 2030. Over 80% of deaths due to CVDs happen in low- and middle-income countries, implying a severe situation for us.

Myocardial infarction (MI) is one of the fatal single diseases usually caused by the

occlusion of coronary arteries due to floating atherosclerotic plaques. The blockades in blood vessels interrupt the supply of oxygen and nutrients immediately, and, if the blockades can't be removed within 15 minutes, the cells in the infarct zone will begin to die and release chemotactic factors, recruiting inflammatory cells into the ischemic zone, followed by acute inflammation and chronic inflammation [61]. In the phase of acute inflammation, macrophages and neutrophils show up and activate the reactive oxygen system (ROS). In the phase of chronic inflammation, fibroblasts start to replace dead cardiomyocytes and form scar tissue in the ischemic area, causing loss of contractility. Eventually, ventricles undergo dilation, the ventricle wall becomes thinner, and finally heart failure turns to be unavoidable. Consequently, patients that survive the initial insult, characterized by regional loss of tissue and function have a high probability of developing heart failure in subsequent years. With the rising global numbers of CVDs, new treatments are greatly needed.

Down to the molecular mechanism, CVDs are controlled and influenced by numerous factors in the “cardiovascular continuum” [62, 63]. One important hormone system involved is the Renin-Angiotensin-Aldosterone System (RAAS), which controls the blood pressure and the fluid balance in the body. The activation of RAAS following ischemic injury initially promotes the recovery of blood pressure, but its continuous stimulation causes vasoconstriction, vascular and cardiac hypertrophy, and fibrosis [64]. Angiotensin II (Ang II), an octa-peptide hormone, which is the end-product of the RAAS, regulates most effects of RAAS [65]. Its overexpression following ischemic injury leads to cardiomyocyte death and hypertrophy, vascular smooth muscle growth, and fibrosis, all of which cause adverse cardiac remodeling, progressive ventricular dysfunction, and finally

heart failure [66]. Therefore, the inhibition of Ang II activation has become a common target for CVD therapy [67].

Ang II receptors

Four plasma membrane receptors have been identified for Ang II, termed as Angiotensin type 1 receptor (AT1R), AT2R, AT3R, and AT4R. Most typical adverse effects of Ang II are mediated via AT1R, including vasoconstriction, sodium retention, aldosterone secretion, fibrosis, cellular proliferation, superoxide formation, inflammation, and thrombosis [62, 66]. AT2R is another important receptor of Ang II, but oppositely it is mostly considered as a protective receptor, triggering vasodilation and anti-proliferation effects. In adult hearts, the large amount of AT1R plays a dominant role in cardiac tissue [68, 69], and its RNA and protein levels further elevate to 2-3 folds after myocardial infarction [68, 70], causing vasoconstriction, increased cardiac contractility, myocyte hypertrophy, myocyte apoptosis, fibroblast proliferation, and fibrosis. This series of events finally lead to progressive ventricle dysfunction and heart failure. To prevent AT1R activation, chemical blockers for AT1R, including candesartan, eprosartan, irbesartan, losartan, olmesartan and telmisartan, have been studied in laboratories and in clinical trials as a treatment following MI and gained function improvement compared to control groups [71-76], and the blockade of AT1R could result in up-regulation of AT2R [22, 77], which is also beneficial for function preservation [78, 79]. However, it requires continuous treatments and sometimes results in minimal reduction in the long-term mortality.

1.4.4 Delivery systems in cardiac tissue

A series of events proceed in heart following the ischemic injury, including CM

death, infiltration of immune cells, degradation of extracellular matrix (ECM), wall thinning, scar formation, eventually left ventricle remodeling and heart failure. With the identification of numerous active factors in the disease development, the direct regulation of the amount or the activity of these genes or proteins through the delivery strategy in cardiac tissue has become an attracting solution. By 2006, this area was dominated by viral vectors, but now an increasing number of non-viral delivery systems have shown their potentials.

Delivery systems realizing the basic requirements

The nature of cargoes determines the basic requirements for the delivery system. The instability against nucleases is one of the major concerns for gene drugs, especially for small RNA molecules, which are more sensitive to enzyme degradation. The anionic phosphate backbone is another obstacle to be overcome, as the repulsive electrostatic interaction between the nucleic acids and cell membranes impedes the gene molecules to diffuse freely into cells. In addition, the short lifetime of gene drugs (e.g. 5 min for siRNA molecules following intravenous injection) also demonstrates the need for a delivery system to improve the pharmacokinetic properties.

To achieve the requirements mentioned above, various types of delivery vehicles, mainly polymeric materials and liposomes, have been studied to compact or load gene cargoes into nano-scaled particles for the delivery in cardiac tissue. The particles protect the integrity of nucleic acids against nuclease and also optimize their pharmacokinetics by the alteration of size and surface properties. Reineke et al. designed a series of poly(glycoamidoamine) (PGAA) materials by incorporating a carbohydrate comonomer within a PEI-like backbone [80, 81]. All PGAAs showed minimal cytotoxicity, and the

tartarate-incorporated T4 glycopolymer complexed with NF- κ B oligodeoxynucleotide (ODN) decoys showed 87% penetration of myocardium in mouse hearts and nearly complete reduction in Cox-2, a well-known NF- κ B dependent gene in heart, with a dose of 10.0 μ g [82]. A facial amphipathic deoxycholic acid-modified PEI (1.8 kDa) (PEI1.8-DA) conjugate was synthesized by Kim et al. to deliver SHP-1 siRNA in a rat IR model [83], and the treatment decreased elevated SHP-1 expression to the normal level and significantly reduced the CM apoptosis and infarct size to 7.7% apoptosis index and 5.4%, respectively.

Unlike gene cargoes, protein cargoes, such as growth factors, demand delivery systems to maintain their activities and also effective concentrations at the site of action. The protein activity may be insulted chemically to the primary structure due to metabolisms (e.g. deamidation, oxidation, beta elimination, incorrect disulfide formation, and racemization) or physically to the secondary or higher structures (e.g. denaturation, aggregation, precipitation, and surface adsorption). Matrix-type particles are able to protect the encapsulated protein drugs against the external attacks, and meanwhile the protein cargoes can diffuse from the vehicles slowly to keep the drug concentration at a relatively high level at the administration spot. VEGF loaded PLGA particles [84] and PlGF-loaded chitosan-alginate nanoparticles [85] were applied through intramyocardial injections in rat MI models, and both studies showed improved cardiac functions and angiogenesis with increased ejection fraction values and vessel densities. Except the matrix-type vehicles, a degradable particle can also release the loaded protein gradually via surface erosion or bulk degradation. Davis et al. utilized degradable polyketal particles with encapsulated superoxide dismutase (SOD) in a rat IR model, and the treatment

increased the production of SOD in hearts and decreased the apoptosis of CMs to the same level as the sham group [86].

Micelles liposomes [87, 88], and silica particles [89-91] were also used as delivery systems in hearts. However, this category of delivery systems that only realized the basic demands are not the mainstream in cardiac applications, as the non-phagocytic CMs set up a high standard for the efficiency of delivery systems.

Delivery systems improving internalization efficiency

To improve the internalization efficiency in cardiac cells, the modification of additional components to the basic vehicles has become a common strategy. Cell penetrating peptide (CPP) is a major category of ligands in this usage, especially TAT and oligo-arginine (R9). The methods to incorporate CPPs into delivery vehicles are diverse, such as complexing with gene cargoes [92], conjugating to DNA or RNA molecules [93], modifying on the surface or scaffolds of liposomes or polymers, [94-96] and decorating on other complicated systems [97]. All the results showed that CPPs did enhance the internalization of delivery systems in CMs. However, CPPs promote the penetration through cell membranes with a non-specific manner, so the delivery systems could be uptake by other types of cells as well. For instance, it's possible that the delivery vehicles may be grabbed by macrophages that accumulate in cardiac tissue after ischemic injury.

To guide delivery systems into a certain type of cells, cell-type-specific ligands were incorporated into vehicles, including carbohydrates, peptides, proteins, etc. GlcNAc is a saccharide ligand specific to CMs screened out from a carbohydrate library, and its conjugation successfully delivered a liposome system and a polyketal system into CMs [98, 99]. As to peptide ligands, at least three candidates have been identified from phage display.

PCM is a ligand that targets to primary CMs [100], and Bull et al. used this peptide in their polymeric systems to deliver siRNA in CMs *in vitro* [93, 95, 101]. Molecules that can recognize the membrane proteins of CMs constitute another type of potential ligands. For example, PGE-2 conjugated siRNA was used in Bull's study to induce the receptor-mediated endocytosis in H9C2 cells [102]. Delivery systems guided by specific ligands do possess superior binding/internalization abilities in CMs compared to un-modified systems; however CPP-guided delivery systems still own the higher delivery efficiency in general. Consequently, the combination of the two types of ligands may become a useful method for developing delivery systems in cardiac tissue, which, in fact, has shown some synergic effects in transfecting CMs *in vitro* and *in vivo* [93, 95, 103, 104].

Delivery systems targeting cardiac tissue

Targeted delivery to the heart through a systemic administration is the ultimate objective of gene therapy in treating cardiovascular diseases. Three categories of strategies have been employed for this purpose so far, including passive targeting, facilitated targeting, and active targeting.

The phenomenon of passive targeting to the heart was claimed by Uskov et al. They observed an increased accumulation of silica nanoparticles with diameters of 6-13 nm in cardiac tissue after ischemic injury compared to normal cardiac tissue [89, 90]. It could pave a way for delivering drugs to damaged myocardium; however the mechanism beneath the cardiac accumulation has not been clarified, leaving the criteria to establish such delivery systems un-cleared. Size of the particles may matter, but how to identify the appropriate range needs to be figured, since another study reported that liposomes of 134nm had similar effects [88].

Facilitated targeting utilizes external sources to lead delivery systems reaching target sites. The ultrasound-targeted microbubble destruction (UTMD) is the most commonly used method in this area. The ultrasound energy is able to enhance the local vascular permeability and meanwhile destruct the gene- or protein-loaded microbubbles into pieces to release the cargoes on site. The delivery efficiency is dependent on time and ultrasound energy. Although quite a few studies have proven the efficacy of UTMD in animal models of MI or IR [105-109], concerns still exist regarding the transformation to human applications, such as the potential risk of tissue damage. Another method is to use the magnetic field to guide magnetic particle-incorporated systems moving to the heart. For instance, Ma et al. used magnetic nanobead/ adenoviral vector complexes to induce VEGF expression in rat hearts successfully with the facilitation of a magnetic field [110]. Compared to UTMD, this strategy avoids tissue damage and is easier to transform to human applications, yet it needs to be further developed to carry other categories of cargoes.

Active targeting involves targeting ligands specific to cardiac tissue, which can be conjugated to established delivery systems. Ideally the targeting ligands recognize cardiac tissue by a specific interaction with certain receptors or markers in myocardium and promote the delivery vehicles to accumulate in the heart. To identify ligands targeted to myocardium, phage display is the common method, and at least three ligands have been screened out. One candidate, named as ischemic myocardium-targeted peptide (IMTP), was conjugated to a cystamine bisacrylamide-diamino hexane polymer with the modification of the R9 peptide (IMTP-CD-9R), and the intravenous injection of IMTP-CD-9R/HO-1 plasmid complexes induced high HO-1 expression in ischemic

injured left ventricle tissue, showing the targeting efficacy of IMTP [103]. Instead of peptides screened from phage display, Kohane et al. used an Ang II sequence on liposome vehicles to recognize the Ang II receptors on cardiac cells, which has an increased expression level after ischemic injury in the heart [111]. Their results showed that the Ang II sequence caused a higher accumulation of liposomes in cardiac cells than the scrambled sequence, but no comparison between different organs was given. The risk of Ang II activation by the peptide sequence is another concern for the safety.

In summary, some efficient delivery systems have been reported for cardiac tissue, but mostly for proteins and plasmids. Safe and efficient delivery systems for small RNA molecules are still needed, as their physical and chemical natures make the task even more difficult.

CHAPTER 2

DEVELOPMENT OF A DEGRADABLE CATIONIC POLYMER TO SILENCE GENE EXPRESSION IN VITRO

2.1 Introduction

It is generally accepted that polymeric materials are superior to small molecule materials when it comes to constructing gene delivery systems, and in fact polymeric materials have been widely used in gene delivery for cancer cells, cell lines, primary cells, and stem cells. Though with great potentials, mechanisms underlying polymers' strengths were not studied thoroughly. Sometimes a subtle variation could cause a significant change on polymers' properties. It is important to identify the factors that matter to the transfection performance and figure out how to optimize the delivery systems. In this chapter, peptide polymers constructed from CPPs were studied as examples.

CPPs have shown their potentials in improving the cell internalization of their carried cargoes in various types of cells. The most representative CPPs include TAT, a peptide sequence of Trans-Activator of Transcription in HIV gene, and nonaarginine, termed as R9. Both TAT and R9 are rich in the arginine residue. Once arginine-rich peptides approach cells, the guanidine groups of arginine residues interact with proteoglycans on cell membranes and stimulate intracellular pathways that cause cytoskeleton rearrangements and finally induce macropinocytosis [45-47], resulting in effective cell membrane penetration [112-114]. However, according to our previous results, commonly used nonaarginine failed to deliver siRNA effectively and constantly [60]. One

possible reason is that the interaction between the short peptide and siRNA molecules is not strong enough, as siRNA has a rod-like structure that can hardly be condensed into tight particles, and the particles formed from siRNA and nonaarginine peptides are likely to dissociate during the transfection, leaving siRNA naked again. Since the short peptides don't have strong affinities with siRNA, polymerized peptides may address the issue by providing more siRNA-binding sites.

To overcome the drawbacks of the short peptides, polymerized oligo-peptides have been developed and applied in gene delivery. Zhang et al. studied a mild oxidation reaction to form disulfide bonds among peptides with cysteine residues, providing a strategy to synthesize peptide polymers from peptide monomers of specific sequences [115]. Seymour group published a series of studies of peptide polymers composed of lysine, or histidine, or their mixture to deliver DNA or siRNA [116-118], using positively charged lysines to complex nucleic acids and using histidines to induce endosome escape. Manickam demonstrated the usage of a polymerized TAT polymer in delivering DNA plasmids in a melanoma cell line [119], and Won reported the study of polymeric nonaarginine peptides in siRNA delivery *in vivo* [120]. It is no doubt that the physical and chemical properties of siRNA-loaded particles would be affected by the polymeric structure of peptides, however, there were few studies focusing on the mechanism of the improved efficiency upon polymerization. The mechanism of their efficiency, especially compared to their monomers, hasn't been well exploited.

Another un-clarified mechanism is that whether the modification of functional ligands is able to improve the delivery efficiency of polymerized peptides, and how much the contribution from the ligands would be. Previous studies only established the method

of polymerizing oligo-peptides, but no further derivation from the peptide scaffolds was demonstrated. For example, few detailed information on how the ligand modification would affect the performance of polymerized peptides was reported, which in fact is one of the major strategies used in targeted delivery. Whether the peptide polymers are efficient enough in gene delivery and how much improvement could be gained from the ligand conjugation need to be figured out.

To address the unsolved issues, in this chapter we developed oligo-arginine based polymeric materials by polymerization with degradable linkages and modifications of a targeting ligand. Unlike the traditional methods of polymer synthesis by adding monomers at the terminal of intermediate products step by step, our materials were synthesized by monomer assemblies in a mild reaction environment, and the molecular weight was controlled by the reaction time. Using this method, it is easier to adjust the properties of the peptide polymer by altering the structure and composition of the monomer. In this study, we used the RGD short peptide as a targeting ligand to improve siRNA delivery efficiency in lung cancer cells and liver cancer cells.

2.2 Results

Synthesis of dPOA polymer

The scheme of synthesis of the degradable poly(oligo-arginine) (dPOA) polymer was illustrated in Figure 2.1. The molecular weight of dPOA ((CR9C)_n), determined by gel permeation chromatography (GPC), was about 140 KDa with a dispersive coefficient of 1.154. To assess the advantages of the peptide polymers toward the short peptide monomer, nonaarginine (R9) and a commercial product poly-L-arginine (PLR) (15- 70 KDa) were

used for comparison in experiments below. The other dPOA (CR9KC)_n was synthesized following the same method, and the molecular weight of the obtained (CR9KC)_n was around 58 KDa with a dispersive coefficient of 3.8. RGD ligands were conjugated to the exposed primary amines on (CR9KC)_n, and ¹H-NMR spectrum showed that about 15% of CR9KC monomers were modified with RGD ligands.

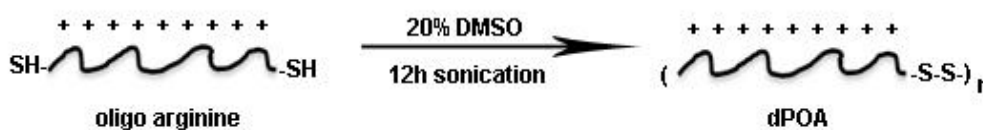


Figure 2.1 Scheme of the synthesis of dPOA. Monomers of CR9C were reacted via oxidative polymerization in 20% DMSO for 12 h with sonication.

Formation of siRNA- loaded arginine peptide particles

Gene Finder exclusive assay was employed for the detection of the formation of siRNA-loaded arginine peptide particles. The decline in the fluorescent intensity indicated to which degree siRNA was complexed by arginine peptides, as only the dye molecules combined with free nucleic acids give strong signals, and the dye molecules would be discarded from siRNA after complexation. With the N/P ratios increased from 3 to 20, the fluorescent intensity of the samples of siRNA-loaded particles dropped quickly till reached a plateau (Figure 2.2), showing arginine peptides' capability of combining siRNA. At N/P =10, 53% of siRNA still remained un-loaded in the R9 group, while only around 20% of free siRNA existed in arginine polymer groups. Among the three peptide materials, dPOA and PLR showed stronger capabilities in complexing siRNA than R9, which indicated that

polymeric peptides own higher siRNA loading efficiencies than the oligo peptide when the same dose of siRNA needs to be applied.

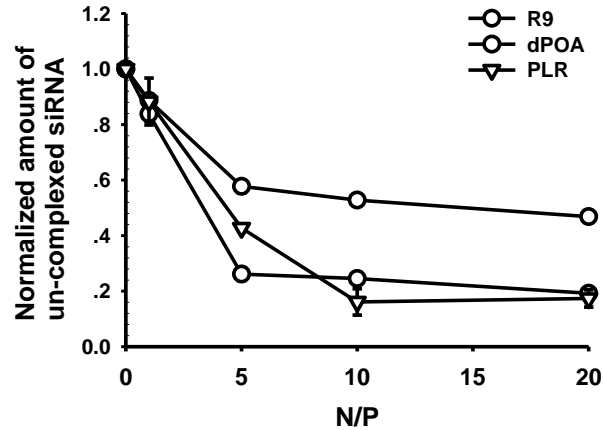


Figure 2.2 siRNA loading capacity of arginine peptides assessed by fluorescent dye exclusive assay. The amount of free siRNA decreased with increasing N/P ratios, indicating the formation of siRNA-loaded arginine peptide particles. Values are mean \pm SEM after normalizing fluorescent intensities of samples to that of a cation-free siRNA solution. $n=3$

Particle size and zeta-potential

Particle sizes and zeta-potentials were determined for siRNA-loaded arginine peptide particles. While R9 failed to form stable particles with siRNA at the low N/P ratios, as they were undetectable by light scattering, the diameters of dPOA/siRNA particles were 208.4 ± 4.8 nm and 190.0 ± 2.6 nm at N/P ratios of 3 and 5, respectively. On the other hand, when arginine peptides were mixed with siRNA under the same N/P ratios, the zeta-potentials of R9/siRNA particles varied from -4.4 to +2.3 mV among triplicates, while dPOA/siRNA particles showed higher and relatively consistent zeta-potentials of around +7mV (Figure 2.3).

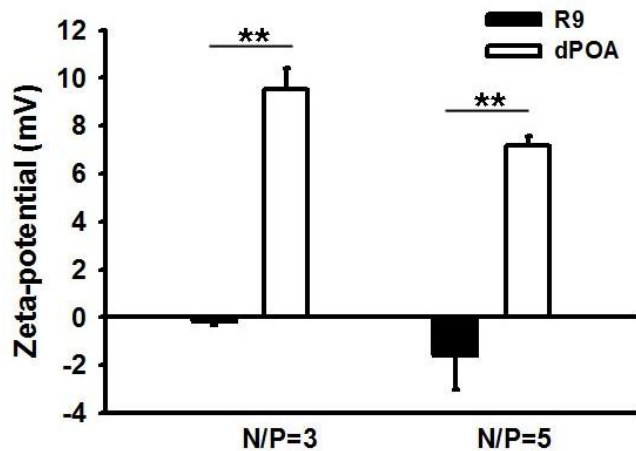


Figure 2.3 Zeta-potentials of R9/siRNA and dPOA/siRNA complexes at N/P=3 and N/P=5. The Zeta-potentials of dPOA/siRNA complexes were significantly higher than those of R9/siRNA at the same N/P ratios. Values are mean \pm SEM. $n=3$. ** $P<0.01$ by student test (t-test).

siRNA stability against RNase treatment

To evaluate arginine peptides' abilities of protecting siRNA, siRNA-loaded arginine peptide particles were treated with RNase at 37 °C for 30 min until naked siRNA was completely degraded. siRNA was released from the particles by polyacrylic acid (PAA), a polyanionic reagent capable of competing with siRNA in combining cationic materials, and escaped siRNA was detected by gel electrophoresis to assess the integrity. It was found that the siRNA loaded with R9 completely disappeared, while the siRNA loaded with dPOA and PLR was still detectable (Figure 2.4), indicating that the polymeric structure is able to enhance the interaction between siRNA and peptides and further increase the stability of siRNA-loaded particles.

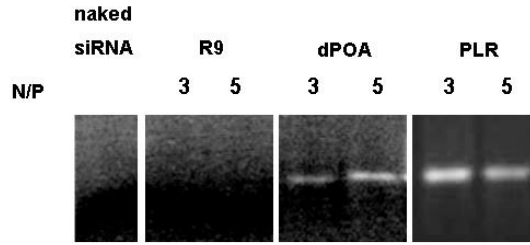


Figure 2.4 Nuclease resistance of siRNA-loaded arginine peptide particles. siRNA-loaded particles at N/P ratios of 3 and 5 were treated with RNase until naked siRNA was degraded completely. The integrity of released siRNA was detected by electrophoresis. siRNA bands only showed in dPOA and PLR groups. Samples were analyzed in 3.5% agarose gel.

GSH treatment

To determine the capability of arginine peptides of releasing siRNA in cytoplasm, dPOA/siRNA and PLR/siRNA particles were treated by glutathione (GSH) for 30 min at 37 °C, and the released siRNA was detected and compared by gel electrophoresis. The gel showed that siRNA was released quickly from dPOA particles, especially at low N/P ratios, as clear siRNA bands were detected after GSH treatment, but no siRNA was observed released from the particles made from the unreducible PLR (Figure 2.5).

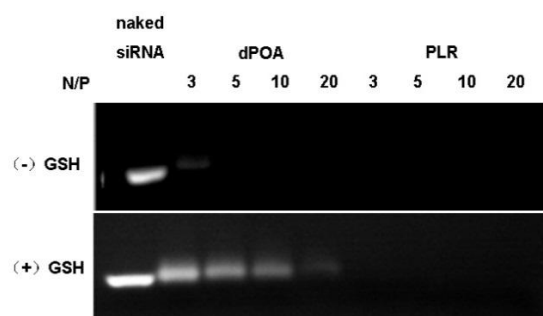


Figure 2.5 GSH treatment for dPOA/siRNA and PLR/siRNA complexes. (a) Before GSH treatment, siRNA were loaded completely by dPOA or PLR at various N/P ratios. (b) After treated with GSH for 30 min, siRNA bands were observed in the dPOA/siRNA group but not in the PLR/siRNA group.

Cytotoxicity

The cytotoxicity of arginine peptides was determined by MTS assay after 6 h incubation. Significant cytotoxicity was observed for the unreducible PLR at the concentrations above 10 $\mu\text{g/ml}$, while R9 and dPOA had minimal effects to the cell viability within the tested concentration range (Figure 2.6), and all groups maintained cell viabilities above 80%.

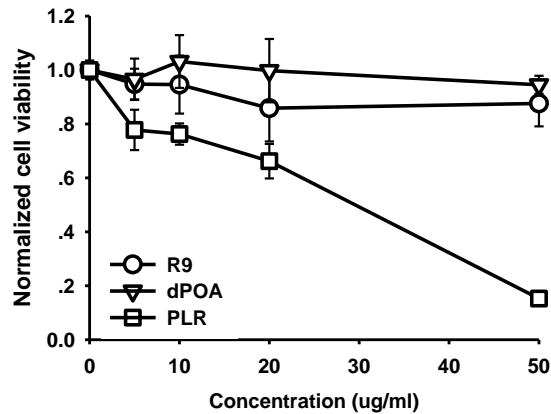


Figure 2.6 Cytotoxicity of arginine peptides. PLR exhibited a significant concentration-dependent cytotoxicity in the tested concentration range, while dPOA and R9 showed minimal effects to the cell viability. Values are mean \pm SEM. $n=3$.

Fluorescence microscopy and flow cytometry analysis

To observe the siRNA distribution and internalization efficacy, cy3-labeled siRNA was complexed with R9 and dPOA, respectively, and incubated with A549-luci cells for 6 h, followed by fluorescence microscopy observation and flow cytometry analysis. Cells treated with dPOA/siRNA particles showed stronger fluorescent signals than those with R9/siRNA particles (Figure 2.7a). 51.6% and 83.7% of cells treated with dPOA/cy3-siRNA were tested fluorescent positive by flow cytometry at N/P ratios of 3 and 5, respectively, while the percentages in R9 group were 7.49% and 25.0% (Figure 2.7b), which corresponded with our observation under fluorescence microscopy.

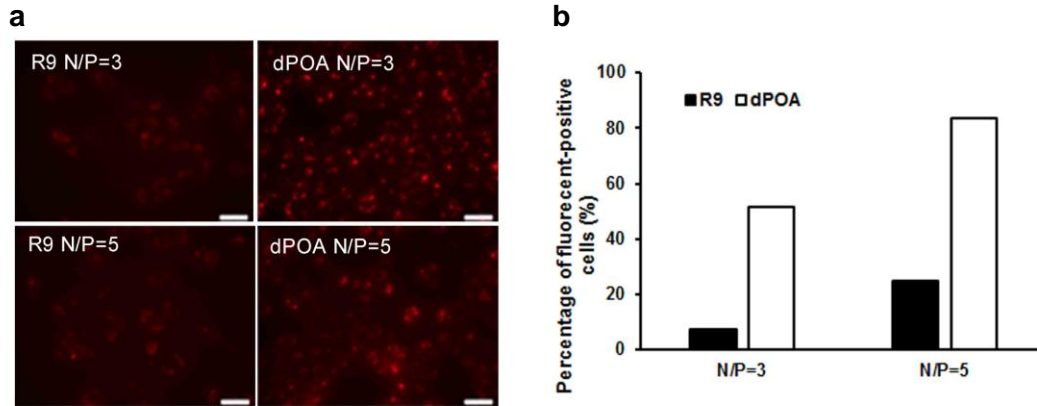


Figure 2.7 Fluorescence microscopy observation and flow cytometry analysis of cy3-siRNA loaded particles. (a) Cy3-labeled siRNA (red) was delivered to A549 cells by R9 and dPOA, respectively, at N/P=3 and 5. (b) Quantization of fluorescent cells by flow cytometry. In both results, dPOA/siRNA group showed stronger intracellular fluorescent intensities than R9/siRNA group.

siRNA delivery efficiency of dPOA and RGD-g-dPOA

At a siRNA concentration of 100 nM, dPOA/siRNA particles tended to induce stronger gene silencing effects in A549-luci cells than R9/siRNA particles at 24, 48, and 72 h after transfection, but not to a significant degree. To further enhance the delivery efficiency of dPOA, a short peptide ligand RGD was conjugated to the synthesized (CR9KC)_n to a conjugation level of 15%, termed as RGD-g-dPOA. Both (CR9KC)_n dPOA and RGD-g-dPOA showed no significant cytotoxicity to cells (Figure 2.8) with cell viabilities above 90% at all tested concentrations.

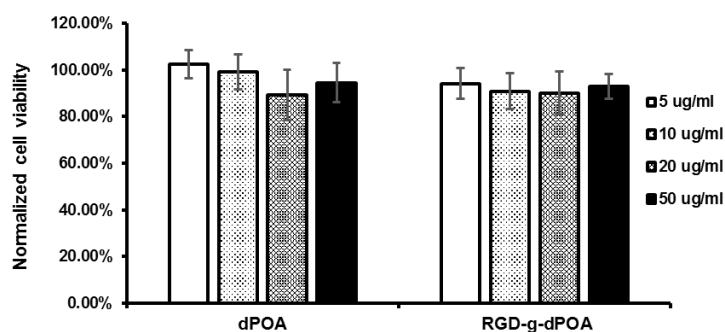


Figure 2.8 Cell viability upon the treatment of dPOA and RGD-g-dPOA. Both peptide polymers showed minimal cytotoxicity to A549 cells with cell viabilities above 90%. Values are mean \pm SEM. $n=3$

In A549-luci cells, RGD-g-dPOA/siRNA particles decreased the luciferase expression levels to $65.4 \pm 3.3\%$, $54.4 \pm 2.8\%$, $48.5 \pm 3.5\%$, and $42.9 \pm 2.0\%$ at N/P ratios of 10, 20, 30, and 40, which were $76.6 \pm 8.5\%$, $79.3 \pm 2.1\%$, $71.8 \pm 12.3\%$, and $56.2 \pm 8.6\%$ in the dPOA/siRNA treatment groups (Figure 2.9a). There was a significant difference at the N/P ratio of 20 ($P<0.01$). In HepG2 cells, the luciferase expression levels were $118.6 \pm 15.8\%$, $64.2 \pm 9.6\%$, $60.9 \pm 7.4\%$, and $55.3 \pm 11.6\%$ at N/P ratios of 10, 20, 30, and 40, respectively, upon RGD-g-dPOA/siRNA treatment, and at N/P ratios of 30 ($P<0.05$) and 40 ($P<0.01$) the expression levels were significantly lower than those with dPOA/siRNA particles (Figure 2.9b).

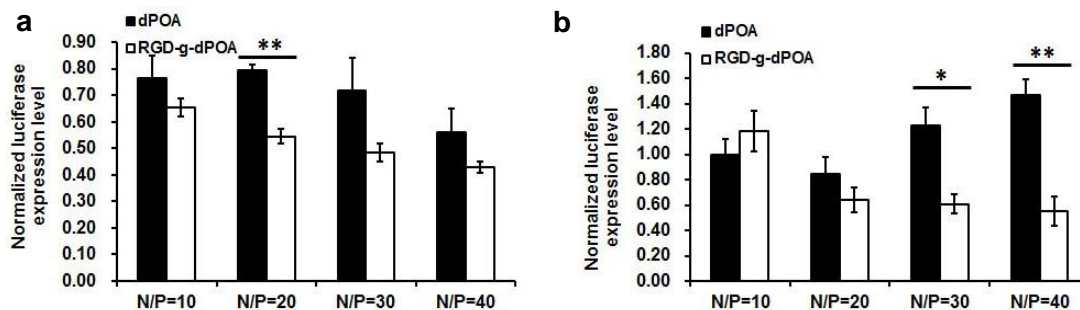


Figure 2.9 Gene silencing efficiency of siRNA-loaded dPOA particles and siRNA-loaded RGD-d-dPOA particles in A549-luci (a) and HepG2 (b) cells. Values are mean \pm SEM after normalizing to the luciferase expression level of the untreated control. In most transfection groups, siRNA-loaded RGD-g-dPOA particles tended to induce higher gene silencing effects against luciferase than the siRNA-loaded dPOA particles. The difference reached statistical significances at N/P=20 in A549-luci cells and N/P=30 and 40 in HepG2 cells. $n=3\sim 4$. * $P<0.05$, ** $P<0.01$ by student test (t-test) between dPOA group and RGD-g-dPOA group.

2.3 Discussion

Arginine rich peptides have been widely used in delivering various types of cargoes, including proteins, plasmids, oligonucleotides, liposomes, etc [121, 122]. In siRNA delivery, some groups used arginine peptides or their derivations to directly combine siRNA for delivery, such as nonaarginine [50], stearylated octaarginine [48], targeting ligand conjugated nonaarginine [49, 52, 53], pentadecaarginine [52], and poly-L-arginine [51]. Though with some positive results, particles formed from the oligo-arginine peptide and siRNA are usually not stable enough against the serum and nucleases, which was also verified by our results, as the electrostatic interaction between these two small molecules is hardly strong. In this study, we used an oxidative polycondensation method to synthesize polymeric arginine peptides, allowing stronger interactions with siRNA. Polymeric peptides were able to complex siRNA at a minimal N/P ratio down to 3, which reduced the

required amount of delivery materials for a given dose of siRNA. Lowering dosage is very important for the real clinical usage, regarding the economic cost, manufacture technology, and patient tolerance. The zeta-potential data also showed the significant distinction between R9 and dPOA materials. The consistency of zeta-potentials of dPOA/siRNA triplicates indicated the better homogeneousness among particles than R9/siRNA, and meanwhile the higher values of zeta-potentials implied dPOA/siRNA particles presented more positive charges on the particle surface at the same N/P ratio. Accordingly, the high positive surface potential enhanced cell uptake by non-specific interactions with cell membranes, resulting in the better performance of dPOA in delivering siRNA than the oligo-arginine peptide.

To further improve the transfection efficiency of dPOA, we conjugated the RGD peptide to the dPOA backbone. RGD is a bioactive ligand that can bind to 11 types of integrins on cell membranes, so it has been widely used for improving the efficacy of delivery systems [123-125]. In our study, the RGD ligation enhanced gene silencing effects both in the lung cancer cell line and liver cancer cell line, especially at high N/P ratios. Higher N/P ratios mean the number of RGD ligands in a particle is more than that at low N/P ratios. This may be a sign implying that a certain density of ligands is needed to fully realize the ligand function. Here dPOA provided a platform for the ligand modification, and a tunable modification of ligands could be achieved by adjusting the ratio between ligands and dPOA. Various ligands could be modified on dPOA, including stabilizing ligands, targeting ligands, fusion ligands, and internalization-improving ligands, to make the design obtain comprehensive and optimized functions and properties.

The advantages of polymeric materials have been increasingly recognized recently,

but the problems on their safety issue haven't been solved. A considerable body of studies reported that the toxicity of cationic polymers or dendrimers is associated with their molecular weights and generations, such as PLL, PEI, and PAMAM. One strategy to reduce such cytotoxicity is the degradable design, and it has been applied to various cationic materials, such as PEI [126-130]. In our study, we used the disulfide bond, a reducible bond in the cytoplasmic environment, to link oligo-arginine peptides (with two cysteine terminals) to form a linear arginine peptide polymer. Compared to the unreducible commercial PLR peptide, dPOA showed a significantly lower cytotoxicity in A549 cells. It is worth noting that the influence of dPOA to cells was very similar to that of R9, which could be an indirect evidence for the degradability of dPOA in cytoplasm, and such degradability is the main reason of the decreased cytotoxicity of cationic polymers. Meanwhile, disulfide bonds also tended to increase the solubility of the polyarginine. In our experiments did commercial PLR tend to form visible precipitations in the phosphate buffer, and it was also reported to precipitate proteins in serum [112], but dPOA showed no similar drawback. Besides the lowered cytotoxicity and increased solubility, the cleavage of disulfide bonds in cytoplasm guaranteed the siRNA release from particles to initiate RNAi process. In fact, too condensed particles, like PLR/siRNA, do not benefit transfection.

As to the comparison of our study to other published data, R9 [50] and R15 [52] were reported to have the capability to deliver siRNA into mammalian cells, but in our study they failed to exhibit substantial functions in improving cell uptake and further gene silencing. One possible reason is that we used R9 at N/P ratios lower than the other groups did, and the formed particles may contain less siRNA, or the surface potentials were not

high enough to overcome the repulsive force from cell membranes. Another possible reason is due to the difference between cell lines. Wang et al. reported to use R9 in siRNA delivery to human gastric carcinoma cells but not A549 cells, although they evaluated the cytotoxicity of R9 in A549 cells. Kim's study pointed out that R9/siRNA particles didn't lead to significant gene silencing effects in 293T cells [60]. Probably different cell types have different preferences for endocytosized particles, such as their sizes and surface potentials, and such preferences may be the crucial factors in the non-specific endocytosis. For further improvements, the ligand-receptor mediated endocytosis could be used to promote cell internalization, by grafting receptor-specific ligands on the reducible arginine backbone, for instance. The reducible arginine peptide polymer has the potential to become an effective low-toxic non-viral delivery system in gene therapeutics.

CHAPTER 3

DEVELOPMENT OF A NEUTRAL CROSSLINKED DENDRIMERIC SYSTEM TO SILENCE GENE EXPRESSION IN VITRO

3.1 Introduction

Most investigations of non-viral siRNA delivery systems mainly focused on cationic carriers [131], such as polymers, lipids and peptides, the materials that can form siRNA-loaded vehicles based on electrostatic interactions under the physiological environment. Among the established cationic delivery systems, dendrimers are the shining stars. A typical dendrimer is composed of three components: the core, the branches, and the peripherals. Dendrimer molecules have tunable structures, as the number of branches and peripherals can be controlled by the growth of generations. Cationic dendrimers can have strong charge interactions with siRNA when the generation of dendrimers is relatively high with rich positive charges presented on the surface, and the high affinity prevents the particles from dissociation during transfection. Dendrimers also provide the sites for ligand modifications with high possibilities of inducing multivalent interactions, especially for saccharide ligands. This property endows dendrimeric materials a great power to target specific cells and enhance cell internalization. Another important advantage of dendrimers is the endosome escape ability due to the buffering amines at the joint points in the structure, which allows the siRNA release into cytoplasm. Consequently, the nature of cationic dendrimers is suitable for constructing siRNA delivery systems.

However, cationic dendrimers bear the similar inherent disadvantages as other cationic systems, possibly even worse due to the high-density charges on the surface. For one thing, cations on dendrimers such as the protonated primary amines easily cause toxicity, resulting from the membrane damage, apoptosis pathway activation, and medium depletion [23-26]. The toxicity of dendrimers is dependent on the generation and molecular weight, as the two parameters determine the number of primary amines on the dendrimer surface. Once the dendrimer surface is substituted with neutral or anionic groups, the toxicity decreases significantly [26, 132-134]. Also dissociation and deformation may happen for polyelectrolyte complexes, because the pure electrostatic interaction can hardly last for a long time, and the aggregation between the polyelectrolyte particles may also happen. For example, the size of polypropyleneimine (PPI)/siRNA was reported to change from 150 ± 22.2 nm to 612.7 ± 45.1 nm during the 48 h in PBS buffer [135], indicating that the particles went through structural changes. Possibly variations in the ionic strength and shear stress may further influence the properties and performance of polyelectrolyte vehicles [136-139]. In addition, since little knowledge has been obtained on how to control electrostatic interactions to maintain or terminate the integrity of polyelectrolyte particles, the timing of siRNA release from polyelectrolyte complexes is unpredictable and uncontrollable, which means the siRNA is possible to be released before reaching the cytoplasm.

In this chapter, we established a neutral crosslinked system which provides stability, safety and controllability for siRNA delivery. The basic idea is to utilize other components in the delivery system to replace the role of primary amines. Traditionally, primary amines are responsible for three tasks: binding siRNA, stabilizing particles, and

interacting with cell membranes. All of the three tasks relate with the charge property of primary amines. Since the pKa of tertiary amines is below 7.4, meaning that they could be protonated temporarily at a low pH environment, tertiary amines were used as the temporary source of positive charges and to load siRNA in this system. A crosslinking method was introduced into the system to stabilize the particles, and meanwhile the crosslinking bond was designed to be reversible at low pH, like the endosomal environment, to guarantee the controllable siRNA release. To enhance the interaction with cells and meanwhile reduce the endocytosis by unspecific cells, the neutral dendrimers were further modified with targeting ligands. This new rational created a low toxic, stable, and targeted delivery system for siRNA.

We used the commonly used cationic dendrimer polyamido amine (PAMAM) as a model molecule to test our idea. The primary amines on PAMAM surface were replaced by neutral crosslinkable hydrazide groups so as to produce the neutral dendrimer, and saccharide ligands were modified to improve the cell targeting. Saccharide ligands were chosen here because they are biocompatible, bioactive, and most importantly, they exert multivalent interactions with membrane receptors when modified on the dendrimer surface. Glutaraldehyde was selected to be the crosslinker, since the hydrazone bond formed by glutaraldehyde and hydrazide is reversible and cleavable in a certain condition, which could endow the system with degradability and the controlled release mechanism. Based on the crosslinking methodology, factors that control the properties of the crosslinked delivery systems were investigated in this part.

3.2 Results

Synthesis of neutral PAMAM-HYD and saccharide-modified PAMAM-HYD

To obtain saccharide-modified neutral dendrimers, G4.0 PAMAM was first expanded to G4.5 by reacting with methyl acrylate, and the G4.5 PAMAM was further modified with hydrazide groups on the surface. The obtained products with theoretically 128 hydrazide groups were termed as PAMAM-HYD. To add the cell targeting capacity, saccharide ligands were modified on PAMAM-HYD. The tested ligands included mannose, glucose, GlcNAc, lactose, galactose, and GalNAc. Figure 3.2 showed the structure of GalNAc-PAMAM-HYD as an example of the saccharide-modified PAMAM-HYD. All the saccharide-modified PAMAM-HYDs have reached the saturate modification levels from 45%- 52% as described in literature [40].

Identification of the targeting ligand for HepG2 cells

To study the interaction between neutral dendrimers and cells, different saccharide-modified PAMAM-HYDs were labeled with fluorescein and then incubated with HepG2 cells to understand the cell binding and cell uptaking properties. Figure 3.1 showed the results from flow cytometry measurements.

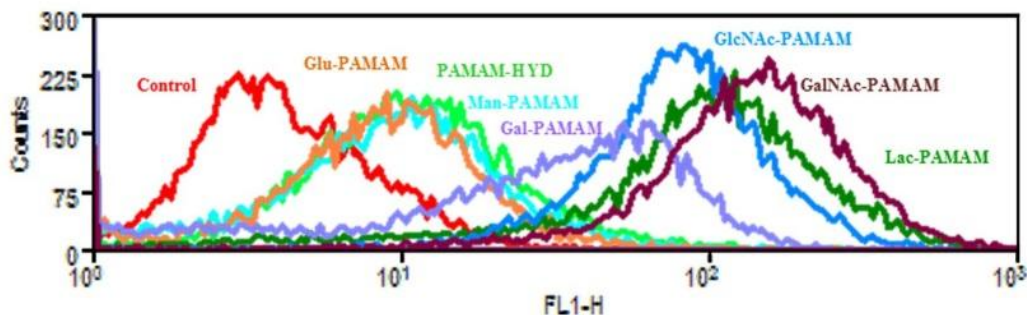


Figure 3.1 Flow cytometry analysis of binding and internalization efficiency of different saccharide-modified PAMAM-HYDs with HepG2 cells. Glu-, Man-, Gal-, GalNAc-, Lac- and GlcNAc-PAMAMs and PAMAM-HYD were labeled with fluorescein and treated with HepG2 cells. Gal, GlcNAc, Lac, and GalNAc showed their abilities to enhance the interaction between dendrimers and HepG2 cells, and GalNAc-PAMAM-HYD showed the strongest cell binding/internalization rate among all the materials.

Among the tested saccharide-modified dendrimers, Gal-, GalNAc-, Lac- and GlcNAc-PAMAM-HYD showed much stronger fluorescent signals in HepG2 cells than other dendrimer materials, indicating the high avidity of these saccharide molecules toward HepG2 cells. GalNAc-PAMAM-HYD showed the strongest fluorescent intensity on a per cell basis, and more than 99% of cells were detected fluorescent-positive. Therefore, GalNAc was identified as the most efficient targeting ligand to HepG2 cells, which accorded with literatures, and was used for the further material development.

Development of the neutral crosslinked system

Figure 3.2a illustrated the chemical structure of the saccharide-modified dendrimer GalNAc-PAMAM-HYD (GPH). By controlling the feed ratio of GalNAc to PAMAM-HYD in the modification reaction, GPHs with varied GalNAc modification levels were obtained. The average GalNAc modification levels were 11.8%, 18.4% and 31.5%, calculated from the H^1 -NMR analysis (Figure 3.2b), and the corresponding

dendrimers were named as GPH-15, GPH-23 and GPH-40, respectively, with the number indicative of the average number of GalNAc ligands on PAMAM-HYD scaffolds.

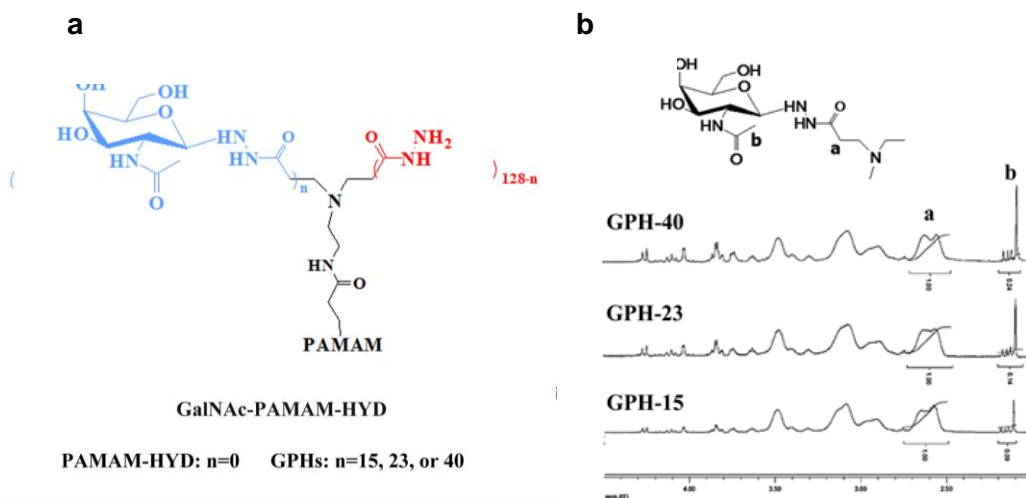


Figure 3.2 Structure of the neutral dendrimer of GalNAc-PAMAM-HYD (GPH) (a) and the ^1H -NMR spectrum of GPHs with varied GalNAc modifications (b). The peripheral amines were substituted with physiologically neutral hydrazide groups and bioactive GalNAc in GPHs. The average numbers of modified GalNAc in each GPH were calculated to be 15, 23, and 40, respectively, according to the ^1H -NMR results (δ 2.1 ($-\text{CH}_3\text{CONH}-$ of GalNAc moiety, 3H), δ 2.6 ($-\text{NCH}_2\text{CH}_2\text{CO}-$ of PAMAM-HYD scaffold, 504H)). Adapted with permission from Liu (2012) [185]. Copyright (2012) American Chemical Society.

A scheme for preparing siRNA-loaded crosslinked particles was shown in Figure 3.3. Since the hydrazide group has a pKa value below 7 [140-143], the PAMAM-HYD and GPHs are expected to be neutral at the physiological pH. On the other hand, as the pKa of tertiary amines was reported between 6 and 7 [144-146], the tertiary amines own the buffering capacity of absorbing protons under the acidic condition. This property allows PAMAM-HYD and GPHs to become internally cationic to bind siRNA within a

certain pH range, resulting in complexes that are crosslinkable to produce siRNA-loaded particles.

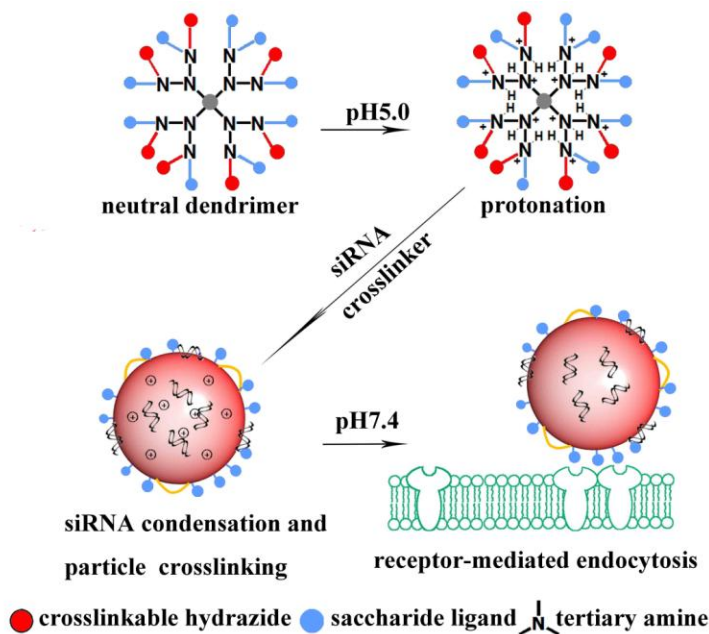


Figure 3.3 Schematic process of preparing siRNA loaded crosslinked particles for siRNA delivery. The whole process includes the mixing of siRNA and neutral dendrimers at pH 5.0, adding the crosslinker, blocking unreacted crosslinkers, recovering the pH to 7.4, and dialysis. Adapted with permission from Liu (2012) [185]. Copyright (2012) American Chemical Society.

Complexation of siRNA with PAMAM-HYD and GPHs at acidic and neutral conditions

To determine whether siRNA was complexed with PAMAM-HYD or GPHs via the internally charged tertiary amines as expected, the Gene Finder exclusive assay was conducted at both neutral and low pHs. At pH 5.0 the amount of free siRNA in solutions gradually decreased with the increasing amount of PAMAM-HYD or GPHs, and the original fluorescent intensity exerted from siRNA-bound Gene Finder decreased to below

10% when the molar ratio between dendrimers and siRNA (D/S) reached 3.5 (Figure 3.4). In addition, the GalNac modification didn't affect the step of siRNA combining with neutral dendrimers at pH 5.0, as the siRNA loading capacities of different GPHs showed no significant distinction. On the other hand, PAMAM-HYD and GPHs didn't cause siRNA complexation at pH 7.4 within the D/S ratios ranged from 0.5 to 3.5.

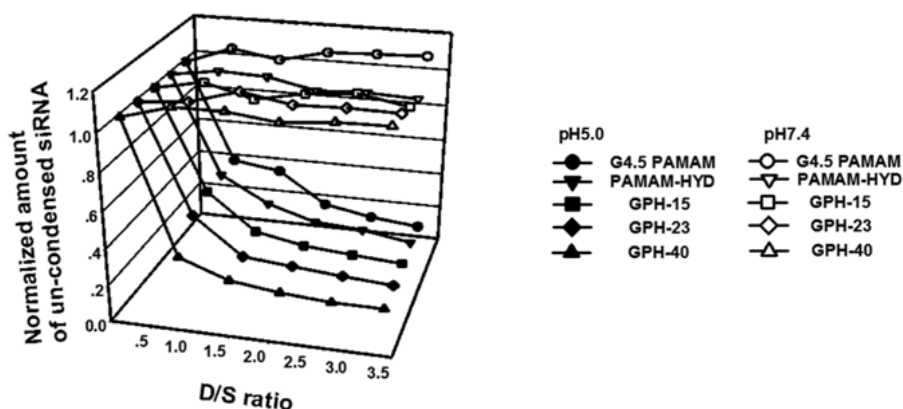


Figure 3.4 Complexation of siRNA with PAMAM-HYD and GPH dendrimers at pH 5.0 and pH 7.4. At pH 5.0, the amount of unloaded siRNA decreased with increasing amount of PAMAM-HYD or GPHs, while at pH7.4, the amount of unloaded siRNA didn't change at any ratio between dendrimers and siRNA. Adapted with permission from Liu (2012) [185]. Copyright (2012) American Chemical Society.

To clearly compare the charge properties at different pHs, zeta-potential measurements were conducted for the dendrimer-siRNA mixtures. The binary mixtures of dendrimers and siRNA possessed positive potentials at pH5.0, ranging from 12 to 15mV (Figure 3.5), while all mixtures had negative potentials when mixed at pH7.4.

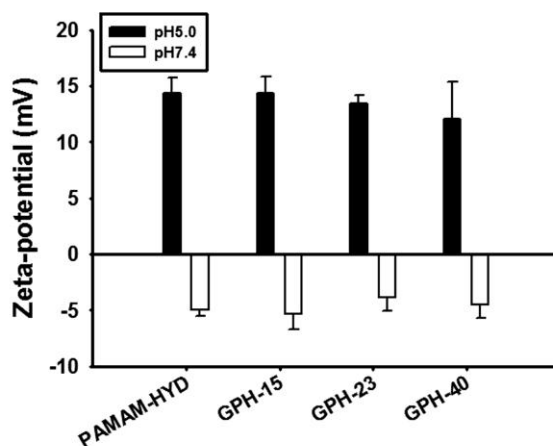


Figure 3.5 Zeta-potentials of dendrimer-siRNA mixtures. All the binary mixtures exhibited positive zeta-potentials above 10 mV at pH 5.0 but showed slightly negative zeta-potentials around -3 to -6 mV at pH 7.4. Values are presented as mean \pm SEM, $n=3$. Adapted with permission from Liu (2012) [185]. Copyright (2012) American Chemical Society.

Preparation of siRNA-loaded crosslinked particles

To construct siRNA-loaded crosslinked particles, glutaraldehyde was added into the mixture of PAMAM-HYD and siRNA at pH5.0 to immobilize the temporarily formed polyelectrolyte parties by establishing linkages between the hydrazide groups on the dendrimer surface. Theoretically, the siRNA and PAMAM-HYD would electrostatically assemble complexes first, followed by crosslinking via glutaraldehyde. Two methods were used simultaneously to terminate the crosslinking reaction: recovering the pH to the physiological condition via buffer exchange and blocking the unreacted glutaraldehyde residues by adding excessive ADHs. Gel electrophoresis was used to detect unloaded siRNA in the systems. When the D/S ratio was settled at 1.7, the amount of unloaded siRNA kept decreasing with increasing concentrations of glutaraldehyde, which means the crosslinking reaction was involved in siRNA encapsulation (Figure 3.6). In contrast,

unlike the situation at pH5.0, the siRNA bands remained visible in the gel after mixed with dendrimers and glutaraldehyde at pH 7.4 following the same protocol (Figure 3.6).

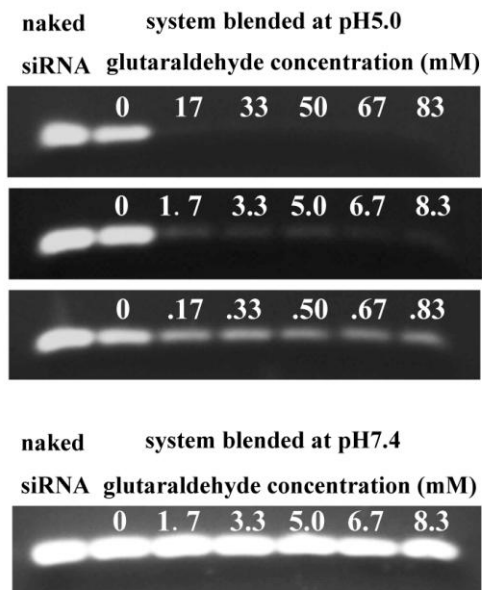


Figure 3.6 siRNA encapsulation efficiency in the crosslinked systems. The amount of encapsulated siRNA increased at pH 5.0 when the glutaraldehyde concentrations were rising in the range from 0.17 mM to 83 mM, but at pH 7.4 no significant siRNA encapsulation was observed in the gel electrophoresis. Adapted with permission from Liu (2012) [185]. Copyright (2012) American Chemical Society.

Similar experiments were conducted with the GalNAc-modified dendrimers so as to test if the method could be used to prepare siRNA-loaded particles after the ligand modification on neutral dendrimers. According to the experiment with Gene Finder, the average siRNA loading efficiencies of PAMAM-HYD and GPHs particles were calculated to be in the range from 79 % to 94 % (Figure 3.7). It showed that at a fixed molar ratio among siRNA, dendrimer, and crosslinker, the siRNA loading efficiency decreased with the increasing GalNAc modification, which is probably due to the

reduced accessibility of crosslinkable hydrazide groups on the dendrimer surface.

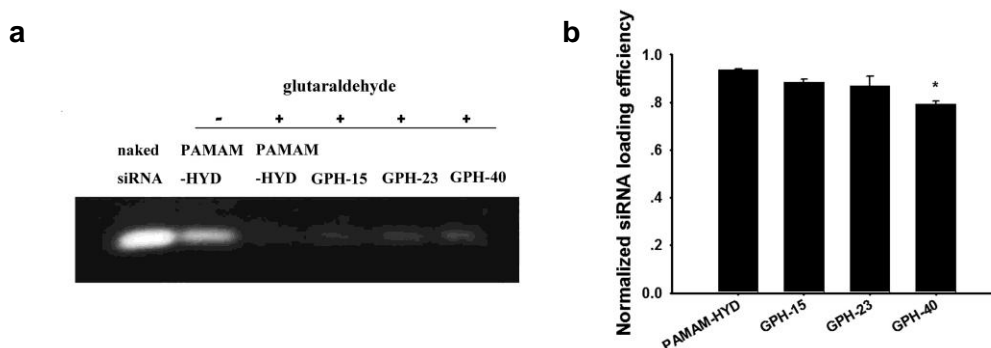


Figure 3.7 siRNA encapsulation efficiency in crosslinked particles made from GPHs with varied GalNAc modification levels. Slightly increasing amount of siRNA were left unloaded when the GalNAc modification levels increased, indicated by the gel electrophoresis (a). According to the quantitative examination by Gene Finder, the siRNA encapsulation efficiency in PAMAM-HYD, GPH-15, GPH-23, and GPH-40 particles were $93.6 \pm 0.3\%$, $88.4 \pm 1.4\%$, $87.0 \pm 3.8\%$, and $79.3 \pm 1.2\%$, respectively. Values are mean \pm SEM. $n=3$, $*P<0.05$, One-way ANOVA followed by the Newman-Keuls post-test. Adapted with permission from Liu (2012) [185]. Copyright (2012) American Chemical Society.

Size and zeta-potential characterization

The measurement of the size of different crosslinked particles could be helpful to understand how the particle diameters vary with the crosslinker concentration and the surface modification of the dendrimer carriers. Again we found the particle size was also dependent on both the crosslinker concentration and the ligand density. Figure 3.8 showed how the particle size changed with these two parameters. Both nano- and micro-scaled particles were obtained from the crosslinked PAMAM-HYD systems. The largest diameter was achieved up to $4.2 \mu\text{m}$ at a medial concentration of glutaraldehyde,

and the particle size declined to about 230 nm when the glutaraldehyde concentration was further increased. When the molar ratio between dendrimer, siRNA, and glutaraldehyde was fixed, the particle size decreased with the increasing GalNAc modification levels on the dendrimers, and the crosslinked GPH-23 and GPH-40 particles exhibited small sizes around 200 nm in the diameter (Figure 3.8b).

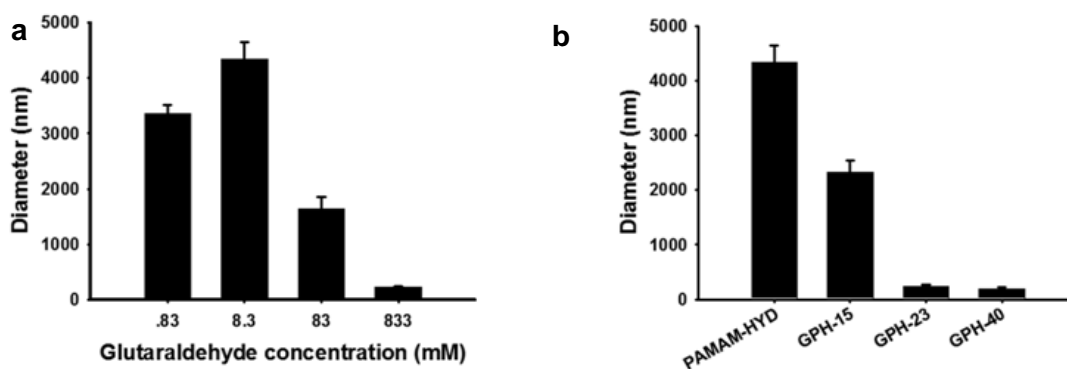


Figure 3.8 Sizes of the siRNA loaded crosslinked particles at varied glutaraldehyde concentrations (a) and GalNAc modification levels (b). Within the glutaraldehyde concentrations ranged from 0.83 mM to 833 mM, the particles reached a largest size of 4.2 μm at 8.3 mM and a smallest size of 230 nm at 833 mM. At the glutaraldehyde concentration of 8.3 mM, the particle size decreased with the increasing GalNAc modification level to around 200 nm in GPH-23 and GPH-40 particles. Adapted with permission from Liu (2012) [185]. Copyright (2012) American Chemical Society.

All the siRNA- loaded particles made from PAMAM-HYD and GPHs were neutral or slightly negatively charged within -3 mV at pH 7.4, detected in the zeta-potential measurement. In contrast, the polyelectrolyte particles made from cationic G5.0 PAMAM and siRNA showed a highly positive zeta-potential around 21 mV (Figure 3.9). Therefore, the siRNA-loaded crosslinked particles can be regarded as neutral vehicles in the physiological environment.

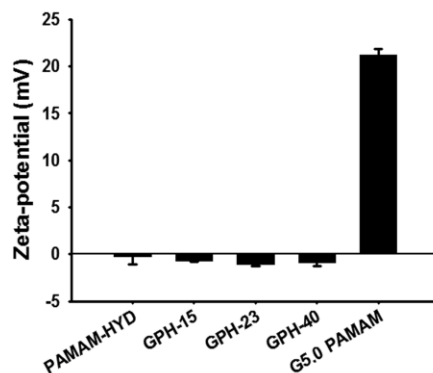


Figure 3.9 Zeta-potentials of siRNA-loaded crosslinked particles. All siRNA loaded crosslinked particles made from neutral dendrimers exhibited slightly negative zeta-potential in the range from 0 to -3 mV. In contrast, the siRNA loaded polyelectrolyte particles made from G5.0 PAMAM had a high positive zeta-potential of 21 mV. Adapted with permission from Liu (2012) [185]. Copyright (2012) American Chemical Society.

Stability of crosslinked particles in aqueous environment

To assess the stability of the crosslinked particles, sizes of the GPH particles were monitored for 24 h in PBS buffer after the particle formulation. At the time points of 4 h and 24 h, the sizes and distributions of GPH-23 particles and GPH-40 particles barely changed over the time (Figure 3.10). Taking the GPH-23 particle as an instance, the average radius decreased only slightly from 122 nm to 111 nm after 24 h incubation in PBS buffer. In contrast, the polyelectrolyte complexes formed by siRNA and cationic G5.0 PAMAM went through a significant change in the size and distribution, with average diameters collapsing from 386 nm to 124 nm.

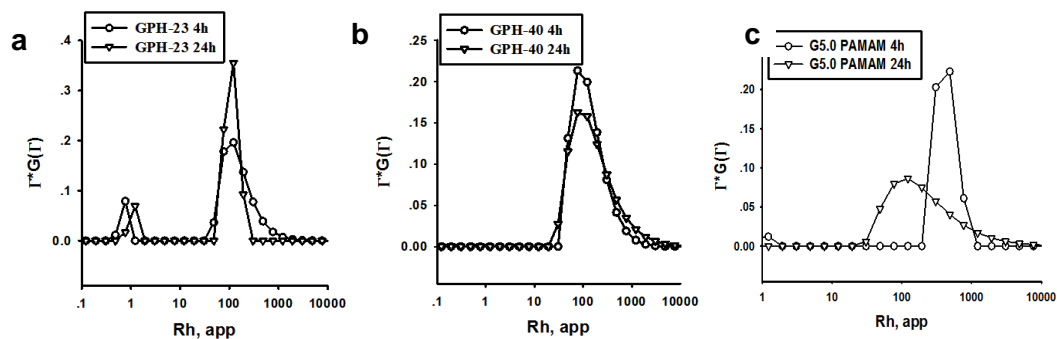


Figure 3.10 Size distribution of siRNA loaded crosslinked particles and polyelectrolyte particles. In both GPH-23 and GPH-40 crosslinked particle samples, no significant variation was observed for the size and distribution of the crosslinked particles at 4 h and 24 h after formulation, while the polyelectrolyte particles made from G5.0 PAMAM showed a shift of the distribution of particle size during the 24 h after formulation.

SiRNA release in the acidic environment

Glutaraldehyde was chosen to be the crosslinker in this system because the formed hydrazone bonds between aldehyde and hydrazide are reversible, which can be cleaved at an acidic condition. To verify the feasibility of the design, the crosslinked particles were incubated at pH 6.0 and pH 7.4 for 3 h, respectively, and the particles were detected by gel electrophoresis. The gel showed that siRNA was released from particles at pH 6.0 after 3 h incubation but remained inside the particles at pH 7.4 (Figure 3.11). This result indicated the controllable release mechanism of the crosslinked particles, implying the degradability of the delivery system under the specific condition.

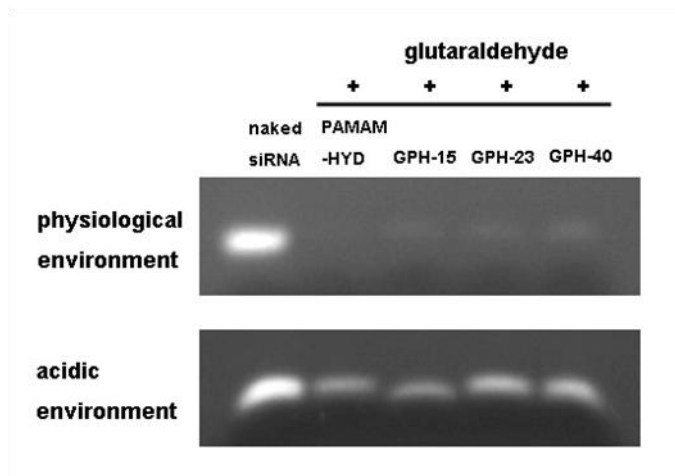


Figure 3.11 siRNA release from the crosslinked particles at the acidic condition. At pH 6.0, siRNA bands were showed in the crosslinked particle samples, while at pH 7.4 siRNA remained encapsulated in the particles, indicative of the controlled release of siRNA in the acidic environment.

Cytotoxicity assay

To determine the safety of the neutral dendrimers, MTS assay was conducted. After incubation with dendrimeric materials for 24 h, above 80% of HepG2 cells remained viable after PAMAM-HYD treatment up to the concentration of 90 nmol/ml, while G5.0 PAMAM induced increasingly severe cytotoxicity with the rising concentrations. A similar pattern was observed when they were tested on the primary human umbilical vein endothelial cells (HUVEC) cells (Figure 3.12b). As to the transfection condition, no significant cytotoxicity was observed, and above 95% of cells maintained alive after the treatment of siRNA-loaded crosslinked particles (Figure 3.13).

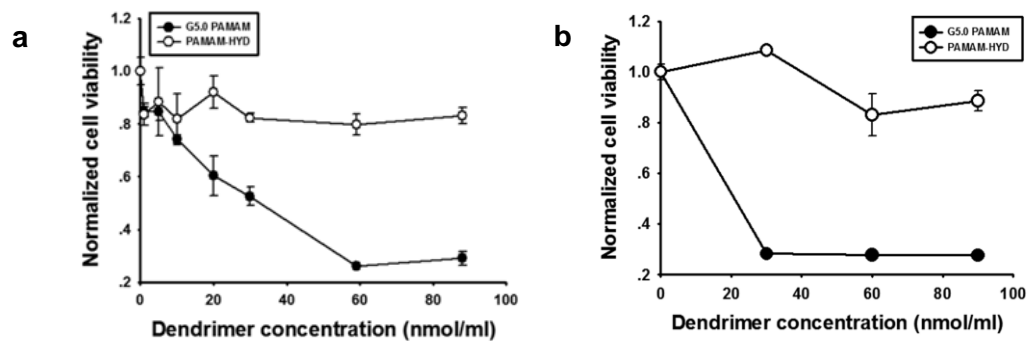


Figure 3.12 Cytotoxicity of neutral dendrimer PAMAM-HYD and cationic dendrimer G5.0 PAMAM on HepG2 cells (a) and HUVECs (b) after 24 h incubation. In both two types of cells, PAMAM-HYD showed minimal effects on the cell viability, while G5.0 PAMAM caused severe cytotoxicity that decreased the cell viabilities below 30%. Adapted with permission from Liu (2012) [185]. Copyright (2012) American Chemical Society.

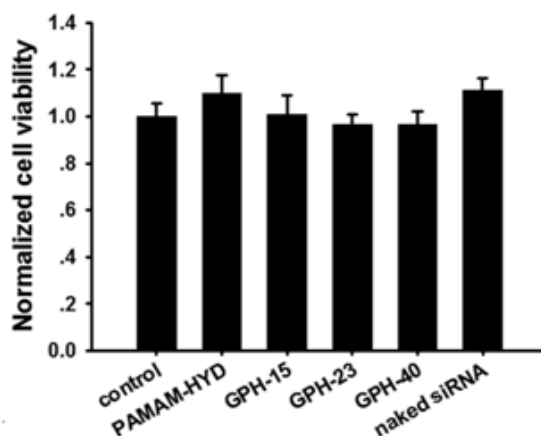


Figure 3.13 Cytotoxicity of siRNA loaded crosslinked particles in HepG2 cells. The crosslinked particles made from PAMAM-HYD and GPHs didn't affect the cell viability of HepG2 cells after 48 h incubation, and all treatment groups had cell viabilities above 90%. Values are mean \pm SEM. $n=3$. Adapted with permission from Liu (2012) [185]. Copyright (2012) American Chemical Society.

Transfection efficiency

siRNA-loaded crosslinked particles were used to treat HepG2 cells at a siRNA concentration of 50 nM in DMEM medium containing 10% serum. Upon the siRNA delivery against luciferase, the luciferase expression levels decreased in the GPH-15, GPH-23, and Lipofectamine 2000 groups (Figure 3.14). The GPH-23 particles obtained the strongest silencing effect of nearly 60% knockdown of the target gene, which was even more efficient than the commercial reagent Lipofectamine 2000. When loaded with scrambled siRNA, no down-regulation of luciferase was observed with any neutral crosslinked delivery system.

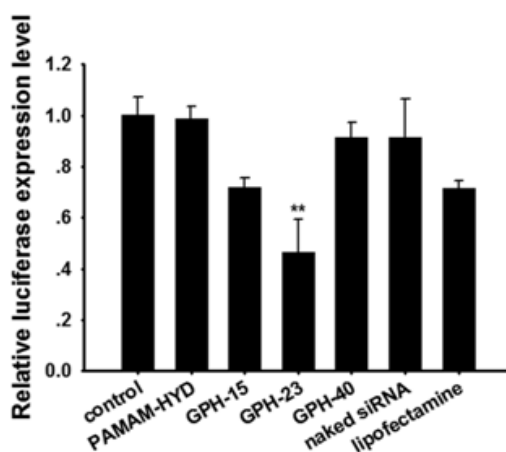


Figure 3.14 Gene silencing effect of the siRNA loaded crosslinked particles. In the serum-containing medium, GPH-23 crosslinked particles showed higher delivery efficiency than the positive control lipofectamine, with a gene down-regulation around 60%. Values are mean \pm SEM, $n=4$, $**P<0.01$, One-way ANOVA followed by the Newman-Keuls post-test. Adapted with permission from Liu (2012) [185]. Copyright (2012) American Chemical Society.

To visualize the internalization of neutral dendrimers, PAMAM-HYD and GPHs were labeled with fluorescein, and the cellular uptake of neutral dendrimers was examined via fluorescence microscopy. Fluorescent signal was barely observed in the

PAMAM-HYD group, but more HepG2 cells were fluorescent-positive in the GPH-23 and GPH-40 treated groups (Figure 3.15a-d). To detect the internalization of the siRNA-loaded crosslinked particles, cy3-siRNA was encapsulated by PAMAM-HYD and GPH materials. PAMAM-HYD particle group only showed some scattered fluorescent spots, while GPH particle groups showed more even distribution of fluorescent signals in HepG2 cells (Figure 3.15e-h). Among all the groups, GPH-23 crosslinked particles seemed to have the highest siRNA internalization in cells, which was expected according to the gene silencing results.

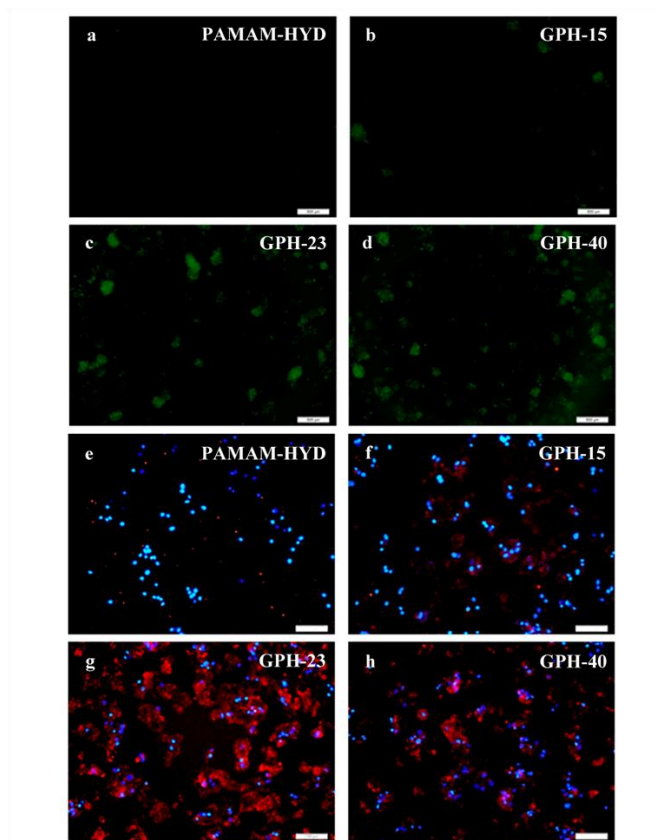


Figure 3.15 Cellular internalization of neutral dendrimers (a-d) and siRNA loaded crosslinked particles (e-h). GPH-23 and GPH-40 dendrimers showed visually higher rates of cell uptake in HepG2 cells, and the siRNA internalization rates of these two types of crosslinked particles were also observed higher than those made from PAMAM-HYD and GPH-15. Adapted with permission from Liu (2012) [185]. Copyright (2012) American Chemical Society.

3.3 Discussion

The design of the neutral dendrimer promotes the translation of synthetic carriers into the real practice. Although cationic materials remain the main fashion to fabricate delivery systems for gene therapy, the safety issue is always a concern when it comes to the translation into clinical use. Cytotoxicity, hemolytic/haematological toxicity and *in vivo* toxicity have been reported in dendrimer-related studies due to the cationic amines on the dendrimer surface. Acetylation of the dendrimer surface to block positive charges was attempted previously [147]; however, this strategy could not address the toxicity issue without compromising the siRNA-binding and delivery capabilities. In this study, the neutral crosslinked system provided a new concept of utilizing primary-amine-free materials. Since it were the tertiary amines that take charge of combining siRNA and the surface saccharide ligands that enhance the cell internalization, the substitution of primary amines didn't compromise the transfection efficiency of dendrimeric materials.

The utilization of buffering amines instead of permanently cationic primary amines to load siRNA is one of the unique features of the new system in this part. The physiologically neutral dendrimers, PAMAM-HYD and GPHs, own two possible sites for protonation, the internal tertiary amines and surface hydrazide groups. The pKa of the tertiary amines within the interior branches of PAMAM dendrimers was reported between 6 and 7 [144-146], while that of carboxylic hydrazide groups was reported down to 3.6 [142]. Consequently, most surface hydrazide groups in neutral dendrimers may remain unprotonated at pH 5.0, and the interaction between siRNA and PAMAM-HYD or GPHs mostly depends on the internally charged tertiary amines. This hypothesis was indirectly approved by the results seen in the siRNA-dendrimer complexation experiment,

in which GPHs with different saccharide modification levels didn't show a significant difference in binding siRNA at all tested D/S ratios. Previous studies on PAMAMs owning neutralized groups on the surface also support the conclusion that dendrimers are capable of interacting with nucleic acids or anionic drugs through the internally charged amines [148-150].

The method of crosslinking was the foundation of the siRNA-loaded neutral particles. Crosslinked systems were previously developed to increase the stability of polyelectrolyte particles made from cationic delivery materials [135, 137, 138, 151-155]. Particularly, the sizes of polyelectrolyte particles made from siRNA and cationic PAMAM were observed kept growing within the 72 h after formulation, while a crosslinking reaction preserved the original size to some degree [156]. In our neutral crosslinked system, the capability of maintaining the morphology of particles was verified again for the crosslinking method, significantly distinct from the un-crosslinked system. The crosslinking strategy did not only stabilize the particles, but also, more importantly, it encapsulated siRNA inside particles without dependence on the electrostatic interaction. This feature minimized the unspecific interaction between neutral crosslinked particles and other components in the extracellular environment. Yet the crosslinking reaction also increased the complexity of the system. In the ternary blends of dendrimer, siRNA, and glutaraldehyde, PAMAM-HYD or GPHs would simultaneously bind with siRNA and react with glutaraldehyde. Crosslinking could occur within the complexes formed from siRNA and dendrimer materials, termed as intra-particle crosslinking. Meanwhile, the initially crosslinked complexes could further assemble with each other as long as hydrazide groups are available, and the secondary

inter-particle crosslinking would lead to the formation of larger particles. Consequently, the average particle size in the system resulted from the dynamic equilibrium between the intra-particle crosslinking and inter-particle crosslinking. The inter-particle crosslinking caused the increased average sizes of PAMAM-HYD systems with the increasing glutaraldehyde concentrations at the beginning. However, when the amount of glutaraldehyde reached a certain threshold capable of saturating the surface hydrazide groups, inter-particle crosslinking would be prevented, allowing the formation of small particles. On the other hand, decorating the dendrimer surface with GalNAc likely increased the surface hydrophilicity and reduced the accessibility of surface hydrazide groups in dendrimers, to some extent preventing the inter-particle assembly after the dendrimer-siRNA complexes were initially crosslinked. In this case, the higher modification levels of GalNAc resulted in smaller size of the crosslinked particles. Thus, the sizes of crosslinked particles can be modulated both by the crosslinker concentration and surface modification.

Controlled release of siRNA is likely to be realized in the crosslinked system. One concern for the cationic delivery vehicles is that the electrostatic forces may restrict the gene cargoes from leaving the delivery system into cytoplasm, and in fact studies already reported that too condensed particles are not efficient for gene delivery [157-161]. In the neutral crosslinked system, the siRNA release could occur upon the breakage of the hydrazone crosslinking bonds in the acidic endosomal environment, when free glutaraldehyde was not present in excess to drive the reaction toward bond formation. Theoretically, the hydrazone bonds would break in endosomes, and then siRNA would dissociate from the particles; at the meantime, the buffering amines inside the dendrimer

would induce the “proton sponge” effect and break the endosomes. Subsequently, siRNA could be released into the cytoplasm.

Saccharide ligands are multi-tasking in the crosslinked system. They provide biocompatibility as well as the controllability on the siRNA loading efficiency and particle size, and also support cell targeting and cell internalization. The fluorescence images demonstrated that GalNAc plays a pivotal role in mediating the cellular uptake of neutral dendrimers and crosslinked particles. The multivalent effects normally exerted by glycodendrimers were likely to further magnify the interaction between GalNAc and its receptors, which made the cell targeting function even more powerful.

CHAPTER 4

DOWN-REGULATION OF AT1R IN CARDIAC TISSUE BY DELIVERING SPECIFIC SIRNA TO PRESERVE CARDIAC FUNCTION POST-MI

4.1 Introduction

The short peptide hormone Ang II is the key player in Renin-Angiotensin-Aldosterone System (RAAS), which would be activated upon ischemic injuries. 4 membrane receptors have been identified for Ang II. Most well-known adverse effects of Ang II are mediated by the Ang II type 1 receptor (AT1R), the activation of which results in worsened cardiac functions after injury [66, 67, 162]. In comparison, another important receptor, the type 2 receptor (AT2R), is generally considered as a protective receptor, leading to improved function recoveries [78, 79, 163]. Consequently, AT1R has become a common target for the management of cardiac diseases. The suppression of AT1R activity can reduce the deleterious effects from Ang II, and meanwhile Ang II can mostly bind AT2R, bringing more beneficial effects upon AT2R activation [164]. Evidence from laboratories and clinical studies showed that Angiotensin receptor blockers (ARBs) are effective to restore blood pressure, prevent fibrosis, and improve cardiac function [71-73, 75, 76].

Despite the obtained positive results so far, some studies demonstrated that the AT1R suppression at the gene expression level holds more advantages to AT1R pharmacological blockade [70, 165]. For instance, the AT1R blockers caused renin and

Ang II levels to increase in plasma, which may further activate the whole RAAS, but the delivery of antisense oligonucleotides against AT1R didn't bring this problem [70]. Possibly the simple blockade interrupts the feedback loop in RAAS, leading to deregulation of other components in the system. In Voros et al.'s study, the overexpression of AT2R significantly reduced the fibrosis degree post-MI in an AT1R-knockout animal model, but such improvement was not observed in the animals treated with AT1R blockers [165]. Apparently, the silencing of AT1R at the gene expression level differs from the direct blockade of the AT1R protein. In addition, an argument about whether the AT1R blockers may increase the risks of MI and cancer is undergoing, which brings more concerns for the traditional therapy. Such situation puts RNAi therapeutics into an important position, as it can selectively control gene expression, and siRNA molecules are the potent initiators to trigger gene silencing.

One crucial challenge for applying RNAi therapeutics to treat CVDs is the development of siRNA delivery systems for cardiac tissue, because the non-phagocytic nature of cardiomyocytes raises the barrier for the delivery of small RNA molecules. Bull and his colleagues did a series of studies using a synthetic polymer carrier to deliver siRNA in a cardiomyoblast cell line, in the form of peptide-conjugated polymers or the peptide-conjugated siRNAs, but no further *in vivo* efficiency was reported so far [93, 95, 101], possibly due to the efficacy issue. Lau et al. used a siRNA-albumin conjugate to silence cardiac genes *in vivo* at a siRNA dose of 1-5 mg/kg. Though a 40% silencing effect was obtained, the usage of a significantly higher dose than those in other studies indicated that the actual performance was not very competitive [166]. Due to the poor efficiency *in vivo*, the demand of potent siRNA delivery systems is still urgent.

In our previous studies, we explored the polymeric materials, the dendrimeric materials, and the CPP ligands, and all of them own unique advantages in siRNA delivery. In this part, we want to combine the strengths of the three components above. A “tadpole” shaped dendrimeric material was developed in this part, composed of a cationic dendron head, a PEG polymer crosslinker, and a CPP tail, and this design allows a strong affinity with siRNA, reduced surface charge density, and enhanced cell membrane penetration. Three tadpole dendrimers were tested and compared *in vitro* first, including one without CPP modification and two with CPP conjugations. The vehicle worked best was further studied in a rat ischemia-reperfusion (IR) model to assess its performance *in vivo*, using AT1R as the gene target.

4.2 Results

Synthesis of tadpole dendrimeric materials

Figure 4.1 showed the design of the tadpole dendrimeric materials. They have a dendron head, a PEG crosslinker in the middle, and a CPP tail. The fan-shape dendron moiety was derived from the reduced cystamine core G4.0 PAMAM, presenting 32 positive charges on the surface, which provide high-density siRNA-binding sites. The hydrophilic and neutral PEG segment would not involve in the charge interaction, possibly presenting on the outer layer of siRNA-loaded particles, which could partially shield the cationic charges on the particles to reduce the potential toxicity. At the same time, the flexibility of PEG could also minimize the steric hindrance between the peptide tails when interact with cell membranes. CPPs were introduced into the tadpole dendrimers to enhance the cell uptake in cardiomyocytes. The three parts were linked via

cleavable disulfide bonds to endow the materials with degradability and the siRNA release mechanism in cytoplasm.

The conjugation of PEG and CPP to the dendron moiety was confirmed by the H^1 -NMR spectra (Figure 4.1b). The high peak in the range of 3.7-3.8 ppm belongs to the PEG segment ($-OCH_2CH_2-$), the relatively wide peak in the range of 2.4-2.6 ppm belongs to PAMAM ($-NCH_2CH_2CO-$), and the two adjacent peaks in the range of 1.5-1.8 ppm belong to the arginine residues ($-HCCCH_2CH_2CH_2NH-$) in the peptides. Qualitative calculations based on the peak area of PAMAM, PEG, and arginine showed the successful conjugation of PEG to the reduced end of PAMAM, and averagely 81.8% and 80.0% of dendron moiety molecules were modified by R9 and TAT, respectively.

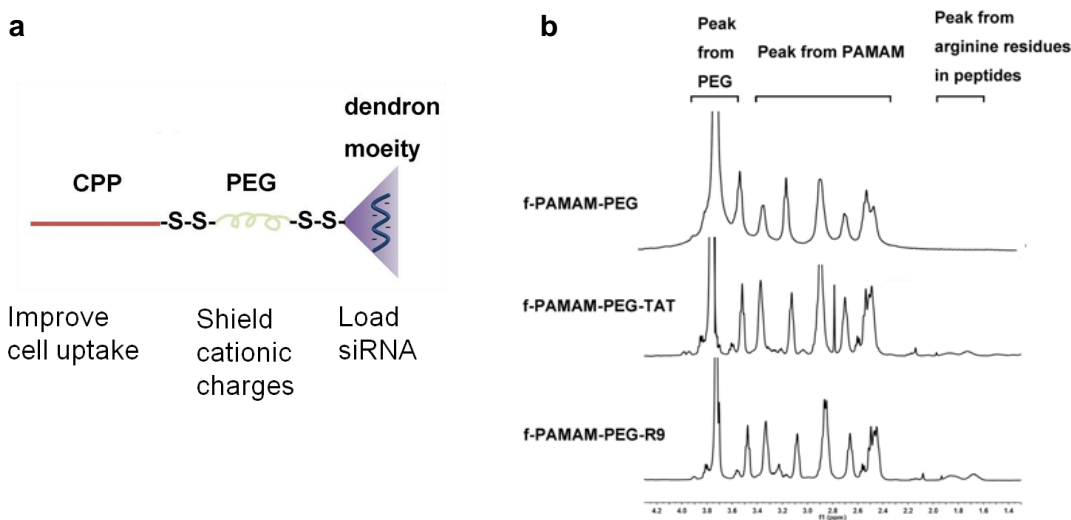


Figure 4.1 Scheme of tadpole dendrimers (a) and H^1 -NMR analysis (b). NMR results showed that the modification rates of R9 and TAT were 81.8% and 80.0% in f-PAMAM-PEG-R9 and f-PAMAM-PEG-TAT tadpole dendrimers, respectively. Adapted with permission from Liu (2013) [96]. Copyright (2013) Elsevier.

Preparation of siRNA-loaded particles

siRNA loading capacity of the tadpole dendrimers was evaluated by the gel retardation assay. Clearly the siRNA bands became fainter in the gel with the increasing N/P ratios, meaning siRNA gradually formed particles based on the electrostatic interaction with the increasing amount of dendrimeric materials. According to the gel pictures, the minimal N/P ratios required to load all siRNA in each system were 10, 60, 60, and 40 for G4.0 PAMAM, f-PAMAM-PEG, f-PAMAM-PEG-TAT, and f-PAMAM-PEG-R9, respectively (Figure 4.2).

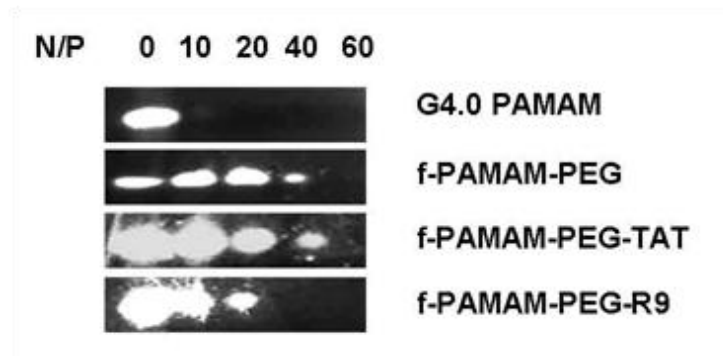


Figure 4.2 Gel retardation assay of G4.0 PAMAM and tadpole dendrimers. siRNA bands became fainter when the N/P ratios were raised higher. The minimal N/P ratios needed to load siRNA completely were 10, 60, 60, and 40 for G4.0 PAMAM, f-PAMAM-PEG, f-PAMAM-PEG-TAT, and f-PAMAM-PEG-R9, respectively.

Dynamic light scattering (DLS) was used to determine the size of siRNA-loaded particles formed by different tadpole dendrimers at the minimal required N/P ratios. The particles made from PAMAM G4.0, f-PAMAM-PEG, f-PAMAM-PEG-TAT, and f-PAMAM-PEG-R9 had diameters of 247 ± 76 nm, 178 ± 13 nm, 302 ± 20 nm, and 143

± 29 nm, respectively (Figure 4.3 and Table 4.1) at N/P ratios of 10, 60, 60 and 40. And the corresponding zeta-potentials of these particles were measured as 29.9 ± 4.1 mV, 10.6 ± 4.3 mV, 15.4 ± 4.0 mV, and 3.2 ± 0.6 mV, respectively.

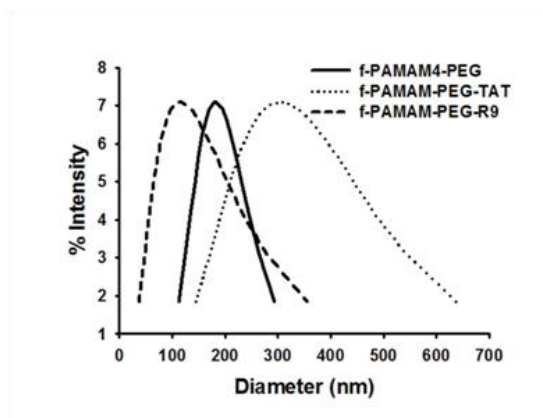


Figure 4.3 Size distribution of siRNA-loaded tadpole dendrimer particles. The f-PAMAM-PEG-R9 formed relatively small particles with siRNA, while f-PAMAM-PEG-TAT formed relatively large particles. Adapted with permission from Liu (2013) [96]. Copyright (2013) Elsevier.

Table 4.1 Size and zeta-potential of siRNA-loaded particles¹

Tadpole dendrimer	Diameter (nm)	Zeta-potential (mV)
PAMAM G4.0	247 ± 76	29.9 ± 4.09
f-PAMAM-PEG	178 ± 14	10.6 ± 4.35
f-PAMAM-PEG-TAT	302 ± 20	15.4 ± 4.01
f-PAMAM-PEG-R9	143 ± 29	3.51 ± 0.6

¹Adapted with permission from Liu (2013) [96]. Copyright (2013) Elsevier.

Though numbers of studies have reported the toxicity of cationic PAMAM [33], no adverse effect from tadpole dendrimers in the metabolic activity was detected in

primary CMs by MTT assay (Figure 4.4), and all particle-treated groups had cell viabilities above 80%, implying the well compatibility of the siRNA-loaded particles.

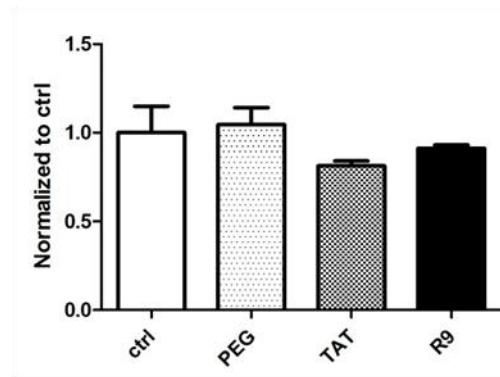


Figure 4.4 Cytotoxicity of siRNA-loaded tadpole dendrimer particles in primary neonatal CMs. The MTT assay showed that cells treated with particles made from f-PAMAM-PEG or f-PAMAM-PEG-R9 had cell viabilities no less than 90%, and cells treated with particles made from f-PAMAM-TAT had cell viabilities above 80%. Adapted with permission from Liu (2013) [96]. Copyright (2013) Elsevier.

siRNA transfection in isolated cardiomyocytes

In our preliminary test, both TAT- and R9-conjugated tadpole dendrimers showed the capability of delivering FITC-siRNA into cardiomyoblast cell line H9C2, as strong fluorescent signals were observed inside cells (Figure 4.5). To determine the transfection efficiency of tadpole dendrimers in primary cardiac cells, we applied the siAT1R-loaded dendrimer particles in neonatal CMs and used qPCR to detect the AT1R expression at the mRNA level. At the siRNA concentration of 50 nM, AT1R expression didn't change significantly upon the treatment of siRNA-loaded particles made from G4.0 PAMAM, f-PAMAM-PEG and f-PAMAM-PEG-TAT compared to the cells treated with the three

empty dendrimeric materials ($104.3 \pm 27.8\%$, $120.8 \pm 24.9\%$ and $96.7 \pm 9.6\%$, respectively), but siRNA-loaded particles made by f-PAMAM-PEG-R9 induced a silencing effect greater than 60% ($36.7 \pm 9.9\%$, $P < 0.01$) (Figure 4.6). Since f-PAMAM-PEG-R9 exhibited the strongest *in vitro* performance with the highest siRNA loading efficiency, the smallest particle size, and the lowest surface positive potential, it continued to be studied *in vivo*.

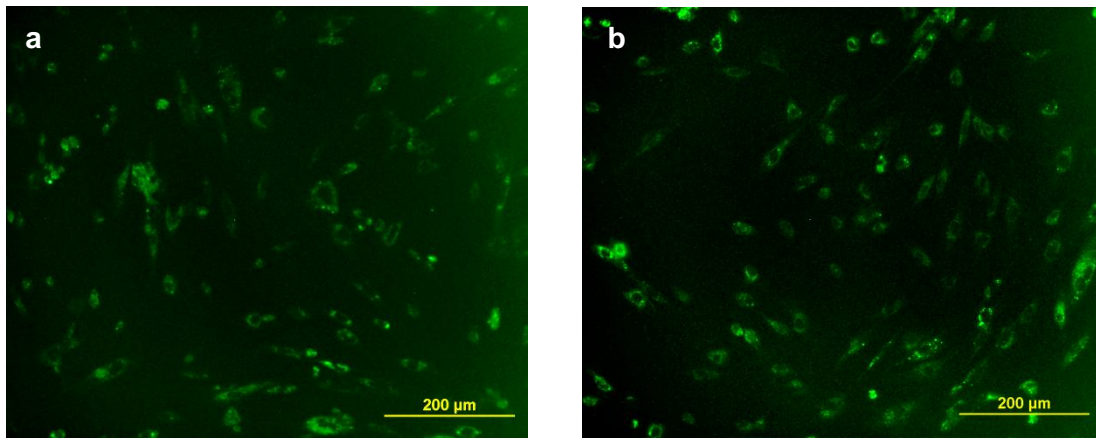


Figure 4.5 Cellular internalization of FITC-siRNA loaded tadpole dendrimer particles in cardiomyoblast H9C2 cells. Cells treated with siRNA-loaded particles made from both f-PAMAM-PEG-TAT (a) or f-PAMAM-PEG-R9 (b) showed positive fluorescent signals in the images. Adapted with permission from Liu (2013) [96]. Copyright (2013) Elsevier.

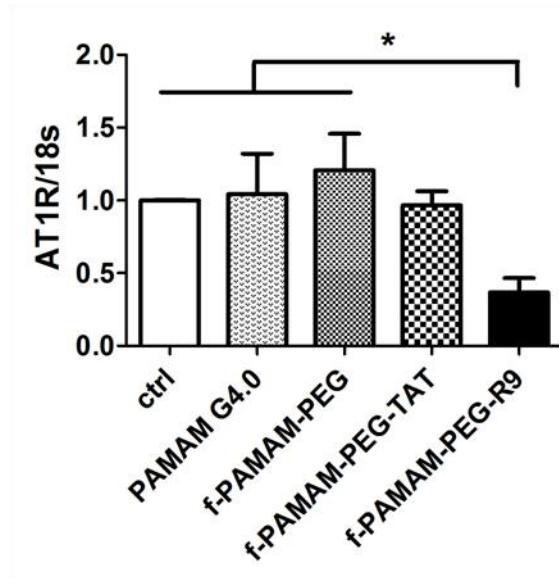


Figure 4.6 AT1R expression upon the treatment of siRNA-loaded tadpole dendrimer particles in primary neonatal CMs. According to the qPCR result, only particles made from f-PAMAM-PEG-R9 induced a significant down-regulation of AT1R *in vitro*, with a silencing effect of 63.3%. The results were normalized to 18S expression (fold change) reported as mean \pm SEM. $n=3-4$, * $P<0.05$, ** $P<0.01$. One-way ANOVA followed by the Tukey post-test.

siRNA delivery *in vivo*

To determine the siRNA delivery efficiency of f-PAMAM-PEG-R9 dendrimer and the therapeutic potential of siRNA delivery in cardiovascular diseases, we conducted animal experiments in a rat IR model. The IR injury was made by surgeries in adult male rats, and the operated animals were randomly divided into three groups that either received the injection of saline alone (IR), or empty tadpole dendrimers (IR+ dendrimer), or siAT1R-loaded particles (IR+ dendrimer/ siRNA) ($n>6$ for each group, $N=36$ total). A group of animals that only went through chest opening without artery ligation was used as the sham group for comparison. On the third day after the injection, gene expression in

left ventricle tissue was determined by qPCR. AT1R expression increased significantly by 1.92 ± 0.26 -fold and 2.01 ± 0.37 -fold ($P < 0.05$) at mRNA levels in IR group and IR+ dendrimer group, respectively, compared to the sham group. In contrast, the AT1R expression in the IR+ dendrimer/siRNA group maintained a similar level (0.94 ± 0.21 fold) as sham animals, significantly lower than that in IR injured animals ($P < 0.05$) (Figure 4.7a).

Except the direct target AT1R, other relative genes in the MI development were also in the scope of detection. The expression of AT2R, the other important receptor of Ang II, slightly decreased in the IR group (0.74 ± 0.20 fold) and IR+ dendrimer group (0.69 ± 0.20 fold) compared to the sham group, while in comparison, the AT2R level increased in the IR+ dendrimer/ siRNA group by 2.14 ± 0.86 -fold, but none of these had statistic significances yet at the 3-day time point (Figure 4.7b). The expression of another relative gene Col-1, which associates with fibrosis formation, was also determined by qPCR. The expression of Col-1 increased by more than 5 folds after the IR injury, while in the siRNA delivery group the Col-1 expression decreased to 2.7 ± 0.85 -fold of the level of the sham group (Figure 4.7c).

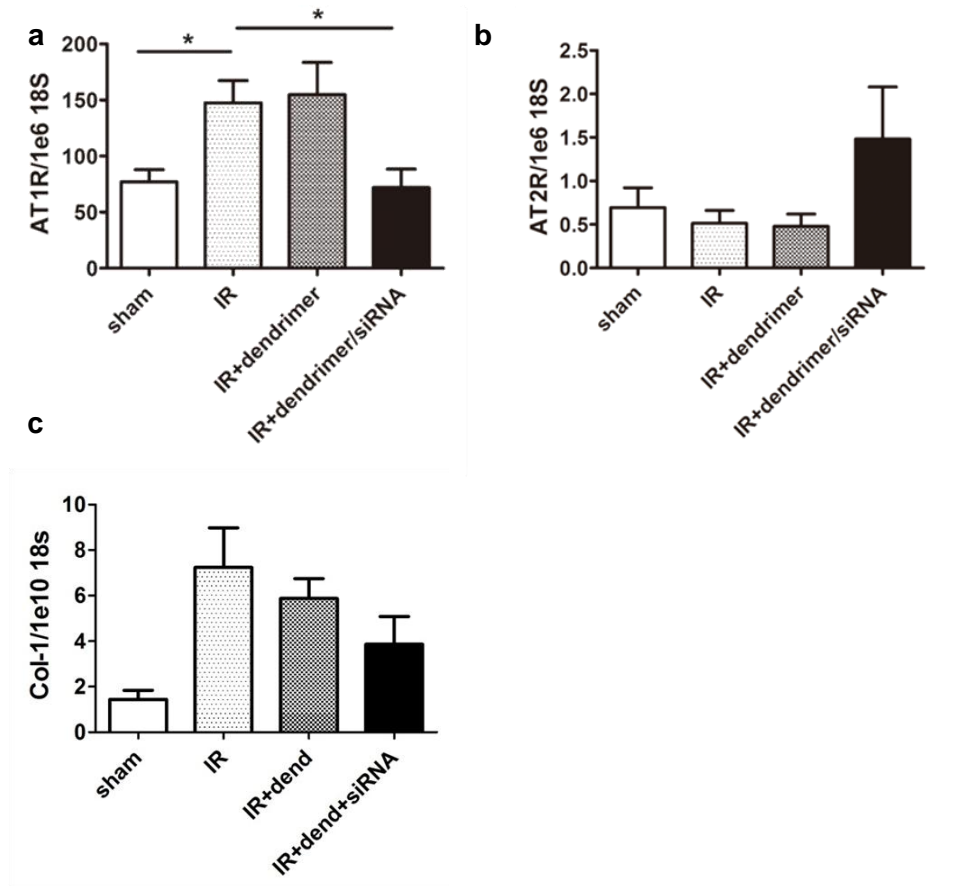


Figure 4.7 Expression of AT1R (a), AT2R (b), and Col-1 (c) in the left ventricle tissue upon the delivery of siRNA loaded tadpole dendrimer particles. At the 3 day after injection, the expression levels of AT1R, AT2R, and Col-1 in the IR+ dendrimer/siRNA group were 0.94 ± 0.21 fold, 2.14 ± 0.86 -fold, and 2.7 ± 0.85 -fold of that of the sham group. Results were normalized to the 18S expression and reported as mean \pm SEM. $n > 6$, $N = 36$, $*P < 0.05$. One-way ANOVA followed by the Tukey post-test. Adapted with permission from Liu (2013) [96]. Copyright (2013) Elsevier.

In vivo cardiac function

To determine whether the siRNA delivery against AT1R by the tadpole dendrimer preserved cardiac functions after the ischemic injury, cardiac functions were evaluated by echocardiography and Pressure-Volume (PV) cardiac hemodynamics ($n > 6$ for each group,

$N=26$ total). Ejection fraction (EF) stands for the percentage of blood pumped out from ventricles in each heart cycle, and rats in the sham group had an average EF value of $74.3 \pm 2.7\%$ that was significantly lower in the IR group ($56.3 \pm 2.4\%$, $P<0.005$) and IR+dendrimer group ($62.0 \pm 2.4\%$, $P<0.01$); however, a significant improvement of EF was observed in the IR+ dendrimer/siRNA group ($71.9 \pm 1.9\%$, $P<0.005$ vs. IR, $P< 0.05$ vs. IR+ dendrimer), reaching a similar EF level as the sham group (Figure 4.8).

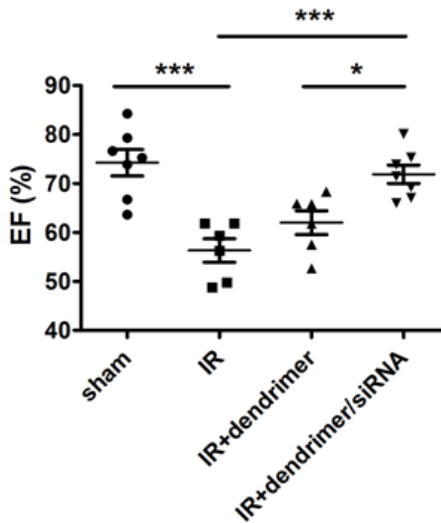


Figure 4.8 Ejection fraction (EF) of different treatment groups at the 3 day after injection. While the EF values of IR and IR + dendrimer groups significantly decreased after the IR injury, the delivery of siAT1R increased the EF value to $71.9 \pm 1.9\%$. Values are mean \pm SEM. $n>6$, $N=26$, $*P<0.01$, $***P<0.005$. One-way ANOVA followed by the Tukey post-test. Adapted with permission from Liu (2013) [96]. Copyright (2013) Elsevier.

The end-systolic volume (ESV) indicates the heart contractility. In IR group, ESV increased significantly to 1.68-fold ($127.8 \pm 6.4 \mu\text{l}$, $P<0.01$) of that in the sham group ($76.0 \pm 6.4 \mu\text{l}$), implying a loss of ventricular contractility and increase in elasticity. The unloaded empty dendrimers didn't cause significant changes ($125.9 \pm 14.5 \mu\text{l}$), but the

treatment of the siRNA-loaded dendrimer particles led to a significant improvement with a lowered ESV of $84.6 \pm 8.6 \mu\text{l}$ ($P < 0.01$ vs. IR, $P < 0.05$ vs. IR+ dendrimer) (Figure 4.9a). Unlike ESV, no significant difference in the end-diastolic volume (EDV) was observed among different treatment groups, and the EDV values of sham, IR, IR+ dendrimer, and IR+ dendrimer/siRNA groups were $222.1 \pm 18.1 \mu\text{l}$, and $250.2 \pm 12.8 \mu\text{l}$, $263.7 \pm 10.2 \mu\text{l}$, and $231.7 \pm 19.8 \mu\text{l}$, respectively (Figure 4.9b).

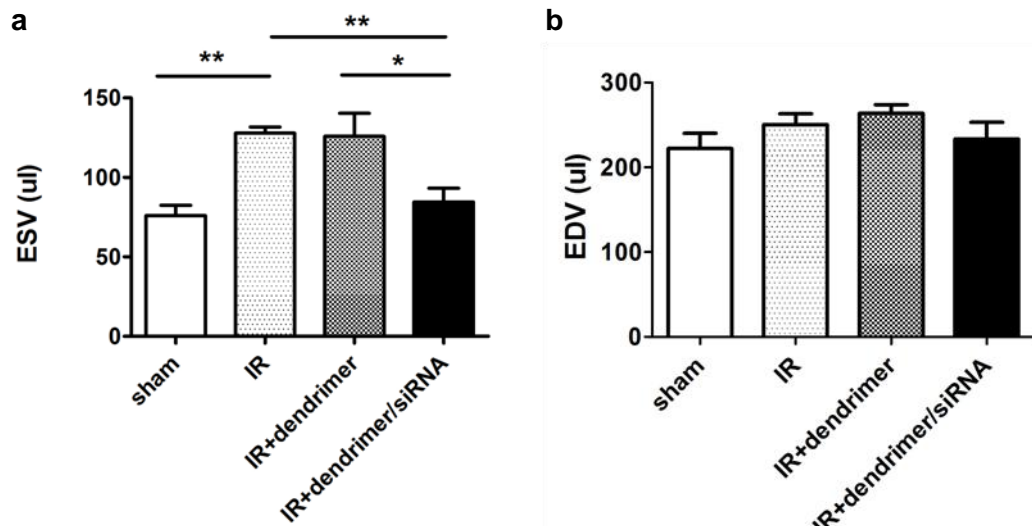


Figure 4.9 End-systolic volume (ESV) (a) and end-diastolic volume (EDV) (b) of different treatment groups. In the acute phase of ischemic injury, the ESV value significantly increased after IR injury, and the delivery of siAT1R-loaded tadpole dendrimer particles decreased the ESV to $84.6 \pm 8.6 \mu\text{l}$. No significant difference among treatment groups was observed for EDV at the 3 day after the surgery. Values are mean \pm SEM. $n > 4$, $N = 21$, $*P < 0.05$, $**P < 0.01$. One-way ANOVA followed by the Tukey post-test. Adapted with permission from Liu (2013) [96]. Copyright (2013) Elsevier.

At the third day following injury, infarct size was measured in different treatment groups using the TTC staining method, and a typical picture would show three color sections: the dark blue area presented the viable tissue, the red presented the area at risk,

and the white presented the dead tissue. The pictures of heart slides showed that in the dendrimer/siRNA group the white area was much smaller than that in the IR group (Figure 4.10a). To quantitative compare the occupation of damaged tissue among groups, the index of infarct size was calculated as infarct area/area-at-risk to avoid the influence from variations in risk areas. By dividing the white area by the sum of white and red areas, the infarct size of the IR group was calculated as $47.8 \pm 4.8\%$. While there was no statistically significant decrease in the IR+ dendrimer group ($37.5 \pm 2.7\%$), the treatment of siAT1R-loaded dendrimer particles significantly reduced the infarct size to $18.4 \pm 3.1\%$ ($P < 0.005$ vs. IR, $P < 0.01$ vs. IR+ dendrimer) (Figure 4.10b).

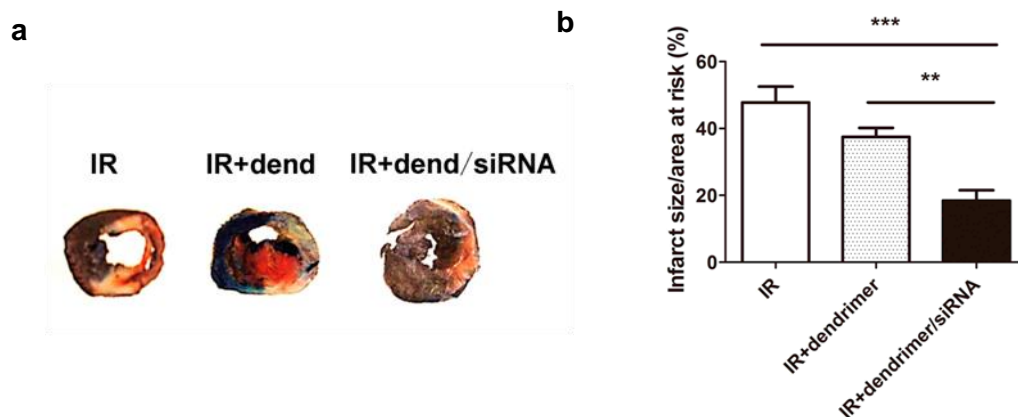


Figure 4.10 Infarct size of different treatment groups. Stained heart slides showed three colors, with the white section indicative of infarcted tissue. Quantitative measurements from Image J showed that the treatment of siRNA-loaded tadpole dendrimer particles reduced the infarct size from $47.8 \pm 4.8\%$ to $18.4 \pm 3.1\%$. Values are mean \pm SEM. $n=5$, $**P < 0.01$, $***P < 0.005$. One-way ANOVA followed by the Tukey post-test. Adapted with permission from Liu (2013) [96]. Copyright (2013) Elsevier.

Optimization of the tadpole dendrimers

To further optimize the tadpole dendrimeric materials, the PEG segment was

shortened from 2 KDa to 1 KDa, and new f-PAMAM-PEG and f-PAMAM-PEG-R9 were produced, termed as f-PAMAM-PEG₁₀₀₀ and f-PAMAM-PEG₁₀₀₀-R9. Both new tadpole dendrimers showed increased siRNA loading efficiency in the gel retardation assay, with the minimal required N/P ratios reduced to 20 and 10 for f-PAMAM-PEG₁₀₀₀ and f-PAMAM-PEG₁₀₀₀-R9, respectively (Figure 4.11a). siRNA-loaded particles formed at the minimal N/P ratios had diameters ranged from 100 nm to 300 nm, which were still acceptable for CMs to uptake (Figure 4.11b).

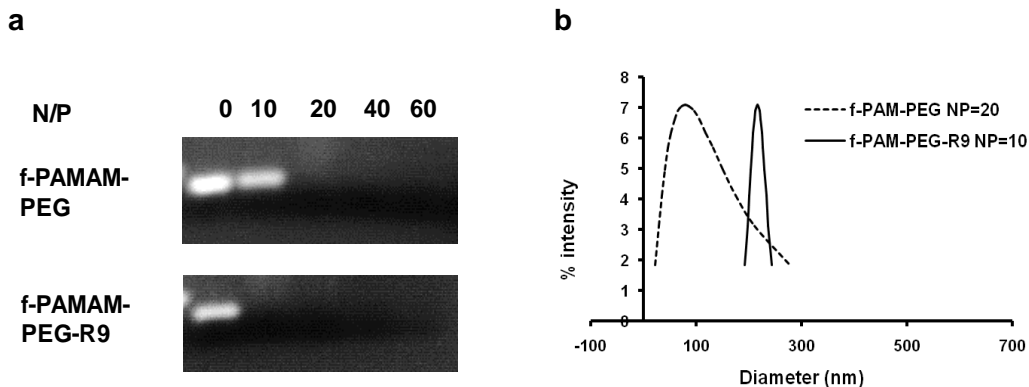


Figure 4.11 Characteristics of the optimized tadpole dendrimers. Gel retardation assay examined the siRNA loading efficiency of tadpole dendrimers after changing the PEG segment. The minimal N/P ratios needed to load siRNA completed reduced to 20 and 10 for f-PAMAM-PEG and f-PAMAM-R9, respectively. siRNA-loaded particles made from the new tadpole dendrimers had average sizes within the range from 100 nm to 300 nm.

4.3 Discussion

Dendrimeric materials are potent candidates for siRNA delivery as described in Chapter 3. Particularly, PAMAM has been widely employed due to its high charge density and the buffering capacity, and successful applications in siRNA delivery *in vitro*

and *in vivo* were reported [167, 168]. Due to the previously good performance, we wanted to exploit the potential of PAMAM to construct a potent delivery system in the non-phagocytic CMs. The cell binding and internalization of a neutral saccharide-modified dendrimer and a cationic dendrimer were compared in cardiomyoblasts first in our primary test. GlcNAc was chosen as the saccharide ligand for CMs to be modified on PAMAM-HYD, since GlcNAc was reported promising in targeting CMs [98, 99]. However, the combination of GlcNAc ligands and the multivalent interaction still could not compete with the cationic PAMAM. The flow cytometry analysis showed that the amount of G5.0 PAMAM bound and uptake by cardiomyoblasts was much more than that of GlcNAc-PAMAM-HYD. In this case, the cationic dendrimer was chosen to establish siRNA delivery system for cardiac tissue.

To improve the performance of cationic dendrimers and meanwhile avoid potential problems, we used a PAMAM moiety as the head of the tadpole dendrimers to load siRNA with a strong affinity, and the CPP tail served to enhance the internalization of siRNA-loaded particles in CMs. To reduce the potential toxicity from the dendron moiety, a PEG segment was introduced into the structure [23-26] to shield the positive charges. The three parts of the tadpole dendrimers are responsible for independent tasks and also cooperate with each other to function as a whole.

PEG segment is an important adjuster in the tadpole dendrimers. With the PEG modification, the zeta-potential of f-PAMAM-PEG particles decreased nearly 3 folds compared to the particles formed by PAMAM G4.0. Similar decreases in zeta-potentials were also observed in the f-PAMAM-PEG-R9 and f-PAMAM-PEG-TAT dendrimer particles. It's likely that PEG presented mostly on the outer layer of the particles,

reducing the exposure of cationic charges. The significantly lowered zeta-potential of R9 dendrimer particles compared to the other tadpole dendrimers was probably due to the smaller N/P ratio required by this material (40 for f-PAMAM-PEG-R9 vs. 60 for f-PAMAM-PEG or f-PAMAM-PEG-TAT). Besides reducing the exposure of positive charges, the PEG segment also affected the siRNA loading efficiency. Without the PEG conjugation, cationic G4.0 PAMAM only needs an N/P ratio of 5 to load siRNA completely, but after conjugation of PEG₂₀₀₀ this value increased to 60 for f-PAMAM-PEG. It's likely that the PEG interrupted the interaction between PAMAM moiety and siRNA, and this hypothesis was confirmed by the new f-PAMAM₁₀₀₀-PEG, as the shorter PEG significantly reduced the minimal required N/P ratio to 20. The same trend also occurred on f-PAMAM₂₀₀₀-R9 and f-PAMAM₁₀₀₀-R9. The appropriate size of PEG could be critical for optimizing the material's property.

In the transfection experiment *in vitro*, PAMAM G4.0 and f-PAMAM-PEG loaded with siAT1R failed to reduce the AT1R expression, implying that the charge interaction alone is not sufficient to translocate the particles into CMs. CPPs are the top choices to enhance the cell internalization, and the two most commonly used CPPs, R9 and TAT, have been reported to enhance the delivery efficiency in cardiac cells and myocardium in literature [95, 103, 104]. In this part, the R9-conjugated tadpole dendrimer caused effective siRNA delivery, but the TAT-conjugated dendrimer failed to do the same. R9 is a short peptide composed of pure arginine residues, while TAT is a longer peptide with two types of basic amino acids, arginine and lysine, and other hydrophobic residues in the sequence. The difference in the transfection efficiency of the two CPP conjugated tadpole dendrimers may be because of the addition of lysine and

phenylalanine residues creating a secondary structure different than that of R9, or the higher number of arginine residues in R9 meets the preference of CMs. In addition, the difference in particle sizes between the two tadpole dendrimers may also affect the transfection efficiency since smaller particles are generally easier to be internalized.

The treatment of siAT1R-loaded dendrimer particles regulated not only the expression of the direct target AT1R but also other relative genes. AT2R is another major receptor that Ang II binds to and exerts mostly beneficial effects. Some studies showed the treatment of AT1R blockers caused increased AT2R expression, while in other studies AT2R wasn't affected [169-171], which was possibly determined together by the type of blockers, the type of injury models, and the time of detection. Yang et al. used an antisense RNA to silence AT1R in an IR model in rat hearts, leading to a decrease in AT2R level [70], potentially mitigating some of the beneficial effects [96]. In our results, the knock-down of AT1R at the mRNA level tended to induce AT2R overexpression compared to the sham group, but not to a significant degree. Since the overexpression of AT2R was reported to be beneficial to cardiac functions in the rat IR model, the RNAi therapy targeting AT1R could gain a double-win from the modulation of AT1R and AT2R. Col-1 is another important gene for cardiac functions, which responds to the fibrosis formation in the infarct area. The synthesis of Col-1 increased upon Ang II activation [172]. In the present study, IR injury increased the Col-1 level, and siAT1R delivery demonstrated a trend at reducing this. It's possible the change in this chronic fibrosis marker will become significant in a long time term.

siRNA delivery against AT1R *in vivo* enhanced CM survival as evidenced by the reduced infarct size, which is indicative of CM necrosis/apoptosis. Since no significant

curing effect of the empty dendrimer was showed in the experiment, the reduced infarct size was a direct result of the AT1R silencing. This is consistent with previous studies demonstrating that Ang II caused cell death in CMs [173, 174], as well as studies demonstrating ARBs capable of reducing infarct size [169, 175, 176]. The improvement in the cell viability further brought the improvements of cardiac function. One representative parameter of cardiac function is the EF. A normal rat has an EF around 60%-80%, and IR injury significantly decreased this value down to 50%. siAT1R delivery by R9 tadpole dendrimer recovered the EF value to the same level of the sham group, indicating the recovery of the heart ability to pump blood. ESV is the volume of ventricles at the end of heart contraction, and a relatively small ESV means a relatively strong capability of contracting. Our result showed that the siAT1R delivery reversed the increasing tendency of ESV after IR injury, implying the preservation of heart contractility. Correspondingly, EDV is the ventricle volume at the end of heart relaxation, but no significant difference of EDV was observed between different treatment groups at the early time point of 3 day. In addition, the CPP ligand R9 is not specific to CMs but generally enhances cell internalization, so the silence of AT1R possibly took place in several types of cells that express AT1R, such as cardiomyocytes, fibroblasts, endothelial cells, and inflammatory cells. The down-regulation of AT1R in multiple types of cells may contribute as a whole to improve the cardiac function recovery after injury.

CHAPTER 5

SUMMARY AND FUTURE DIRECTIONS

5.1 Peptide polymers in siRNA delivery

Chapter 2 described the synthesis and usage of a degradable arginine peptide polymer in siRNA delivery *in vitro* and the comparison with an oligo arginine peptide and an undegradable peptide polymer. This part verified three basic hypotheses in polymer materials. First, the polymerization strategy of oligo peptides is effective in enhancing the interaction between siRNA and peptides and further enhancing the stability of siRNA- loaded particles. Second, the degradable design of peptide polymers is able to reduce the cytotoxicity from cationic charges. Third, the conjugation of functional ligands benefits the delivery efficiency of delivery systems. In fact, several studies have synthesized CPP polymers via the linkage of disulfide bonds for gene delivery, and similar advantages of polymeric structures compared to their monomers were found, but the conjugation of functional ligands to CPP polymers was not reported before.

Although CPP polymers gained improved performance compared to CPP monomers, the simple polymerization of CPPs could hardly create ideal delivery systems. The highest gene silencing effect detected in our study was about 50% in serum-free medium, which was much lower than the 92% from the positive control lipofectamine. Undoubtedly, CPPs are good at penetrating cell membranes, but they lack the capability of endosome escape. Therefore the retention in endosomes may be the reason for the low transfection efficiency of CPPs. Stability is another concern that limits CPPs'

performance. When the dPOA/siRNA particles and RGD-g-dPOA/siRNA particles were used in serum-containing medium, the gene silencing effects disappeared, indicating that the particles formed from peptide polymers were not stable against serum proteins. As a conclusion, CPPs alone are not the ideal candidates to become the hardcore of a delivery system, and instead the collaboration between CPPs and other components would become the future direction for the utilization of CPPs. Several studies decorated CPPs and other types of targeting ligands together on delivery vehicles, and synergetic effects in enhancing cell internalization were observed compared to the usage of the ligands separately[93, 95]. CPPs would perform as good supporters to improve the delivery efficiency of gene delivery systems, especially to the difficult targets.

How to use ligands wisely needs to be considered in the future. Not only in my results but also in literatures, the significant improvement of ligand-modified systems always showed at relatively high N/P ratios [95, 101], maybe when the ligand density meets a bottom limit. To increase the density of ligands, dendrimers offer a promising solution. The rich peripherals on the dendrimer surface provide the sites for ligand modification, and the ligand density can be regulated in the chemical reaction. Saccharide ligands on dendrimers have been verified to have a special multivalent interaction with their receptors, which magnifies the interaction by more than 100 folds [177-179]. Unlike saccharide ligands, peptide ligands on dendrimers don't have such magnitudes of elevation, but such pattern also showed benefits to cell binding, cell recognizing, and cell internalization [39, 180-182]. Gray et al. conjugated the multivalent RGD or R9 peptides to a dendrimeric material, and both modification strategies exhibited improved delivery

efficiency of microRNA to HUVEC cells compared to the unmodified materials [183], showing the benefits from multifunctional ligands.

Degradability will become a necessary character of cationic polymers in the future. The difference between R9 and PLR demonstrated that the high-density positive charges were the origin of cytotoxicity, and the degradable design addressed the issue in our results. In addition, the degradation of carriers allows the release of siRNA from the delivery vehicles to initiate RNAi process; otherwise siRNA can't perform its function. Thus the degradability is critical for both safety and function of cationic delivery systems.

5.2 Neutral crosslinked dendrimeric systems

The neutral crosslinked system brings a new concept in constructing gene delivery systems, by using the combination of the buffering amines, a crosslinking method, and surface ligands to replace the role of primary amines in cationic materials. The established delivery vehicles are superior to traditional cationic delivery vehicles at five aspects. First, the replacement of primary amines significantly reduces the toxicity compared to the original cationic materials. The distinct performance between G5.0 PAMAM and PAMAM-HYD in MTS assay provided solid evidence for this point. Second, the neutrality of the crosslinked particles minimizes the non-specific interaction with extracellular components, reducing the risk of unexpected particle dissociation. It is very common for cationic particles to interact with anionic proteins in serum or ECM, which is one major reason attributed to their instability, but the neutral crosslinked particles avoid such drawback. Third, the crosslinking bonds hold the neutral particles stable from deformation and dissociation, further prolonging the effective time window of delivery vehicles. It was reported that the cationic delivery particles continued with

secondary self-assembling between each other over time, and the particle size exhibited a growing tendency after formulation [156]. Such deformation of particles caused the decreased transfection efficiency in cells, but the transfection efficiency could be preserved when the particles were crosslinked [156]. In our study, the crosslinking strategy benefited the neutral particles in the same way. Forth, the neutral crosslinked system is tunable regarding the siRNA loading efficiency, the particle size, and the targeting capability. The final transfection efficiency is a combinational result from these factors, and each of them can be finely adjusted by the crosslinker concentration and the surface ligand density. In contrast, the charge-interaction based particles are generally formed dependent on random self-assemblies without controllability. Fifth, the neutral crosslinked particles have the potential to release siRNA into cytoplasm when the cleavage of crosslinking bonds is triggered under a specific environment, but the timing of siRNA release from cationic delivery vehicles is vague and uncontrolled. To sum up, the neutral crosslinked dendrimeric system provides safety, stability, and controllability for siRNA delivery, which can be considered as a breakthrough in this area.

The choice of ligands is critical for the efficiency of the neutral crosslinked system. Due to the absence of charge interactions with cell membranes, the cell internalization of neutral particles basically depends on the surface ligands. The suitable ligands promote the cell binding, cell recognizing, and cell internalization, and with the multivalent effects brought by the dendrimeric structure such enhancement could be magnified. Yet on the other hand, inappropriate ligands with multivalent effects may become barriers between particles and cells, lowering the rate of cell uptake of the

delivery vehicles. Accordingly, if the neutral crosslinked particles need to be applied to other types of cells, a potent ligand needs to be identified before the particle formulation.

The concept of the neutral crosslinked system is not restricted to the PAMAM dendrimer, and in fact any dendrimer, polymer, or other types of materials containing buffering amines in their structures can be considered for this idea. For instance, PEI, which is very famous of its high transfection efficiency as well as the high cytotoxicity, is being kept away from human studies due to the safety concern. If the PEI is transformed into a neutral material that preserves the outstanding delivery capacity and meanwhile alleviates the toxicity, the hurdle that prevents PEI from clinical applications could be removed. Considering the low cost of PEI compared to the PAMAM dendrimer, the neutral delivery system based on PEI is actually more promising to be finally translated into manufacture and medical practices.

The current rational of the neutral crosslinked system need to be further optimized. Right now the formulation procedure of the crosslinked particles is relatively complicated, containing multiple steps. The main reason is actually the concern for the toxicity of glutaraldehyde, so blocking with small molecules and dialysis are used in the protocol to remove all unreacted glutaraldehyde. To simplify the procedure, a biocompatible crosslinker should be introduced into the system, and the peripheral of the neutral dendrimer should be changed to a corresponding group that can react with the new crosslinker. To make sure the whole system preserves the degradability and the siRNA controlled-release mechanism, the crosslinking bond is better to be reversible at intracellular environments, such as the disulfide bond, acetal linkage, ester linkage, and even enzyme-sensitive linkages. Except the crosslinking bond, the degradability of the

main body of the material or the crosslinker can also serve to release siRNA under specific conditions. With a simplified formulation procedure, the translation of the neutral crosslinked delivery system into clinical practices could become expectable.

5.3 Dendrimeric delivery systems in cardiac tissue

The R9-conjugated tadpole dendrimer developed in Chapter 4 paves a way for using RNAi therapeutics in treating cardiovascular diseases. The safety of the materials was confirmed by the MTT assay in primary CMs *in vitro*, and the delivery efficiency was verified by the regulated gene expression and the improved cardiac functions. Thus the tadpole dendrimers are promising non-viral gene delivery systems in cardiac tissue, and they are not restricted for siRNA but maybe also suitable for other small nucleic acid molecules, such as microRNA. Moreover, an increasing number of cardiac-specific microRNAs that can enhance cardiac regeneration [19-21] have been discovered recently. To fully exploit the usage of the tadpole dendrimers, new targets and new therapeutic molecules could be applied.

The behavior of siRNA after delivery is worthy being further studied. In the current tadpole dendrimers, CPPs are used as the functional ligands, which enhance the cell internalization of carried cargoes. Although we expected the cell uptake of siRNA-loaded particles in CMs could be improved by the CPP conjugation, it was possible that other types of cells also endocytosized the delivery vehicles and had down-regulated AT1R expression. For instance, the R9 was reported to promote the microRNA delivery to HUVECs based on a dendrimeric material [183]. In this case, the AT1R expression may also reduced in fibroblasts, endothelial cells, and inflammatory

cells that poured in after injury happened. The remaining question is whether the improved cardiac functions resulted solely from the AT1R down-regulation in CMs or not. Telling apart the contribution made from different types of cells may give us a hint if the specific targeting to one type of cells is highly required or the general gene regulation in cardiac tissue also works well. Undoubtedly, the situation may be different depending on the target gene, but a small study on the distribution of delivered siRNA in cardiac tissue would be helpful in the future.

The design of tadpole dendrimers allows the chance for the systemic and targeted delivery by replacing the CPP ligand with a targeting ligand. In particular for cardiac tissue, the collaboration between CPPs and targeting ligands is encouraged, as the CPP played a crucial role to enhance the cell uptake of the delivery vehicles in CMs in our study. In fact, Bull et al. compared TAT and a CM-specific ligand PCM in their polymeric system and tried the combination of the two ligands. According to their results, TAT-conjugated vehicles had higher transfection efficiency *in vitro*, while PCM-conjugated vehicles showed stronger capability of specifically targeting to CMs other than fibroblasts. The mixture of the two ligands actually exhibited synergetic effects with better performance than the two single ligands. Therefore, the cooperation between CPPs and targeting ligands could be a potent tool for systemic delivery, and such strategy could be tried on the tadpole dendrimers in the future.

The incorporation of gene delivery systems into other biomedical engineering methods may also be a future direction. Currently, the majority of gene delivery systems focus on the transient gene regulation, but many diseases need a regulation in a long time period of the chronic phase. For instance, the AT1R expression increased within a time

window from 3 day to weeks post-MI. To suppress the AT1R activation during this time period, traditional pharmacological AT1R blockers can be orally administrated every day, easy and convenient; however, as to siRNA delivery, current techniques can hardly fully cover this time period without repeated injections, which would bring more painful experience if translated to patients. Therefore, the controlled release of siRNA-loaded particles instead of siRNA itself will become an upcoming issue. One possible idea is to incorporate siRNA-loaded delivery vehicles into hydrogels, such as alginate hydrogel used by Cohen's group to repair damage tissue in hearts [184]. siRNA-loaded particles could diffuse from the hydrogel over time, which wouldn't affect the release of gel-loaded growth factors into the environment if there's any. In this case, such system could combine the healing function from hydrogels and the gene regulation function from the delivery vehicles, and meantime preserve the protein delivery function of the gel. Similarly, tissue-engineering scaffold attached with siRNA-loaded particles may also be considered for the further development.

5.4 Concluding remark

Three innovations were demonstrated in the dissertation.

1. The dissertation described the investigation of the CPP polymers to illustrate the strengths of polymeric materials and the contribution of functional ligands to the transfection efficiency of CPP polymers.
2. The dissertation described the development of the neutral crosslinked dendrimeric system, which brings a new concept for the development of gene delivery systems.
3. The dissertation described the application of siRNA delivery systems in

modulating gene expression in cardiac tissue and demonstrated the usage of RNAi therapeutics in a cardiac IR model, which promotes the development of gene therapy in the cardiovascular disease management.

This dissertation developed effective polymeric and dendrimeric siRNA delivery systems with reduced toxicity as well as enhanced stability and targeting efficiency, and they are paving ways for novel non-viral siRNA delivery systems for gene therapy. With the rapid progress in the area of gene delivery, gene therapy will become a powerful weapon for the management of critical diseases and personalized therapy to improve human health.

APPENDIX A

MATERIALS AND METHODS

Synthesis of degradable poly(oligo-arginine) (dPOA) polymers

dPOA was produced by an oxidative polycondensation method in a mild oxidative environment. Briefly, Ac-CRRRRRRRRRC-NH₂ (CR9C) (or Ac-CRRRRRRRRRKC-NH₂ (CR9KC)) and Ac-CRRRRRRRRR-NH₂ (CR9) were mixed as a molar ratio of 3:1 in 20% DMSO (DMSO: DPBS volume ratio =2:8) to a concentration of 20 mg/ml, and the mixture was incubated in water bath at 70 °C with sonication for 12 h. The products were purified against extensive dialysis using a cellulose membrane (MWCO 7 kDa, Union Carbide, NY). The final products were lyophilized and stored at -20 °C for future use. The molecular weight of the polymers was determined by gel permeation chromatography (GPC).

Synthesis of RGD-g- dPOA

(CR9KC)_n was dissolved in DPBS at a concentration of 10 mg/ml and reacted with N-succinimidyl-3-(2-pyridyldithiol)propionate (SPDP) of 0.2 molar equivalents of CR9KC monomers in DPBS at room temperature for 2 h, followed by a reaction with excess Ac-CGRGDS-NH₂ peptides at room temperature for 24 h. The obtained RGD-g-dPOA was purified against extensive dialysis using a cellulose membrane (MWCO 7 kDa, Union Carbide, NY) and lyophilized and stored at -20 °C for future use.

Preparation of siRNA-loaded polyelectrolyte particles and gel retardation analysis

siRNA in DPBS (2 μ M) was added to an equal volume of solutions of cationic materials (such as the arginine peptides and tadpole dendrimers) at indicated concentrations to achieve varied N/P ratios, and the samples were incubated at room temperature for 20 min. Gel electrophoresis was performed to visualize the unloaded siRNA in solutions. Samples were detected in a 3.5% agarose gel in pH 8.5 TBE buffer, and images were captured by a Tanon-1600 Gel Documentation System (Tanon, Shanghai, China).

Fluorescent dye exclusive assay

100 \times Gene Finder was mixed with a 0.2 μ M siRNA solution at a volume ratio of 1:50, followed by incubation at room temperature for 5 min. The Gene Finder-combined siRNA was mixed with cationic materials as described above. The fluorescent signals of the samples were determined by a SpectraMax M2 microplate reader (MD, USA) to detect unloaded siRNA in solutions (Ex: 488nm, Em: 522nm).

RNase protection assay and GSH treatment

siRNA-loaded arginine peptide particles were treated with 5 unit RNase at 37 $^{\circ}$ C for 30 min, and the treatment was terminated by a 1% SDS solution. Samples were treated with excess polyacrylic acid (PAA) to release siRNA from particles, followed by electrophoresis in a 3.5% agarose gel in 0.5 \times TBE buffer (0.045mol/L Tris, 0.045mol/L boric acid, 0.001mol/L EDTA). Images were captured by a Tanon-1600 Gel Documentation System (Tanon, Shanghai, China).

For the GSH treatment assay, siRNA-loaded arginine peptide particles were treated with a 5 mM glutathione solution (GSH) at 37 $^{\circ}$ C for 1 h, followed by the treatment of

excess PAA at room temperature for 30 min, and then samples were analyzed by electrophoresis in a 3.5% agarose gel.

Particle size and zeta-potential analysis

To characterize the particle size and zeta-potential of the siRNA-loaded particles, samples were prepared as described in their corresponding sections and diluted 10 times by deionized water, followed by analysis through light scattering experiments with a ZetaPALS machine (Brookhaven Instruments, NY).

Establishment of the luciferase stably expressing cell line

Luciferase expressing plasmid pGL4.51 was transfected into A549 cells with Lipofectamine 2000 according to the manufacturer's protocol, followed by 800 µg/ml G418's selection for two weeks. Survival clones were transferred into a 96-well plate and selected by 400 µg/ml G418 for another 2 months. The luciferase expression was measured by a Bright-Glo luciferase assay system (Promega). The obtained stable transfectants were termed as A549-luci and cultured in F12 nutrient medium with 10% FBS and 1% streptomycin and penicillin.

MTS assay

MTS assay was performed according to the manufacturer's protocol. In brief, cells were seeded into a 96-well plate at a confluency around 80%. Tested materials or delivery particles were added to cells at indicated concentrations and incubated with cells for 6- 48 h according to the transfection experiments. The cell culture supernatants were replaced by 100 µl of fresh medium and 20 µl of MTS reagent. After incubation at 37 °C with 5% CO₂ for 1 h, the light absorbance at 490 nm of each well was recorded by the SpectraMax M2

microplate reader.

siRNA transfection

A549-luci cells (or HepG2 cells) were seeded into a 96-well plate at a density of 1.2×10^4 cells/well one day before transfection. siRNA-loaded dPOA particles or RGD-g-dPOA particles were added to cells in serum-free F12 (or DMEM) medium at a siRNA concentration of 100 nM, and after 6 h incubation the medium was replaced by fresh culture medium. Luciferase expression and total protein amount were determined by a Bright-Glo luciferase assay system and BCA protein assay 48 h after transfection.

Fluorescence microscopy and flow cytometry analysis

The procedure of cy3-siRNA transfection was the same as the non-labeled siRNA described in their corresponding sections. After transfection, cells were washed twice with DPBS, and nuclei were stained with DAPI for 10 min. Images were captured by an IX71 fluorescence microscopy (Olympus, Japan), and cellular uptake rates of materials were compared. For flow cytometry analysis, cy3-siRNA transfected cells were washed by DPBS twice and detached from the plate bottom after trypsin treatment. Flow cytometry was conducted by FASCalibur (Becton, Dickinson and Company, NJ), and data were processed using Summit 4.0 software.

Synthesis of PAMAM-hydrazide (PAMAM-HYD) and saccharide-modified

PAMAM-HYDs

PAMAM-HYD and saccharide-modified PAMAM-HYD dendrimers were synthesized following a published method in our lab [40]. 50 mg/ml G4.0 PAMAM solution was reacted with methyl acrylate of 10 molar equivalents of the primary amines

at 37 °C for 48 h, followed by rotary evaporation to remove the unreacted methyl acrylate at 65 °C. The obtained G4.5 PAMAM was further reacted with hydrazine hydrate of 10 molar equivalents of the methyl esters for 24 h at 55 °C under reflux, followed by rotary evaporation and extensive dialysis. The synthesis of PAMAM-HYD was conducted by Xiaopeng Liu, who was a graduate student in our lab.

To conjugate saccharide ligands, 10 mg/ml PAMAM-HYD was reacted with saccharide molecules of 10 molar equivalents of hydrazide groups in pH 5.0 phosphate buffer for 24 h at 50 °C. The crude saccharide-modified dendrimers were purified via dialysis. ¹H-NMR was used to determine the saccharide modification level in each product. The tested saccharides included mannose, glucose, GlcNAc, galactose, and lactose, termed as Man-, Glu-, GlcNAc-, Gal-, and Lac-PAMAM. The synthesis of these glycodendrimers was conducted by Xiaopeng Liu [40].

To synthesize GalNAc-PAMAM-HYDs with different GalNAc modification levels, PAMAM-HYD was reacted with GalNAc of 0.5, 1 or 1.5 molar equivalents of the hydrazide groups according to the same protocol described above. The GalNAc modification level was analyzed by ¹H-NMR.

Screening of the efficient ligand for HepG2 cells

To identify the potent saccharide ligand for HepG2 cells, different saccharide-modified PAMAM-HYDs were labeled with fluorescein and incubated with HepG2 cells at a concentration of 1.6 μM for 24 h. The cells were washed with DPBS, detached from the culture plate, and subjected to flow cytometry analysis by a FASCalibur instrument (Becton, Dickinson and Company, NJ).

Preparation of crosslinked delivery systems

To study the complexation between siRNA and neutral dendrimers, 2 μM siRNA was added to an equal volume of dendrimer solutions of indicated concentrations at pH 5.0 and 7.4, respectively.

To prepare crosslinked systems, 2 μM siRNA and 25 mM glutaraldehyde were first mixed at pH 5.0 for 5 min, and then the dendrimer solution was added to the mixture, allowing the incubation at 37 $^{\circ}\text{C}$ for 1 h. To terminate the crosslinking reaction, excessive adipic acid dihydrazide (ADH) molecules were added to block the unreacted glutaraldehyde, and meanwhile the solution pH was adjusted to 7 using a NaOH solution. To purify the siRNA-loaded crosslinked particles, the samples were subjected to dialysis in PBS at pH 7.4 [185].

Gel retardation analysis and fluorescent dye exclusive assay

To determine whether siRNA interacted with the neutral dendrimers or was loaded in the crosslinked particles, gel electrophoresis was performed to visualize the unloaded siRNA in solution. Samples were detected in a 3.5% agarose gel in pH 8.5 TBE buffer, and images were captured by a Tanon-1600 Gel Documentation System (Tanon, Shanghai, China).

Unloaded siRNA was also quantitatively analyzed by nucleic acid fluorescent dye. Briefly, siRNA-dendrimer complexes or siRNA-loaded crosslinked particles were prepared as described above, and Gene Finder was added to the obtained solutions. After 5 min incubation, the fluorescent signal was measured and recorded by a SpectraMax M2 microplate reader (Molecular Devices, CA) (excitation: 488 nm; emission: 522 nm).

RNAi experiments

First, luciferase-expressing HepG2 cells were produced by the transfection of pGL4.51 plasmid (Promega) with Lipofectamine 2000. 24 h after the plasmid transfection, 10 pmol siRNA against the firefly luciferase gene was loaded in crosslinked particles as described above, and the particles were added to HepG2 cells in DMEM medium containing 10% FBS, allowing a siRNA concentration of 50 nm during transfection. The luciferase protein expression was measured by a Bright-Glo luciferase assay system after 48 h, and the total protein was measured via a BCA protein assay kit.

Fluorescence microscopy analysis

To visualize the cell uptake, neutral dendrimers were labeled with NHS-fluorescein molecules and incubated with HepG2 cells for 24 h before imaged. Meanwhile, cy3-siRNA loaded crosslinked particles were prepared as described above and incubated with HepG2 cells for 12 h. Cells were washed with DPBS thrice before fluorescence images were captured by an IX71 fluorescence microscope (Olympus, Japan).

Synthesis of tadpole dendrimeric materials

The synthesis of the tadpole dendrimeric materials was divided into three steps. First, 10 mg/ml cystamine core G4.0 PAMAM (Sigma) was reacted with dithiothreitol (DTT, Sigma) of 10 molar equivalents of disulfide bonds for 24 h in PBS, followed by ultrafiltration via 3 KDa MWCO Amicon® Ultra Centrifugal Filters (Millipore). Second, the reduced PAMAM with exposed thiol groups was reacted with Py-PEG-Py (Jiaxing Biomatrix Inc.) of 5 molar equivalents of thiol groups for 24 h, and the intermediates

were purified by extensive dialysis. Third, Ac-CRRRRRRRRR-NH₂ (R9), Ac-CGGWRKKRRQRRR-NH₂ (TAT) (GL Biochem Ltd), or cysteine (Sigma) of 1.5 molar equivalents of PEG was reacted, respectively, with the intermediates for 24 h, followed by dialysis using a 7 kDa MWCO cellulose membrane. The structure of tadpole dendrimeric materials and the peptide modification level in each product were analyzed by ¹H-NMR [96].

Particle size and zeta-potential

Particle sizes were analyzed by a 90Plus Particle Size Analyzer instrument, and the zeta-potentials were measured by a Zeta Sizer Nano ZS90 instrument.

siAT1R transfection in CMs

CMs were isolated from Sprague–Dawley (SD) rat pups (Charles River Labs) as described in literature [99], and cells were allowed to grow to 80% confluency before further experiments. Tadpole dendrimers loaded with or without siRNA against AT1R (5'-UGAAGAGCCUGAUCAAAUAdTdT-3' (sense) and 3'-dTdTACUUCUCGGACUAGUUUAU-5' (antisense), Dharmacon) were prepared as described above in DMEM, and the siRNA-loaded particles were incubated with CMs in DMEM medium containing 2% serum for 24 h before RNA isolation [96].

qPCR to detect gene expression level

Total RNA was isolated using Trizol reagent according to the manufacturer's protocol, followed by reverse transcription by an M-MLV kit (Invitrogen) to produce cDNA. cDNA was subjected to quantitative real-time PCR (qPCR) by Power SYBR Green (Invitrogen) in an Applied Biosystems StepOne Plus real time PCR system with

the primers below. Gene expression levels were normalized relative to that of the housekeeping gene 18S, and the results were presented as fold changes for siRNA-loaded particles relative to the empty dendrimer vehicles for the *in vitro* transfection [96].

Table A.1 Primer sequences used in qPCR

Gene name	Forward primer	Reverse primer
AT1R	TTCTCAATCTCGCCTTGGCTG ACT	AAGGAACACACTGGCGTAGAGG TT
AT2R	AATATGCTCAGTGGTCTGCTG GGA	CACAACAGCAGCTGCCATCTTC AA
Col-1	TGCTGCTTGCAGTAACGTCG	TCAACACCATCTCTGCCTCG
18S	TTCCTTACCTGGTTGATCCTG CCA	AGCGAGCGACCAAAGGAACCAT AA

Animal studies

To get the IR injury model, adult SD rats were anesthetized with 1-3% isoflurane followed by heart exposure, and the left descending coronary artery was occluded for 30 min before releasing the suture. Operated animals were randomly divided into 3 groups, and immediately after blood flow recovery, 80 µl samples were injected intramyocardially at 3 regions of the border zone: saline (IR group), saline containing empty dendrimer (IR + dendrimer group), or saline containing siRNA- loaded particles (IR + dendrimer/siRNA group). siRNA was given at a dose of 5 µg/kg. Animals that only

went through chest opening without artery ligation were kept as sham animals. After injection, chests were closed and rats were allowed to recover on a heating pad. All animal studies were approved by Emory University Institutional Animal Care and Use Committee [96].

At the 3-day time point, cardiac functions of the animals were measured by echocardiography and Pressure-Volume (PV) cardiac hemodynamics, and then animals were subjected to scarification. Total RNA was isolated from the left ventricle tissue using Trizol reagent, and the copy number of genes was determined by qPCR using a standard curve method and normalized to 18S [96].

Infarct size measurement

Three days after injection, rats were anesthetized with inhaled isoflurane, and the coronary artery was re-occluded at the same place of occlusion as the initial surgery. 10% filtered Evan's blue dye was used to perfuse the heart through the aorta until the blue dye fulfilled the tissue beyond the infarct area. Hearts were sliced and soaked in a 1% 2,3,5-triphenyltetrazolium chloride (TTC) solution for 15-20 min. Finally, the heart slides were fixed in 4% paraformaldehyde over night before imaged. ImageJ was used to trace the areas of three different colors: the blue stands for the viable tissue, the red stands for the area at risk, and the white stands for the infarcted area [96].

REFERENCES

- [1] Venter JC, Adams MD, Myers EW, Li PW, Mural RJ, Sutton GG, et al. The sequence of the human genome. *Science*. 2001;291:1304-51.
- [2] Oh YK, Park TG. siRNA delivery systems for cancer treatment. *Adv Drug Deliv Rev*. 2009;61:850-62.
- [3] Takahashi Y, Nishikawa M, Takakura Y. Nonviral vector-mediated RNA interference: its gene silencing characteristics and important factors to achieve RNAi-based gene therapy. *Adv Drug Deliv Rev*. 2009;61:760-6.
- [4] Whitehead KA, Langer R, Anderson DG. Knocking down barriers: advances in siRNA delivery. *Nat Rev Drug Discov*. 2009;8:129-38.
- [5] Bennett CF, Swayze EE. RNA targeting therapeutics: molecular mechanisms of antisense oligonucleotides as a therapeutic platform. *Annu Rev Pharmacol*. 2010;50:259-93.
- [6] Pecot CV, Calin GA, Coleman RL, Lopez-Berestein G, Sood AK. RNA interference in the clinic: challenges and future directions. *Nat Rev Cancer*. 2011;11:59-67.
- [7] Elbashir SM, Harborth J, Weber K, Tuschl T. Analysis of gene function in somatic mammalian cells using small interfering RNAs. *Methods*. 2002;26:199-213.
- [8] Tokatlian T, Segura T. siRNA applications in nanomedicine. *Wiley Interdiscip Rev Nanomed Nanobiotechnol*. 2010;2:305-15.
- [9] Thomas C, Ehrhardt A, Kay M. Progress and problems with the use of viral vectors for gene therapy. *Nat Rev Genet*. 2003;4:346-58.
- [10] De Smedt SC, Demeester J, Hennink WE. Cationic polymer based gene delivery systems. *Pharm Res*. 2000;17:113-26.
- [11] Duncan R. The dawning era of polymer therapeutics. *Nat Rev Drug Discov*. 2003;2:347-60.
- [12] Svenson S. Dendrimers as versatile platform in drug delivery applications. *Eur J Pharm Biopharm*. 2009;71:445-62.

- [13] Lee CC, MacKay JA, Frechet JM, Szoka FC. Designing dendrimers for biological applications. *Nat Biotechnol.* 2005;23:1517-26.
- [14] Burnett JC, Rossi JJ, Tiemann K. Current progress of siRNA/shRNA therapeutics in clinical trials. *Biotechnol J.* 2011;6:1130-46.
- [15] Watts JK, Corey DR. Clinical status of duplex RNA. *Bioorg Med Chem Lett.* 2010;20:3203-7.
- [16] Koldehoff M, Steckel NK, Beelen DW, Elmaagacli AH. Therapeutic application of small interfering RNA directed against bcr-abl transcripts to a patient with imatinib-resistant chronic myeloid leukaemia. *Clin Exp Med.* 2007;7:47-55.
- [17] Santel A, Aleku M, Keil O, Endruschat J, Esche V, Fisch G, et al. A novel siRNA-lipoplex technology for RNA interference in the mouse vascular endothelium. *Gene Ther.* 2006;13:1222-34.
- [18] Davis ME, Zuckerman JE, Choi CH, Seligson D, Tolcher A, Alabi CA, et al. Evidence of RNAi in humans from systemically administered siRNA via targeted nanoparticles. *Nature.* 2010;464:1067-70.
- [19] Porrello ER, Mahmoud AI, Simpson E, Johnson BA, Grinsfelder D, Canseco D, et al. Regulation of neonatal and adult mammalian heart regeneration by the miR-15 family. *Proc Natl Acad Sci U S A.* 2013;110:187-92.
- [20] Eulalio A, Mano M, Dal Ferro M, Zentilin L, Sinagra G, Zacchigna S, et al. Functional screening identifies miRNAs inducing cardiac regeneration. *Nature.* 2012;492:376-81.
- [21] Jayawardena TM, Egemnazarov B, Finch EA, Zhang L, Payne JA, Pandya K, et al. MicroRNA-mediated in vitro and in vivo direct reprogramming of cardiac fibroblasts to cardiomyocytes. *Circ Res.* 2012;110:1465-73.
- [22] Xu L, Anchordoquy T. Drug delivery trends in clinical trials and translational medicine: challenges and opportunities in the delivery of nucleic acid-based therapeutics. *J Pharm Sci.* 2011;100:38-52.
- [23] Hunter AC. Molecular hurdles in polyfectin design and mechanistic background to polycation induced cytotoxicity. *Adv Drug Deliv Rev.* 2006;58:1523-31.
- [24] Jain K, Kesharwani P, Gupta U, Jain NK. Dendrimer toxicity: let's meet the challenge. *Int J Pharm.* 2010;394:122-42.

- [25] Mukherjee SP, Davoren M, Byrne HJ. In vitro mammalian cytotoxicological study of PAMAM dendrimers - towards quantitative structure activity relationships. *Toxicol In Vitro*. 2010;24:169-77.
- [26] Stasko NA, Johnson CB, Schoenfisch MH, Johnson TA, Holmuhamedov EL. Cytotoxicity of polypropylenimine dendrimer conjugates on cultured endothelial cells. *Biomacromolecules*. 2007;8:3853-9.
- [27] Symonds P, Murray JC, Hunter AC, Debska G, Szewczyk A, Moghimi SM. Low and high molecular weight poly(L-lysine)s/poly(L-lysine)-DNA complexes initiate mitochondrial-mediated apoptosis differently. *FEBS Lett*. 2005;579:6191-8.
- [28] Koo H, Kang H, Lee Y. Analysis of the relationship between the molecular weight and transfection efficiency/cytotoxicity of poly-L-arginine on a mammalian cell line. *Bull Korean Chem Soc*. 2009;30:927-30.
- [29] Fischer D, Bieber T, Li Y, Elsasser HP, Kissel T. A novel non-viral vector for DNA delivery based on low molecular weight, branched polyethylenimine: effect of molecular weight on transfection efficiency and cytotoxicity. *Pharm Res*. 1999;16:1273-9.
- [30] Florea BI, Meaney C, Junginger HE, Borchard G. Transfection efficiency and toxicity of polyethylenimine in differentiated Calu-3 and nondifferentiated COS-1 cell cultures. *AAPS PharmSci*. 2002;4:1-11.
- [31] Svenson S, Tomalia DA. Dendrimers in biomedical applications-reflections on the field. *Adv Drug Deliv Rev*. 2005;57:2106-29.
- [32] Sebestik J, Niederhafner P, Jezek J. Peptide and glycopeptide dendrimers and analogous dendrimeric structures and their biomedical applications. *Amino Acids*. 2011;40:301-70.
- [33] Liu J, Gray WD, Davis ME, Luo Y. Peptide- and saccharide-conjugated dendrimers for targeted drug delivery: a concise review. *Interface Focus*. 2012;2:307-24.
- [34] Lee RT, Lee YC. Affinity enhancement by multivalent lectin-carbohydrate interaction. *Glycoconj J*. 2000;17:543-51.
- [35] Lundquist JJ, Toone EJ. The cluster glycoside effect. *Chem Rev*. 2002;102:555-78.
- [36] Shukla R, Thomas TP, Peters J, Kotlyar A, Myc A, Baker JR. Tumor angiogenic vasculature targeting with PAMAM dendrimer-RGD conjugates. *Chem Commun*.

2005;5739-41.

- [37] Dijkgraaf I, Rijnders AY, Soede A, Dechesne AC, van Esse GW, Brouwer AJ, et al. Synthesis of DOTA-conjugated multivalent cyclic-RGD peptide dendrimers via 1,3-dipolar cycloaddition and their biological evaluation: implications for tumor targeting and tumor imaging purposes. *Org Biomol Chem*. 2007;5:935-44.
- [38] Hill E, Shukla R, Park SS, Baker JR, Jr. Synthetic PAMAM-RGD conjugates target and bind to odontoblast-like MDPC 23 cells and the predentin in tooth organ cultures. *Bioconjug Chem*. 2007;18:1756-62.
- [39] McNerny DQ, Kukowska-Latallo JF, Mullen DG, Wallace JM, Desai AM, Shukla R, et al. RGD dendron bodies; synthetic avidity agents with defined and potentially interchangeable effector sites that can substitute for antibodies. *Bioconjug Chem*. 2009;20:1853-9.
- [40] Liu X, Liu J, Luo Y. Facile glycosylation of dendrimers for eliciting specific cell-material interactions. *Polym Chem*. 2012;3:310-3.
- [41] Roberts JC, Bhalgat MK, Zera RT. Preliminary biological evaluation of polyamidoamine (PAMAM) Starburst dendrimers. *J Biomed Mater Res*. 1996;30:53-65.
- [42] Kieburg C, Lindhorst TK. Glycodendrimer synthesis without using protecting groups. *Tetrahedron Lett*. 1997;38:3885-8.
- [43] Malik N, Wiwattanapatapee R, Klopsch R, Lorenz K, Frey H, Weener JW, et al. Dendrimers: relationship between structure and biocompatibility in vitro, and preliminary studies on the biodistribution of ¹²⁵I-labelled polyamidoamine dendrimers in vivo. *J Control Release*. 2000;65:133-48.
- [44] Agashe HB, Dutta T, Garg M, Jain NK. Investigations on the toxicological profile of functionalized fifth-generation poly (propylene imine) dendrimer. *J Pharm Pharmacol*. 2006;58:1491-8.
- [45] Melikov K, Chernomordik LV. Arginine-rich cell penetrating peptides: from endosomal uptake to nuclear delivery. *Cell Mol Life Sci*. 2005;62:2739-49.
- [46] Meade BR, Dowdy SF. Enhancing the cellular uptake of siRNA duplexes following noncovalent packaging with protein transduction domain peptides. *Adv Drug Deliv Rev*. 2008;60:530-6.

- [47] Nakase I, Takeuchi T, Tanaka G, Futaki S. Methodological and cellular aspects that govern the internalization mechanisms of arginine-rich cell-penetrating peptides. *Adv Drug Deliv Rev.* 2008;60:598-607.
- [48] Tonges L, Lingor P, Egle R, Dietz GPH, Fahr A, Bahr M. Stearylated octaarginine and artificial virus-like particles for transfection of siRNA into primary rat neurons. *RNA.* 2006;12:1431-8.
- [49] Kumar P, Wu HQ, McBride JL, Jung KE, Kim MH, Davidson BL, et al. Transvascular delivery of small interfering RNA to the central nervous system. *Nature.* 2007;448:39-43.
- [50] Wang YH, Hou YW, Lee HJ. An intracellular delivery method for siRNA by an arginine-rich peptide. *J Biochem Bioph Meth.* 2007;70:579-86.
- [51] Kim EJ, Shim G, Kim K, Kwon IC, Oh YK, Shim CK. Hyaluronic acid complexed to biodegradable poly L-arginine for targeted delivery of siRNAs. *J Gene Med.* 2009;11:791-803.
- [52] Kim SW, Kim NY, Bin Choi Y, Park SH, Yang JM, Shin S. RNA interference in vitro and in vivo using an arginine peptide/siRNA complex system. *J Control Release.* 2010;143:335-43.
- [53] Subramanya S, Kim SS, Abraham S, Yao JH, Kumar M, Kumar P, et al. Targeted delivery of small interfering RNA to human dendritic cells to suppress dengue virus infection and associated proinflammatory cytokine production. *J Virol.* 2010;84:2490-501.
- [54] Zhang C, Tang N, Liu X, Liang W, Xu W, Torchilin VP. siRNA-containing liposomes modified with polyarginine effectively silence the targeted gene. *J Control Release.* 2006;112:229-39.
- [55] Nakamura Y, Kogure K, Futaki S, Harashima H. Octaarginine-modified multifunctional envelope-type nano device for siRNA. *J Control Release.* 2007;119:360-7.
- [56] Kogure K, Akita H, Yamada Y, Harashima H. Multifunctional envelope-type nano device (MEND) as a non-viral gene delivery system. *Adv Drug Deliver Rev.* 2008;60:559-71.
- [57] Kim SH, Jeong JH, Kim TI, Kim SW, Bull DA. VEGF siRNA delivery system using arginine-grafted bioreducible poly(disulfide amine). *Mol Pharm.* 2009;6:718-26.

- [58] Merkel OM, Mintzer MA, Librizzi D, Samsonova O, Dicke T, Sproat B, et al. Triazine dendrimers as nonviral vectors for in vitro and in vivo RNAi: the effects of peripheral groups and core structure on biological activity. *Mol Pharm.* 2010;7:969-83.
- [59] Noh SM, Park MO, Shim G, Han SE, Lee HY, Huh JH, et al. Pegylated poly-L-arginine derivatives of chitosan for effective delivery of siRNA. *J Control Release.* 2010;145:159-64.
- [60] Kim WJ, Christensen LV, Jo S, Yockman JW, Jeong JH, Kim YH, et al. Cholesteryl oligoarginine delivering vascular endothelial growth factor siRNA effectively inhibits tumor growth in colon adenocarcinoma. *Mol Ther.* 2006;14:343-50.
- [61] Ertl G, Frantz S. Wound model of myocardial infarction. *Am J Physiol Heart Circ Physiol.* 2005;288:H981-3.
- [62] Dzau V, Braunwald E. Resolved and unresolved issues in the prevention and treatment of coronary artery disease: a workshop consensus statement. *Am Heart J.* 1991;121:1244-63.
- [63] Dzau VJ, Antman EM, Black HR, Hayes DL, Manson JE, Plutzky J, et al. The cardiovascular disease continuum validated: clinical evidence of improved patient outcomes: part II: Clinical trial evidence (acute coronary syndromes through renal disease) and future directions. *Circulation.* 2006;114:2871-91.
- [64] Probstfield JL, O'Brien KD. Progression of cardiovascular damage: the role of renin-angiotensin system blockade. *Am J Cardiol.* 2010;105:10A-20A.
- [65] Dzau VJ. Theodore Cooper Lecture: Tissue angiotensin and pathobiology of vascular disease: a unifying hypothesis. *Hypertension.* 2001;37:1047-52.
- [66] Ferrario CM, Strawn WB. Role of the renin-angiotensin-aldosterone system and proinflammatory mediators in cardiovascular disease. *Am J Cardiol.* 2006;98:121-8.
- [67] Ma TK, Kam KK, Yan BP, Lam YY. Renin-angiotensin-aldosterone system blockade for cardiovascular diseases: current status. *Br J Pharmacol.* 2010;160:1273-92.
- [68] Meggs LG, Coupet J, Huang H, Cheng W, Li P, Capasso JM, et al. Regulation of angiotensin II receptors on ventricular myocytes after myocardial infarction in rats. *Circ Res.* 1993;72:1149-62.

- [69] Suzuki J, Matsubara H, Urakami M, Inada M. Rat angiotensin II (type 1A) receptor mRNA regulation and subtype expression in myocardial growth and hypertrophy. *Circ Res.* 1993;73:439-47.
- [70] Yang BC, Phillips MI, Zhang YC, Kimura B, Shen LP, Mehta P, et al. Critical role of AT1 receptor expression after ischemia/reperfusion in isolated rat hearts: beneficial effect of antisense oligodeoxynucleotides directed at AT1 receptor mRNA. *Circ Res.* 1998;83:552-9.
- [71] Cohn JN, Tognoni G. A randomized trial of the angiotensin-receptor blocker valsartan in chronic heart failure. *N Engl J Med.* 2001;345:1667-75.
- [72] Daniels MC, Keller RS, de Tombe PP. Losartan prevents contractile dysfunction in rat myocardium after left ventricular myocardial infarction. *Am J Physiol Heart Circ Physiol.* 2001;281:H2150-8.
- [73] Dahlof B, Devereux RB, Kjeldsen SE, Julius S, Beevers G, de Faire U, et al. Cardiovascular morbidity and mortality in the Losartan Intervention For Endpoint reduction in hypertension study (LIFE): a randomised trial against atenolol. *Lancet.* 2002;359:995-1003.
- [74] Granger CB, McMurray JJ, Yusuf S, Held P, Michelson EL, Olofsson B, et al. Effects of candesartan in patients with chronic heart failure and reduced left-ventricular systolic function intolerant to angiotensin-converting-enzyme inhibitors: the CHARM-Alternative trial. *Lancet.* 2003;362:772-6.
- [75] Lithell H, Hansson L, Skoog I, Elmfeldt D, Hofman A, Olofsson B, et al. The Study on Cognition and Prognosis in the Elderly (SCOPE): principal results of a randomized double-blind intervention trial. *J Hypertens.* 2003;21:875-86.
- [76] Corinne Berthonneche, Thierry Sulpice, Stéphane Tanguy, Stephen O'Connor, Jean-Marc Herbert, Philippe Janiak, et al. AT1 receptor blockade prevents cardiac dysfunction and remodeling and limits TNF- α generation early after myocardial infarction in rats. *Cardiovasc Drugs Ther.* 2005;19:251-9.
- [77] Jugdutt BI, Menon V. Valsartan-induced cardioprotection involves angiotensin II type 2 receptor upregulation in dog and rat models of in vivo reperfused myocardial infarction. *J Card Fail.* 2004;10:74-82.
- [78] Yang Z, Bove CM, French BA, Epstein FH, Berr SS, DiMaria JM, et al. Angiotensin II type 2 receptor overexpression preserves left ventricular function after myocardial infarction. *Circulation.* 2002;106:106-11.

- [79] Kaschina E, Grzesiak A, Li J, Foryst-Ludwig A, Timm M, Rompe F, et al. Angiotensin II type 2 receptor stimulation: a novel option of therapeutic interference with the renin-angiotensin system in myocardial infarction? *Circulation*. 2008;118:2523-32.
- [80] Liu Y, Wenning L, Lynch M, Reineke TM. New poly(d-glucaramidoamine)s induce DNA nanoparticle formation and efficient gene delivery into mammalian cells. *J Am Chem Soc*. 2004;126:7422-3.
- [81] Liu Y, Reineke TM. Poly(glycoamidoamine)s for gene delivery: stability of polyplexes and efficacy with cardiomyoblast cells. *Bioconjug Chem*. 2006;17:101-8.
- [82] Tranter M, Liu Y, He S, Gulick J, Ren X, Robbins J, et al. In vivo delivery of nucleic acids via glycopolymer vehicles affords therapeutic infarct size reduction in vivo. *Mol Ther*. 2012;20:601-8.
- [83] Kim D, Hong J, Moon HH, Nam HY, Mok H, Jeong JH, et al. Anti-apoptotic cardioprotective effects of SHP-1 gene silencing against ischemia-reperfusion injury: Use of deoxycholic acid-modified low molecular weight polyethyleneimine as a cardiac siRNA-carrier. *J Control Release*. 2013;168:125-34.
- [84] Simon-Yarza T, Tamayo E, Benavides C, Lana H, Formiga FR, Grama CN, et al. Functional benefits of PLGA particulates carrying VEGF and CoQ in an animal of myocardial ischemia. *International journal of pharmaceutics*. *Int J Pharm*. 2013;454:784-90.
- [85] Binsalamah ZM, Paul A, Khan AA, Prakash S, Shum-Tim D. Intramyocardial sustained delivery of placental growth factor using nanoparticles as a vehicle for delivery in the rat infarct model. *Int J Nanomedicine*. 2011;6:2667-78.
- [86] Seshadri G, Sy JC, Brown M, Dikalov S, Yang SC, Murthy N, et al. The delivery of superoxide dismutase encapsulated in polyketal microparticles to rat myocardium and protection from myocardial ischemia-reperfusion injury. *Biomaterials*. 2010;31:1372-9.
- [87] Paulis LE, Geelen T, Kuhlmann MT, Coolen BF, Schafers M, Nicolay K, et al. Distribution of lipid-based nanoparticles to infarcted myocardium with potential application for MRI-monitored drug delivery. *J Control Release*. 2012;162:276-85.
- [88] Takahama H, Minamino T, Asanuma H, Fujita M, Asai T, Wakeno M, et al. Prolonged targeting of ischemic/reperfused myocardium by liposomal adenosine augments cardioprotection in rats. *J Am Coll Cardiol* . 2009;53:709-17.

- [89] Galagudza MM, Korolev DV, Sonin DL, Alexandrov IV, Minasian SM, Postnov VN, et al. Passive and active target delivery of drugs to ischemic myocardium. *Bull Exp Biol Med.* 2011;152:105-7.
- [90] Galagudza M, Korolev D, Postnov V, Naumisheva E, Grigorova Y, Uskov I, et al. Passive targeting of ischemic-reperfused myocardium with adenosine-loaded silica nanoparticles. *Int J Nanomedicine.* 2012;7:1671-8.
- [91] Galagudza MM, Korolev DV, Sonin DL, Postnov VN, Papayan GV, Uskov IS, et al. Targeted drug delivery into reversibly injured myocardium with silica nanoparticles: surface functionalization, natural biodistribution, and acute toxicity. *Int J Nanomedicine.* 2010;5:231-7.
- [92] Paul A, Binsalamah ZM, Khan AA, Abbasia S, Elias CB, Shum-Tim D, et al. A nanobiohybrid complex of recombinant baculovirus and Tat/DNA nanoparticles for delivery of Ang-1 transgene in myocardial infarction therapy. *Biomaterials.* 2011;32:8304-18.
- [93] Nam HY, Kim J, Kim SW, Bull DA. Cell targeting peptide conjugation to siRNA polyplexes for effective gene silencing in cardiomyocytes. *Mol Pharm.* 2012;9:1302-9.
- [94] Torchilin VP, Levchenko TS, Rammohan R, Volodina N, Papahadjopoulos-Sternberg B, D'Souza GG. Cell transfection in vitro and in vivo with nontoxic TAT peptide-liposome-DNA complexes. *Proc Natl Acad Sci U S A.* 2003;100:1972-7.
- [95] Nam HY, Kim J, Kim S, Yockman JW, Kim SW, Bull DA. Cell penetrating peptide conjugated bioreducible polymer for siRNA delivery. *Biomaterials.* 2011;32:5213-22.
- [96] Liu J, Gu C, Cabigas EB, Pendergrass KD, Brown ME, Luo Y, et al. Functionalized dendrimer-based delivery of angiotensin type 1 receptor siRNA for preserving cardiac function following infarction. *Biomaterials.* 2013;34:3729-36.
- [97] Clemons TD, Viola HM, House MJ, Iyer KS, Hool LC. Examining efficacy of "TAT-less" delivery of a peptide against the L-type calcium channel in cardiac ischemia-reperfusion injury. *ACS Nano.* 2013;7:2212-20.
- [98] Aso S, Ise H, Takahashi M, Kobayashi S, Morimoto H, Izawa A, et al. Effective uptake of N-acetylglucosamine-conjugated liposomes by cardiomyocytes in vitro. *J Control Release.* 2007;122:189-98.

- [99] Gray WD, Che P, Brown M, Ning X, Murthy N, Davis ME. N-acetylglucosamine conjugated to nanoparticles enhances myocyte uptake and improves delivery of a small molecule p38 inhibitor for post-infarct healing. *J Cardiovasc Transl Res.* 2011;4:631-43.
- [100] McGuire MJ, Samli KN, Johnston SA, Brown KC. In vitro selection of a peptide with high selectivity for cardiomyocytes in vivo. *J Mol Biol.* 2004;342:171-82.
- [101] Nam HY, McGinn A, Kim PH, Kim SW, Bull DA. Primary cardiomyocyte-targeted bio-reducible polymer for efficient gene delivery to the myocardium. *Biomaterials.* 2010;31:8081-7.
- [102] Kim SH, Jeong JH, Ou M, Yockman JW, Kim SW, Bull DA. Cardiomyocyte-targeted siRNA delivery by prostaglandin E(2)-Fas siRNA polyplexes formulated with reducible poly(amido amine) for preventing cardiomyocyte apoptosis. *Biomaterials.* 2008;29:4439-46.
- [103] Won YW, McGinn AN, Lee M, Bull DA, Kim SW. Targeted gene delivery to ischemic myocardium by homing peptide-guided polymeric carrier. *Mol Pharm.* 2013;10:378-85.
- [104] Ko YT, Hartner WC, Kale A, Torchilin VP. Gene delivery into ischemic myocardium by double-targeted lipoplexes with anti-myosin antibody and TAT peptide. *Gene Ther.* 2009;16:52-9.
- [105] Vancraeynest D, Havaux X, Pouleur AC, Pasquet A, Gerber B, Beauloye C, et al. Myocardial delivery of colloid nanoparticles using ultrasound-targeted microbubble destruction. *Eur Heart J.* 2006;27:237-45.
- [106] Fujii H, Li SH, Wu J, Miyagi Y, Yau TM, Rakowski H, et al. Repeated and targeted transfer of angiogenic plasmids into the infarcted rat heart via ultrasound targeted microbubble destruction enhances cardiac repair. *Eur Heart J.* 2011;32:2075-84.
- [107] Saliba Y, Mougnot N, Jacquet A, Atassi F, Hatem S, Fares N, et al. A new method of ultrasonic nonviral gene delivery to the adult myocardium. *J Mol Cell Cardiol.* 2012;53:801-8.
- [108] Chen S, Shimoda M, Chen J, Grayburn PA. Stimulation of adult resident cardiac progenitor cells by durable myocardial expression of thymosin beta 4 with ultrasound-targeted microbubble delivery. *Gene Ther.* 2013;20:225-33.

- [109] Chen ZY, Liang K, Qiu RX, Luo LP. Ultrasound- and liposome microbubble-mediated targeted gene transfer to cardiomyocytes in vivo accompanied by polyethylenimine. *J Ultrasound Med.* 2011;30:1247-58.
- [110] Zhang Y, Li W, Ou L, Wang W, Delyagina E, Lux C, et al. Targeted delivery of human VEGF gene via complexes of magnetic nanoparticle-adenoviral vectors enhanced cardiac regeneration. *PloS one.* 2012;7:e39490.
- [111] Dvir T, Bauer M, Schroeder A, Tsui JH, Anderson DG, Langer R, et al. Nanoparticles targeting the infarcted heart. *Nano Lett.* 2011;11:4411-4.
- [112] Mitchell DJ, Kim DT, Steinman L, Fathman CG, Rothbard JB. Polyarginine enters cells more efficiently than other polycationic homopolymers. *J Pept Res.* 2000;56:318-25.
- [113] Futaki S, Nakase I, Suzuki T, Zhang YJ, Sugiura Y. Translocation of branched-chain arginine peptides through cell membranes: flexibility in the spatial disposition of positive charges in membrane-permeable peptides. *Biochemistry.* 2002;41:7925-30.
- [114] Jones SW, Christison R, Bundell K, Voyce CJ, Brockbank SMV, Newham P, et al. Characterisation of cell-penetrating peptide-mediated peptide delivery. *Brit J Pharmacol.* 2005;145:1093-102.
- [115] Tam J.P., Wu C.R., Liu W., W. ZJ. Disulfide bond formation in peptides by dimethyl sulfoxide. Scope and applications. *J Am Chem Soc.* 1991;113:6657-62.
- [116] Oupicky D, Parker AL, Seymour LW. Laterally stabilized complexes of DNA with linear reducible polycations: strategy for triggered intracellular activation of DNA delivery vectors. *J Am Chem Soc.* 2002;124:8-9.
- [117] Read ML, Bremner KH, Oupicky D, Green NK, Searle PF, Seymour LW. Vectors based on reducible polycations facilitate intracellular release of nucleic acids. *J Gene Med.* 2003;5:232-45.
- [118] Read ML, Singh S, Ahmed Z, Stevenson M, Briggs SS, Oupicky D, et al. A versatile reducible polycation-based system for efficient delivery of a broad range of nucleic acids. *Nucleic Acids Res.* 2005;33:e86.
- [119] Soundara Manickam D, Bisht HS, Wan L, Mao G, Oupicky D. Influence of TAT-peptide polymerization on properties and transfection activity of TAT/DNA polyplexes. *J Control Release.* 2005;102:293-306.

- [120] Won YW, Yoon SM, Lee KM, Kim YH. Poly(oligo-D-arginine) with internal disulfide linkages as a cytoplasm-sensitive carrier for siRNA delivery. *Mol Ther*. 2011;19:372-80.
- [121] Rothbard JB, Garlington S, Lin Q, Kirschberg T, Kreider E, McGrane PL, et al. Conjugation of arginine oligomers to cyclosporin A facilitates topical delivery and inhibition of inflammation. *Nat Med*. 2000;6:1253-7.
- [122] Dietz GPH, Bahr M. Delivery of bioactive molecules into the cell: the Trojan horse approach. *Mol Cell Neurosci*. 2004;27:85-131.
- [123] Yonenaga N, Kenjo E, Asai T, Tsuruta A, Shimizu K, Dewa T, et al. RGD-based active targeting of novel polycation liposomes bearing siRNA for cancer treatment. *J Control Release*. 2012;160:177-81.
- [124] Vader P, Crielaard BJ, van Dommelen SM, van der Meel R, Storm G, Schiffelers RM. Targeted delivery of small interfering RNA to angiogenic endothelial cells with liposome-polycation-DNA particles. *J Control Release*. 2012;160:211-6.
- [125] Zhang YF, Wang JC, Bian DY, Zhang X, Zhang Q. Targeted delivery of RGD-modified liposomes encapsulating both combretastatin A-4 and doxorubicin for tumor therapy: in vitro and in vivo studies. *Eur J Pharm Biopharm*. 2010;74:467-73.
- [126] Ahn CH, Chae SY, Bae YH, Kim SW. Biodegradable poly(ethylenimine) for plasmid DNA delivery. *J Control Release*. 2002;80:273-82.
- [127] Forrest ML, Koerber JT, Pack DW. A degradable polyethylenimine derivative with low toxicity for highly efficient gene delivery. *Bioconjug Chem*. 2003;14:934-40.
- [128] Gosselin MA, Guo WJ, Lee RJ. Efficient gene transfer using reversibly cross-linked low molecular weight polyethylenimine. *Bioconjug Chem*. 2001;12:989-94.
- [129] Kim YH, Park JH, Lee M, Park TG, Kim SW. Polyethylenimine with acid-labile linkages as a biodegradable gene carrier. *J Control Release*. 2005;103:209-19.
- [130] Peng Q, Hu C, Cheng J, Zhong Z, Zhuo R. Influence of disulfide density and molecular weight on disulfide cross-linked polyethylenimine as gene vectors. *Bioconjug Chem*. 2009;20:340-6.
- [131] Zhang SB, Zhao B, Jiang HM, Wang B, Ma BC. Cationic lipids and polymers

- mediated vectors for delivery of siRNA. *J Control Release*. 2007;123:1-10.
- [132] Kolhatkar RB, Kitchens KM, Swaan PW, Ghandehari H. Surface acetylation of polyamidoamine (PAMAM) dendrimers decreases cytotoxicity while maintaining membrane permeability. *Bioconjug Chem*. 2007;18:2054-60.
- [133] Luo D, Haverstick K, Belcheva N, Han E, Saltzman WM. Poly(ethylene glycol)-conjugated PAMAM dendrimer for biocompatible, high-efficiency DNA delivery. *Macromolecules*. 2002;35:3456-62.
- [134] Yang H, Lopina ST, DiPersio LP, Schmidt SP. Stealth dendrimers for drug delivery: correlation between PEGylation, cytocompatibility, and drug payload. *Journal of materials science Materials in medicine*. 2008;19:1991-7.
- [135] Taratula O, Garbuzenko OB, Kirkpatrick P, Pandya I, Savla R, Pozharov VP, et al. Surface-engineered targeted PPI dendrimer for efficient intracellular and intratumoral siRNA delivery. *J Control Release*. 2009;140:284-93.
- [136] Adami RC, Collard WT, Gupta SA, Kwok KY, Bonadio J, Rice KG. Stability of peptide-condensed plasmid DNA formulations. *J Pharm Sci*. 1998;87:678-83.
- [137] Adami RC, Rice KG. Metabolic stability of glutaraldehyde cross-linked peptide DNA condensates. *J Pharm Sci*. 1999;88:739-46.
- [138] McKenzie DL, Smiley E, Kwok KY, Rice KG. Low molecular weight disulfide cross-linking peptides as nonviral gene delivery carriers. *Bioconjug Chem*. 2000;11:901-9.
- [139] Zezin AB, Kabanov VA. A new class of complex water-soluble polyelectrolytes. *Makromol. Chem., Suppl*. 1984;6:259-76.
- [140] Alfaro JF, Gillies LA, Sun HG, Dai SJ, Zang TZ, Klaene JJ, et al. Chemo-enzymatic detection of protein isoaspartate using protein Isoaspartate methyltransferase and hydrazine trapping. *Anal Chem*. 2008;80:3882-9.
- [141] Raddatz S, Mueller-Ibeler J, Kluge J, Wass L, Burdinski G, Havens JR, et al. Hydrazide oligonucleotides: new chemical modification for chip array attachment and conjugation. *Nucleic Acids Res*. 2002;30:4793-802.
- [142] Radushev AV, Chekanova LG, Gusev VY, Sazonova EA. Determination of hydrazides and 1,2-diacylhydrazines of aliphatic carboxylic acids by conductometric titration. *J Anal Chem*. 2000;55:445-8.

- [143] Schlupe T, Cooney CL. Purification of plasmids by triplex affinity interaction. *Nucleic Acids Res.* 1998;26:4524-8.
- [144] Cakara D, Kleimann, J. & Borkovec, M. Microscopic protonation equilibria of poly(amidoamine) dendrimers from macroscopic titrations. *Macromolecules.* 2003;36:4201-7.
- [145] Diallo MS, Christie S, Swaminathan P, Balogh L, Shi X, Um W, et al. Dendritic chelating agents. 1. Cu(II) binding to ethylene diamine core poly(amidoamine) dendrimers in aqueous solutions. *Langmuir.* 2004;20:2640-51.
- [146] Niu YH, Sun, L. & Crooks, R. A. . Determination of the intrinsic proton binding constants for poly(amidoamine) dendrimers via potentiometric pH titration. *Macromolecules.* 2003;36:5725-31.
- [147] Waite CL, Sparks SM, Uhrich KE, Roth CM. Acetylation of PAMAM dendrimers for cellular delivery of siRNA. *BMC Biotechnol.* 2009;9:38-47.
- [148] Yang K, Weng LA, Cheng YY, Zhang HF, Zhang JH, Wu QL, et al. Host-guest chemistry of dendrimer-drug complexes. 6. Fully acetylated dendrimers as biocompatible drug vehicles using dexamethasone 21-phosphate as a model drug. *J Phys Chem B.* 2011;115:2185-95.
- [149] Patil ML, Zhang M, Taratula O, Garbuzenko OB, He H, Minko T. Internally cationic polyamidoamine PAMAM-OH dendrimers for siRNA delivery: effect of the degree of quaternization and cancer targeting. *Biomacromolecules.* 2009;10:258-66.
- [150] Lee JH, Lim YB, Choi JS, Lee Y, Kim TI, Kim HJ, et al. Polyplexes assembled with internally quaternized PAMAM-OH dendrimer and plasmid DNA have a neutral surface and gene delivery potency. *Bioconjug Chem.* 2003;14:1214-21.
- [151] Kakizawa Y, Harada A, Kataoka K. Glutathione-sensitive stabilization of block copolymer micelles composed of antisense DNA and thiolated poly(ethylene glycol)-block-poly(L-lysine): A potential carrier for systemic delivery of antisense DNA. *Biomacromolecules.* 2001;2:491-7.
- [152] Oupicky D, Carlisle RC, Seymour LW. Triggered intracellular activation of disulfide crosslinked polyelectrolyte gene delivery complexes with extended systemic circulation in vivo. *Gene Ther.* 2001;8:713-24.
- [153] McKenzie DL, Kwok KY, Rice KG. A potent new class of reductively activated

- peptide gene delivery agents. *J Biol Chem.* 2000;275:9970-7.
- [154] Yang YH, Park Y, Man SH, Liu YH, Rice KG. Cross-linked low molecular weight glycopeptide-mediated gene delivery: Relationship between DNA metabolic stability and the level of transient gene expression in vivo. *J Pharm Sci.* 2001;90:2010-22.
- [155] Miyata K, Kakizawa Y, Nishiyama N, Harada A, Yamasaki Y, Koyama H, et al. Block cationic polyplexes with regulated densities of charge and disulfide cross-linking directed to enhance gene expression. *J Am Chem Soc.* 2004;126:2355-61.
- [156] Zhou J, Liu J, Shi T, Xia Y, Luo Y, Liang L. Phase separation of siRNA-polycation complex and its effect on transfection efficiency. *Soft Matter.* 2013;9:7.
- [157] Redlich O. The Dissociation of Strong Electrolytes. *Chem. Rev.* 1946;39:333-56.
- [158] Dong CL, Wen GL, Ai JZ, Shu JS, Nan C, Gang G, et al. Pre-deliver chitosanase to cells: A novel strategy to improve gene expression by endocellular degradation-induced vector unpacking. *Int J Pharm.* 2006;314:63-71.
- [159] Zhou LZ, Gan L, Li HB, Yang XL. Studies on the interactions between DNA and PAMAM with fluorescent probe [Ru(phen)(2)dppZ]2(+). *J Pharmaceut Biomed.* 2007;43:330-4.
- [160] Godbey WT, Wu KK, Mikos AG. Tracking the intracellular path of poly(ethylenimine)/DNA complexes for gene delivery. *Proc Natl Acad Sci U S A.* 1999;96:5177-81.
- [161] Liu XH, Yang JW, Miller AD, Nack EA, Lynn DM. Charge-shifting cationic polymers that promote self-assembly and self-disassembly with DNA. *Macromolecules.* 2005;38:7907-14.
- [162] Harada K, Sugaya T, Murakami K, Yazaki Y, Komuro I. Angiotensin II type 1A receptor knockout mice display less left ventricular remodeling and improved survival after myocardial infarction. *Circulation.* 1999;100:2093-9.
- [163] Ichihara S, Senbonmatsu T, Price E, Jr., Ichiki T, Gaffney FA, Inagami T. Targeted deletion of angiotensin II type 2 receptor caused cardiac rupture after acute myocardial infarction. *Circulation.* 2002;106:2244-9.
- [164] Oishi Y, Ozono R, Yoshizumi M, Akishita M, Horiuchi M, Oshima T. AT2

receptor mediates the cardioprotective effects of AT1 receptor antagonist in post-myocardial infarction remodeling. *Life Sci.* 2006;80:82-8.

- [165] Voros S, Yang Z, Bove CM, Gilson WD, Epstein FH, French BA, et al. Interaction between AT1 and AT2 receptors during postinfarction left ventricular remodeling. *Am J Physiol Heart Circ Physiol.* 2006;290:H1004-10.
- [166] Lau S, Graham B, Cao N, Boyd BJ, Pouton CW, White PJ. Enhanced extravasation, stability and in vivo cardiac gene silencing via in situ siRNA-albumin conjugation. *Mol Pharm.* 2012;9:71-80.
- [167] Kesharwani P, Gajbhiye V, Jain NK. A review of nanocarriers for the delivery of small interfering RNA. *Biomaterials.* 2012;33:7138-50.
- [168] Xu QX, Wang CH, Pack DW. Polymeric carriers for gene delivery: chitosan and poly(amidoamine) dendrimers. *Curr Pharm Design.* 2010;16:2350-68.
- [169] Jugdutt BI, Menon V. AT1 receptor blockade limits myocardial injury and upregulates AT2 receptors during reperfused myocardial infarction. *Mol Cell Biochem.* 2004;260:111-8.
- [170] Jugdutt BI, Menon V. Upregulation of angiotensin II type 2 receptor and limitation of myocardial stunning by angiotensin II type 1 receptor blockers during reperfused myocardial infarction in the rat. *J Cardiovasc Pharmacol Ther.* 2003;8:217-26.
- [171] Nio Y, Matsubara H, Murasawa S, Kanasaki M, Inada M. Regulation of gene transcription of angiotensin II receptor subtypes in myocardial infarction. *J Clin Invest.* 1995;95:46-54.
- [172] Horio T, Nishikimi T, Yoshihara F, Matsuo H, Takishita S, Kangawa K. Effects of adrenomedullin on cultured rat cardiac myocytes and fibroblasts. *Eur J Pharmacol.* 1999;382:1-9.
- [173] Cigola E, Kajstura J, Li B, Meggs LG, Anversa P. Angiotensin II activates programmed myocyte cell death in vitro. *Exp Cell Res.* 1997;231:363-71.
- [174] Grishko V, Pastukh V, Solodushko V, Gillespie M, Azuma J, Schaffer S. Apoptotic cascade initiated by angiotensin II in neonatal cardiomyocytes: role of DNA damage. *Am J Physiol Heart Circ Physiol.* 2003;285:H2364-72.
- [175] Flynn JD, Akers WS. Effects of the angiotensin II subtype 1 receptor antagonist

losartan on functional recovery of isolated rat hearts undergoing global myocardial ischemia-reperfusion. *Pharmacotherapy*. 2003;23:1401-10.

- [176] Jalowy A, Schulz R, Dorge H, Behrends M, Heusch G. Infarct size reduction by AT1-receptor blockade through a signal cascade of AT2-receptor activation, bradykinin and prostaglandins in pigs. *J Am Coll Cardiol*. 1998;32:1787-96.
- [177] Mammen M, Choi SK, Whitesides GM. Polyvalent interactions in biological systems: implications for design and use of multivalent ligands and inhibitors. *Angew Chem Int Ed*. 1998;37:2754-94.
- [178] Kiessling LL, Gestwicki JE, Strong LE. Synthetic multivalent ligands in the exploration of cell-surface interactions. *Curr Opin Chem Biol*. 2000;4:696-703.
- [179] Niederhafner P, Sebestik J, Jezek J. Glycopeptide dendrimers. Part I. *J Pept Sci*. 2008;14:2-43.
- [180] Waite CL, Roth CM. PAMAM-RGD conjugates enhance siRNA delivery through a multicellular spheroid model of malignant glioma. *Bioconjug Chem*. 2009;20:1908-16.
- [181] Pandita D, Santos JL, Rodrigues J, Pego AP, Granja PL, Tomas H. Gene delivery into mesenchymal stem cells: a biomimetic approach using RGD nanoclusters based on poly(amidoamine) dendrimers. *Biomacromolecules*. 2011;12:472-81.
- [182] Wood KC, Azarin SM, Arap W, Pasqualini R, Langer R, Hammond PT. Tumor-targeted gene delivery using molecularly engineered hybrid polymers functionalized with a tumor-homing peptide. *Bioconjug Chem*. 2008;19:403-5.
- [183] Gray WD, Wu RJ, Yin X, Zhou J, Davis ME, Luo Y. Dendrimeric bowties featuring hemispheric-selective decoration of ligands for microRNA-based therapy. *Biomacromolecules*. 2013;14:101-9.
- [184] Landa N, Miller L, Feinberg MS, Holbova R, Shachar M, Freeman I, et al. Effect of injectable alginate implant on cardiac remodeling and function after recent and old infarcts in rat. *Circulation*. 2008;117:1388-96.
- [185] Liu J, Zhou J, and Luo Y. SiRNA delivery systems based on neutral crosslinked dendrimers. *Bioconjug Chem*. 2012;23:174-83
- [186] Figure 4.1, 4.3, 4.4, 4.5, 4.7, 4.8, 4.9, 4.10 and table 4.1 were adapted from *Biomaterials*, 34, Liu J et al., Functionalized dendrimer-based delivery of

Angiotensin type 1 receptor siRNA for preserving cardiac function following infarction, 3729-36, Copyright (2013), with permission from Elsevier.

VITA

Jie was born in Tianjin, China, and received her early education till high school there. As she was curious about the secret of life, she chose biology for bachelors and earned her Bachelor of Science in Biological Science from Peking University in 2008. To better apply the obtained biological knowledge to meet the unmet clinical needs, she chose the field of engineering for her further studies and joined Peking University to pursue her doctoral degree in Biomedical Engineering. In 2009 Jie enrolled in the Joint PhD Program between Georgia Institute of Technology/Emory University/Peking University. She spent one year on Emory campus to conduct research in a collaborative lab in 2012. Outside the lab she prefers to spend her time in traveling, swimming, and calligraphy. She also likes cooking and tasting all kinds of food.